UROKIN: A novel software for kinematic analysis of urogenital motion using transperineal ultrasound imaging

Catriona Czyrnyj

A thesis submitted to the Faculty of Graduate and Postdoctoral Studies
in partial fulfillment of the requirements for the degree of

MASTER OF APPLIED SCIENCE

in Biomedical Engineering

Ottawa-Carleton Institute for Biomedical Engineering
University of Ottawa
Ottawa, Canada

February 2017

Abstract

Dynamic transperineal ultrasound (TPUS) video allows for kinematic analysis of urogenital morphology and mobility, however, measures are often limited to peak displacements of anatomical landmarks and are vulnerable to error incurred by probe rotation during imaging. This thesis aimed to (1) develop an algorithm to calculate kinematic curves of urogenital landmark motion from TPUS video and to (2) investigate the error incurred in these kinematic measures due to in-plane ultrasound probe rotation. UROKIN, a semi-automated software, was developed and, as a proof of concept, was used to identify differences in urogenital kinematics during pelvic floor muscle maximum voluntary contractions between women with and without stress urinary incontinence. A mathematical model revealed that the error incurred by TPUS probe rotation in the x- (anterior-posterior) and y- (cranial-caudal) directions, was a factor of: r, the radius of rotation; Θ, the in-plane angular probe rotation; and α, the angular deviation between the anatomical planes and the coordinate system in which error was calculated. As an absolute measure, the error incurred by in-plane probe rotation is reduced to a factor of only r and Θ. Moving forward, UROKIN must be adapted to include findings from (1), and must be tested for validity and reliability.

Acknowledgements

It is my pleasure to have the opportunity to thank all those who were instrumental in the completion of this thesis. I have been very lucky to be surrounded by outstanding researchers for whom I have the utmost respect and who have taught me so much over the past few years. First of all, I would like to thank the members of my committee, Dr. Adrian Chan and Dr. Ryan Graham, for donating their time and insight to aid in the completion of this thesis. I could not have dreamed of having two reviewers whom I admire more. I am very excited to gain the valuable feedback and experience that will come with the defense of this work.

I would like to express my gratitude to Dr. Michel Labrosse, my co-supervisor. Dr. Labrosse took me on as a student part way through my degree and dove head-first into a subject area with which he was not well acquainted. Dr. Labrosse's insight, calm and collected attitude, and extensive knowledge of biomedical engineering and biomechanics were an asset throughout the conception and execution of this thesis. Special thanks also go to my husband, Joel Gadde, who has supported me throughout my Master's and who has allowed me the privilege to support him in return. As well, I must extend my sincerest thanks to my lab mates in Ottawa, Kaylee Brooks and Marie-Ève Bérubé. These strong and wonderful women put up with my antics on a regular basis and make going into work something to look forward to.

Lastly, these acknowledgements would not be complete without the most heart-felt thank you to my supervisor and mentor, Dr. Linda McLean. Linda was kind enough to take a chance on me and to give me the support and the space to develop as a researcher and as a person. Linda's clear passion for this field and her unique and very special skill set have provided an environment where I can thrive and achieve much more than I ever thought possible. Thank you so much for everything you have done, I am forever in your debt.

Ethics and Collaboration

Ethics approval was granted by the Queens University Research Ethics Board (6006245), the Ottawa Hospital Research Ethics Board (2011625-01H) and the University of Ottawa Heath Sciences and Science Research Ethics Board (H10-14-18B & H08-15-29). I, the student, was responsible for all of the background research, development of the software, formulation of the mathematical derivation for the correction of rotational errors, development of processing and analysis procedures for all kinematic data, execution of all methods, and original drafts of all thesis chapters. Dr. Linda McLean was instrumental in guiding the development of the methodologies used, helping to establish data collection and processing parameters, and the interpretation of results obtained. She was also responsible for guiding the development of my understanding in the areas of anatomy, urogenital mechanics, ultrasound imaging, and statistics for the successful execution of all aspects of this thesis. All sections of the thesis were edited by Dr. McLean to ensure the best possible product. Dr. Michel Labrosse provided feedback on all methods and writings and helped to ensure that the technical and engineering aspects of the thesis were accurate. Dr. Ryan Graham provided insight into the use of 3D motion capture hardware and software and provided background on biomechanical phenomena, as necessary. Dr. Andy Adler provided extremely useful feedback on the mathematical derivation of error incurred due to probe motion. Kaylee Brooks, Yousef Bader, Martin Legendre, and myself were responsible for processing preliminary data using the UROKIN software to aid in the debugging process. As paid research assistants, Yousef Bader and Martin Legendre performed the image processing of the data presented in Chapter 4, using the UROKIN software. I performed the image processing presented in Chapter 3 and all bulk processing of the data presented in Chapter 3 and Chapter 4. Statistical testing was guided by Dr. McLean and executed by myself.

Copyright

Table of Contents

List of Figures

List of Tables

1 Introduction

Pelvic floor disorders (PFD) are defined as sensory or emptying abnormalities of the lower urinary and gastrointestinal tracts [1]. PFDs affect 25-35% of the population [1], [2] and present most commonly as different forms of urinary incontinence [1], [3]. Stress urinary incontinence (SUI) is the leakage of urine during tasks that increase intra-abdominal pressure (IAP) such as exertion, coughing, or sneezing [3] and accounts for 50% of all urinary incontinence (UI) cases [3]–[5]. SUI will affect up to half of all women at some point in their lives [1], [3]–[6] and is seen in both parous [7] and nulliparous women [2]. Stress incontinence is systematically underreported by women, likely making the actual prevalence estimate much higher than the 18.7% reported in the literature [3], [5], [6]. Population surveys have found that approximately 3.3 million Canadians suffer from urinary incontinence [4], leading to a cumulative cost of $8.5 billion annually [8]. SUI has also been linked to lower health-related quality of life and negative effects on psychosocial functioning [5], [6], [9]. With an aging global population and increased risk of PFDs in older women [1], [4], [6], [8], [10], prevalence of PFDs is expected to increase at least 55% by 2050 [10], exacerbating the need for effective SUI treatments.

In general, SUI is thought to result from defects in pelvic organ support [11]–[14], urethral hypermobility [13], [15], [16], and/or urethral sphincter dysfunction [11], [17]. When a woman physically exerts herself, there is a contraction of the abdominal muscles and expansion of the diaphragm; the IAP increases thereby causing an increase in bladder pressure. In a woman with SUI, urine leakage will occur if the bladder pressure exceeds the urethral closure force. While SUI risk factors include old age [1], [4], [6], [8], [10], obesity [3], [18], parity [1], [3], [5], [6], and ethnicity [1], [6], [19], [20], the underlying cause is most likely some combination of these biomechanical factors.

Treatment options for SUI currently include physical therapies, pessaries, urethral bulking agents, and surgery [4]. Physical therapy sees success rates approaching 50% [21] and involves pelvic floor muscle

(PFM) exercise to induce improved motor control and hypertrophy of the PFMs [21], [22] and urethral sphincter [22]. Pessaries are devices inserted into the vagina and are meant to stabilize the urethra. Pessaries are effective in approximately 45-55% of patients [23], but come with a risk of irritation and/or damage to the vaginal wall [24], [25] and do not provide a permanent solution. More recently, clinicians have begun using urethral bulking agents: the injection of collagen into the urethra. This method has similar reported success rates of 48% at one year post-injection, though the efficacy of bulking agents decreases with time due to natural breakdown of the collagen [4], [26]. Surgery, usually involving the enhancement of urethral stability through the insertion of a mid-urethral sling, is effective in approximately 80% of women [4], but is accompanied by a 15% chance of complications [27]. Although several management options exist for SUI, none is ideal and it is difficult to predict which would be optimal for a given individual.

Recent studies have suggested that specific treatments may be correlated with higher success rates when targeted to specific biomechanical defects identified through clinical testing. For example, if a woman exhibits urethral hypermobility and weak PFMs, physiotherapy will be more likely to succeed than if she had demonstrated stronger PFMs [28]. As well, smaller urethral cross-sectional areas have been correlated with lower success rates in surgeries involving mid-urethral sling insertion [29]. In these cases, urethral bulking agents or PFM training may be a better option [30]. Identification of the specific defect(s) contributing to an individual's SUI could allow for the personalization of care and the optimization of treatment outcomes.

There is currently no gold standard for the diagnosis and evaluation of urinary incontinence. SUI is generally assessed through subjective reports of leakage frequency and severity [1], [3], [6], [9], [10], [20]. Clinical techniques, such as the Q-tip test [11], [13], [23], [31], urethral profilometry [11], [17], [19], [29], [32], [33], and flow cystometry [19], [29], [34]–[37], have been developed to obtain objective measures in women with SUI, though their validity has been largely discredited [31], [32], [34]. The Q-

tip test is designed to measure urethral mobility during Valsalva. As a woman performs the bearing down maneuver, a Q-tip inserted into the distal urethra changes its angle with the strain. If the angular displacement of the Q-tip exceeds 30°, the patient is thought to exhibit urethral hypermobility (i.e. a loss of urethral support) [31] warranting treatment. When tested in a sample of 114 women, the Q-tip test failed to accurately identify urethral hypermobility in 75% of cases when compared to urethral excursion measured on sagittal plane ultrasound [31]. Urethral profilometry measures urethral function through pressure sensors embedded within a catheter that is inserted into the urethra and the bladder. Unfortunately, data acquired using urethral profilometry have been unable to detect the presence or severity of SUI [32]. Flow cystometry involves filling the bladder to capacity with saline solution to measure the pressure at which the bladder leaks urine (i.e. leak point pressure). In flow cystometry, the type of stress test and catheter used can influence measurements taken, reducing the reliability and validity of this method [34]. The most prominent limitation of these objective methods is the invasive insertion of a catheter. A catheter inserted into the urethra can alter the biomechanics and neuromuscular responses of the urogenital system, thereby impacting the validity of the results [38].

More recently, imaging techniques such as MRI and transperineal ultrasound (TPUS) have been used to assess female continence function. These methods allow the user to take measures of the morphology and kinematics of relevant pelvic structures [14], [15], [33], [39], [40]. In particular, dynamic sagittal plane TPUS has become popular due to its capacity for rapid sampling rates, affordability, availability, and ease of use. Further, images can be acquired non-invasively without inserting any instrumentation into the vagina or urethra. Ultrasound images have allowed the quantification of urethral support by objective measurement of bladder neck and urethral mobility [11], [13], [15], [16], [31], bladder neck descent [39], and urethral length [7], [11], [15], [17], [19]. Using ultrasound images, the motion of urogenital structures resulting PFM contractions has been quantified by measurement of anorectal angle displacement and change in levator plate length (i.e. the distance from the postero-caudal pubic symphysis and the anorectal angle) [14], [35], [41], [42]. While these measurements may provide valuable information to

describe the pathokinetics associated with PFDs, image analysis can be time and labour intensive. These measurements are also potentially fraught with error due to the unavoidable motion of the TPUS probe with respect to the patient that occurs as a result of the clinician's attempts to retain all essential anatomical landmarks in the image frame. As such, robust methods are required to process clinically acquired TPUS images.

Clinical urogynecology researchers often analyze a single rest frame and a frame representing the maximal displacement of urogenital landmarks observed during a task (i.e. a cough, PFM contraction, or Valsalva manoeuver). These rest and peak frames are used to compute net displacements of anatomical landmarks in an effort to quantify the extent of pathology (e.g. urethral mobility) in the case of incontinence or pelvic organ descent in the case of prolapse. While this strategy can identify structural differences between women with and without SUI [37], [43], [44], it omits potentially valuable details associated with the task mechanics [14], [45]. Further, whether analysing a complete dynamic task or simply peak displacements, processing must compensate for probe motion or there will be inherent error in the measurements. In the literature, there has been relatively little investigation into the effects of in-plane probe motion on measurements taken from TPUS images [14], [45], [46].

To optimize treatment for SUI, the underlying biomechanical mechanism(s) must be identified and understood. To accomplish this, reliable, objective, and valid measurements of urogenital mechanics are required. Before this is possible, the current limitations of dynamic TPUS processing and analysis must be quantified and improved to create measurements that truly reflect the kinematics of the urogenital organs and tissues. The purposes of this research were therefore to (1) develop a semi-automated software that compensates for in-plane TPUS probe motion in order to improve accuracy in dynamic sagittal plane TPUS analysis and (2) examine the effects of in-plane probe rotation on measurements taken using TPUS.

2 Background

2.1 Urogenital Anatomy

Urinary continence is maintained through complex interactions between the organs, muscles and connective tissues of the urogenital system. The urogenital system, as considered here, consists of the organs involved in maintaining continence and providing support to the continence system: the bladder, urethra, vagina, and rectum (Figure 2.1). These organs sit within the pelvic cavity and, as a group, are bordered anteriorly by the pubic symphysis – a secondary cartilaginous joint of the lateral pubic bones – laterally by the pubic bones themselves, and posteriorly by the sacrum and coccyx (Figure 2.2).

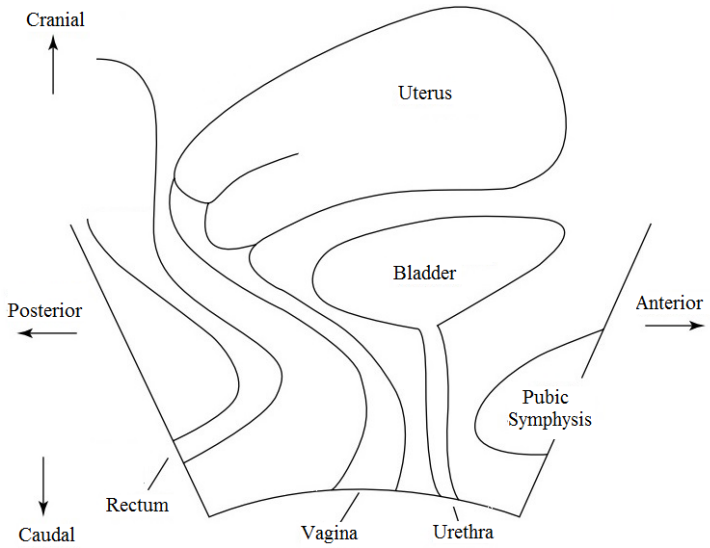

Figure 2.1 A mid-sagittal plane diagram of the female urogenital system including the urethra, bladder, vagina, and rectum. The uterus and pubic symphysis are also included. Adapted with permission from [39].

The main pelvic organ support structure, referred to as the pelvic floor, is composed of a complex array of connective tissues and is an integral part of the urogenital system [14], [47]. The urogenital organs rest inside the pelvic cavity, supported by the anterior pelvic bones, the bony sacrum and the pelvic floor [21], and a collection of muscles and fascia spanning the pelvic outlet (Figure 2.2). The levator ani is the primary muscle of the pelvic floor involved in continence control [48] and has several muscular subcomponents: the pubococcygeus, puborectalis, and iliococcygeus. Each of these subcomponents has two lateral components, one each on the left and right side of the body. Each side of the pubococcygeus

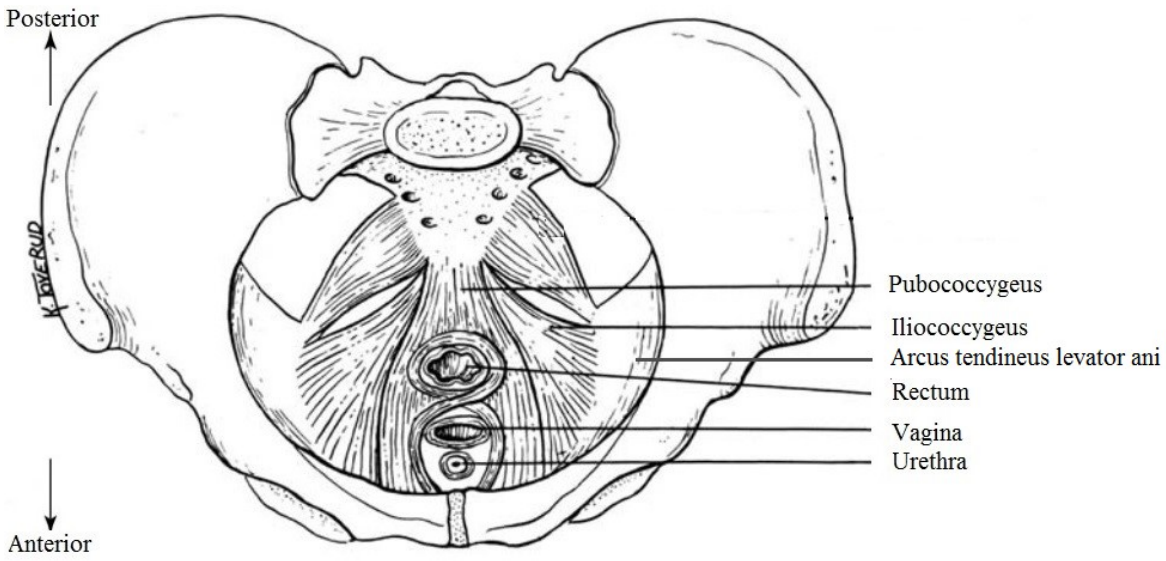

Figure 2.2 Anatomical drawing of an axial plane view of the pelvis, pelvic floor muscles (pubococcygeus, iliococcygeus, and puborectalis) and the external openings of the urethra, vagina, and rectum. Adapted with permission from [21].

attaches to the anterior pelvis at the pubic symphysis, and runs along its respective side of the urethra, vagina, and rectum to attach to the posterior pelvis, at the coccyx (Figure 2.2). Each side of the puborectalis muscle attaches anteriorly at the pubic symphysis and runs laterally along either side of the urethra and vagina to attach at the posterior aspect of the rectum, like a sling (Figure 2.2, Figure 2.3). The sling formed by the puborectalis around the posterior rectum causes a slight anterior bend to the rectal tract, referred to as the anorectal angle or anorectal junction (Figure 2.3) [49], [50]. The third

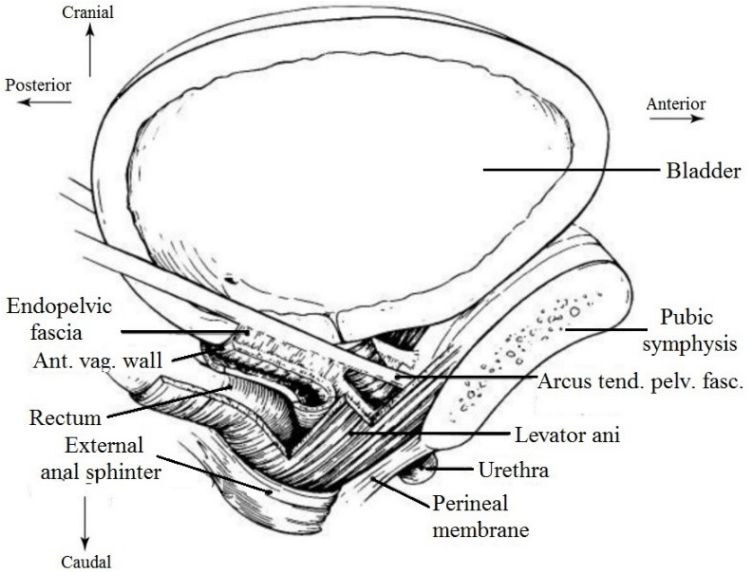

Figure 2.3 Lateral view of the urogenital organs and the muscle and tissue support structure of the urogenital system. Modified with permission from [48].

muscle of the levator ani, the iliococcygeus, is often referred to as the “shelf” that supports the urogenital system [48]. The iliococcygeus spans the width of the pelvic outlet and attaches bilaterally at the arcus tendineus levator ani (Figure 2.2). These subcomponents of the levator ani are composed primarily of type I slow twitch muscle fibers with a lower proportion of type II fast twitch muscle fibers [51]. The type I muscle fibers presumably allow the PFMs to remain tonically active [48], [52], providing pelvic organ support through most activities of daily living, with the recruitment of type II fibers as required. The levator ani are encased in connective tissue, which also aids in providing passive support to the pelvic organs [53]. Further, there is abundant connective tissue, the endopelvic fascia, which is involved in stabilizing and securing the urogenital organs and muscles (Figure 2.3) [47]. The urogenital hiatus or levator hiatus is often used to describe the transverse cross-section the female urogenital system bordered by the levator ani muscles and connective tissue; the portion of the pelvic floor through which the urethra, vagina, and rectum pass (Figure 2.2).

Urethral anatomy is also relevant to urinary continence function (Figure 2.4) [23], [36], [48]. The urethra originates at its proximal connection to the bladder (referred to as the bladder neck, urethrovesical neck, or urethrovesical angle) and extends distally to the external urethral meatus. In a healthy female, the urethra is supported by the levator ani muscles, the anterior vaginal wall, the endopelvic fascia, the

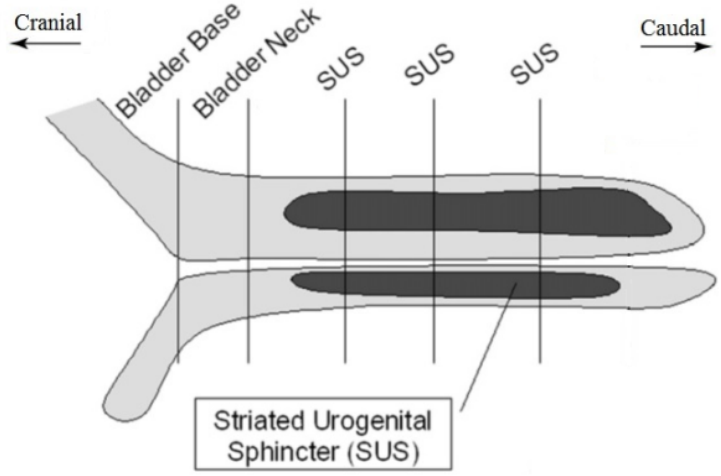

Figure 2.4 Mid-sagittal plane diagram of the urethra and striated urethral sphincter. Modified with permission from [17].

arcus tendineous fasciae, and the pelvis. Additionally, the pubourethral ligaments attach the urethra to the pubis. The external urethral sphincter, the smooth and striated muscle with fibers running longitudinally as well as circumferentially around the distal half of the urethra, also aids in maintaining urinary continence [48]. There is also an internal urethral sphincter, composed solely of smooth muscle, which may also contribute to continence function [54].

2.2 Female Urogenital Mechanics

Measuring the contractile ability, strength, and compliance of the PFMs and observing their effect on the bladder neck are important methods of investigating the continence mechanism [21], [22], [28], [30]. Anatomical landmarks in the midsagittal plane can be measured and tracked using TPUS, allowing researchers to assess urogenital kinematics [14], [16] and changes in urogenital morphology [55], [56] during dynamic tasks. These anatomical landmarks can be used as a means of quantifying dynamic PFM behavior [14], [22], [35], [41], [45], [50], [57] and urethral mobility [15], [22], [41], [43], [44], [58], factors thought to be extremely relevant to SUI and the continence mechanism [11]–[16]. Further, tasks such as coughing, maximal voluntary contraction (MVC or Kegel), and the Valsalva manoeuver incorporate controlled or reflexive contraction or relaxation of the PFMs – muscle functions thought to be essential to urinary continence [11], [47], [58]. These three tasks are often used in the study pelvic floor mechanics [37], [45], [59] and, when captured using dynamic 2D TPUS, they allow for direct observation of the motion of various midsagittal anatomical landmarks which provides insight into continence mechanics [15], [39], [48], [60]. The value of midsagittal, anatomical landmarks on 2D TPUS and their use to describe healthy and pathological urogenital mechanics during coughing, MVC, and Valsalva tasks are discussed further below.

2.2.1 Midsagittal Landmarks Relevant to Continence Function

2.2.1.1 Measures of Bladder Neck and Urethral Motion

Bladder neck position measured in the midsagittal plane can be assessed using TPUS during a variety of tasks and the magnitude of net bladder neck descent has been strongly associated with SUI [39], [61]. However, a recent study that included dynamic TPUS video of 31 women with and 42 women without SUI performing coughing tasks, found that five expert urologists and urogynecologists with significant experience in the evaluation of urethral hypermobility on ultrasound were unable to identify any patterns of bladder neck motion during coughing which could be used to accurately diagnose SUI [13]. Even using quantitative measures of bladder neck excursion, researchers have had difficulty in generating cut-off values of bladder neck excursion to objectively diagnose SUI [43], [62], [63], perhaps due to the multifactorial nature of the disorder. While bladder neck excursion during PFM MVC has previously been shown to correlate with PFM strength measured by palpation, and perineometry [12], it must be understood that the change in position of the bladder neck is an artifact of the muscle contraction and is not equivalent to direct measures PFM force during contraction. It was recently shown that the correlation between change in levator plate length (i.e. motion of the anorectal angle), measured by TPUS, and PFM activity, measured using electromyography (EMG), is significantly higher than the correlations of both bladder neck, and urethral motion, with PFM activity during PFM MVC [64]. Additionally, the literature shows that SUI can occur due to dysfunction of the PFMs, urethral sphincter, or the connective tissue supporting the urethra [21]. Based on this information, the anorectal angle appears to be the most valid anatomical landmark in the midsagittal plane through which to observe PFM activity using TPUS [14], [35], [45], [46], [57]. Bladder neck kinematics are more likely better measures for quantifying urethral mobility [11], [22], [37], [43] and potentially the integrity of the connective tissue supporting the urethra [65] as discussed below.

Acceptable levels of inter- and intra-examiner reliabilities have been observed in the measurement of peak bladder neck excursion during coughing and Valsalva tasks. (Section 2.3.2) [44], [59], [60], [66]. To

better understand changes in urethral support induced by vaginal childbirth, Shek and Dietz [16] developed a systematic approach to study the bladder neck and urethral mobility. This methodology involved manual identification of the urethral midline, running from the bladder neck to the external urethral meatus, at rest, and at peak Valsalva. This line was then divided equally to yield six points and the net displacement of each point was plotted to observe how net urethral excursion changes from the proximal to the distal end. In 44 nulligravid and 73 primiparous women, examined both pre- and post-partum, they saw reproducible measurements of urethral mobility (ICC = 0.80) and trends towards marked changes occurring after vaginal instrumental delivery. Their results also showed that the distal urethra was consistently less mobile than the proximal urethra, which is anatomically logical considering that the distal urethra passes the pubic symphysis where the muscles of the levator ani and connective tissues of the pelvic floor anchor at the anterior pelvis. Increased connective tissue surrounding and supporting the urethra in this region would likely decrease mobility of the distal urethral mobility. Pirpiris et al. [15] expanded on this work to further show the importance of observing the motion of the entire urethra. Using the methods of Shek and Dietz [16], their group found that peak displacement of the mid-urethra was most strongly associated with SUI. While these studies demonstrate the importance of quantifying the kinematics of the entire urethra, there are limitations to the methods employed. There was no compensation for probe rotation (Section 2.3.3), thus the effects on in-plane probe rotation on these measures are unknown. Additionally, the urethra was traced from the bladder neck to the external urethral meatus. As the meatus is located on the perineum, which is made of soft tissue, pressure of the ultrasound probe throughout a task can alter its position and the apparent length and curvature of the distal urethra.

To date, Constantinou's group [46] has conducted the only study to include dynamic tracking of urethral motion. Twenty-two continent women and nine women with SUI were imaged during a coughing task. Their results showed differences between cohorts in antero-posterior and cranio-caudal kinematics (Table 2.1). These differences were evident both in the anterior and posterior urethral walls. Specifically, there were between-cohort differences in the minimal antero-posterior and both minimal and maximal cranio-

caudal accelerations of the urethral walls. When the displacement curves of the urethra were aligned and averaged with respect to the synchronization point (Section 2.2.1.2), women with SUI exhibited peak urethral excursions more than double those seen in continent women, though differences in directions of urethral motion, velocity, and acceleration were not investigated. This study yielded large volumes of highly relevant information, suggesting that bladder neck and urethral kinematic curves may be useful in discriminating between women with and without SUI. However, the small sample size, the use of unmatched cohorts in terms of relevant demographic characteristics (i.e. age, body mass index), and parametric statistical testing on small samples, leave gaps in the literature that must be addressed.

	Anterior Urethra		Posterior Urethra	
Mean ± SD	**Anterior-Posterior**	**Cranial-Caudal**	**Anterior-Posterior**	**Cranial-Caudal**
Peak Displacement (cm)				
Continent	-0.43 ± 0.28	-0.66 ± 0.25	-0.41 ± 0.21	-0.80 ± 0.27
SUI	-1.22 ± 0.48	-1.7 ± 0.51	-1.1 ± 0.42	-1. 7 ± 0.61
p-value	<0.0001	0.0002	0.0009	0.0014
Peak Velocity Before Synchronization Point (cm/s)				
Continent	-2.8 ± 1.4	-3.4 ± 1.3	-2.5 ± 1.4	-3.7 ± 1.4
SUI	-4.2 ± 1.3	-5.1 ± 1.3	-3.9 ± 1.1	-5.4 ± 1.6
p-value	0.011	0.0015	0.0021	0.0044
Peak Velocity After Synchronization Point (cm/s)				
Continent	2.8 ± 1.3	3.1 ± 1.0	2.5 ± 1.2	4.2 ± 1.7
SUI	4.5 ± 2.3	6.3 ± 2.6	4.0 ± 2.1	5.8 ± 2.4
p-value	0.0072	0.0031	0.034	0.0031

Peak Acceleration (cm/s^2)	**Maximum**	**Minimum**	**Maximum**	**Minimum**	**Maximum**	**Minimum**	**Maximum**	**Minimum**
Continent	35 ± 17	-25 ± 9.2	38 ± 13	-28 ± 9.4	31 ± 13	-24 ± 9.2	33 ± 24	-39 ± 16
SUI	39 ± 17	-34 ± 16	55 ± 19	-48 ± 21	37 ± 13	-34 ± 16	55 ± 16	-47 ± 16
p-value	0.27	0.030	0.0052	0.012	0.11	0.021	0.0060	0.12

Table 2.1 Peak values of anterior and posterior urethral kinematics in women with stress urinary incontinence (SUI) and without (continent) centered about the maximum caudal anorectal angle displacement during a coughing task. Reproduced with permission from [46].

2.2.1.2 Measures of Pelvic Floor Muscle Kinematics

PFM behavior during dynamic tasks can be quantified in the midsagittal plane by tracking the anorectal angle or the levator plate line: a line running from the postero-caudal pubic symphysis to the anorectal angle in the sagittal plane [42] (Figure 2.5). The anorectal angle, and thus the levator plate line, have anatomical significance, as they represent the mid-sagittal cross-section of the puborectalis, pubococcygeus, and connective tissues of the levator ani. In three dimensions, the levator plate line

(Figure 2.5) represents the midsagittal view of the oblique axial plane that is coincident with the urogenital hiatus (Figure 2.6). Three-dimensional TPUS is required to image the urogenital hiatus and provide insight into changes occurring in urogenital hiatus during dynamic tasks [41], [56], [67], [68]. However, due to limitations on sampling rates of 3D TPUS, we are not yet able to track dynamic behavior of the urogenital hiatus. As such, the levator plate line and anorectal angle are used to observe dynamic behavior of the PFMs in the midsagittal plane [22], [35], [41], [69]. Measures of the levator plate line can be similar to tracking the motion of the anorectal angle, however changes in levator plate length often eliminate potentially relevant directional information regarding antero-posterior and cranial-caudal aspects of the motion.

In 2006, two different research groups reported that changes levator plate length and geometry of the anorectal angle in the midsagittal plane were associated with PFM function during dynamic tasks [35], [57]. Huang et al. [35] used measures of the levator plate length and change in levator plate length on Valsalva maneuver in an investigation of correlations between measures of the urogenital hiatus and the lower urinary tract. In a group of 396 women with pelvic organ prolapse, ranging from Stage I to Stage III (ICS POP-Q) [70], there were small but significant correlations ($p<0.05$) between levator plate length

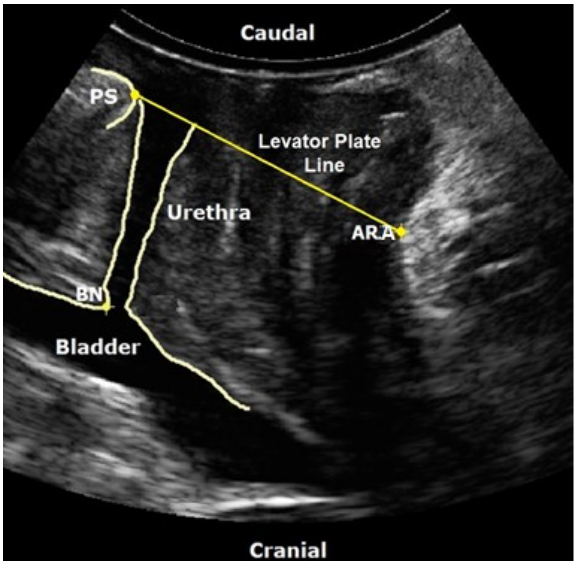

Figure 2.5 Sagittal plane transperineal ultrasound image of the female urogenital system. Relevant anatomical landmarks are labelled including the pubic symphysis (PS), anorectal angle (ARA), bladder neck (BN), bladder, and urethra. The levator plate line, a line running from the postero-caudal PS to the ARA that characterized PFM behavior, can also be seen.

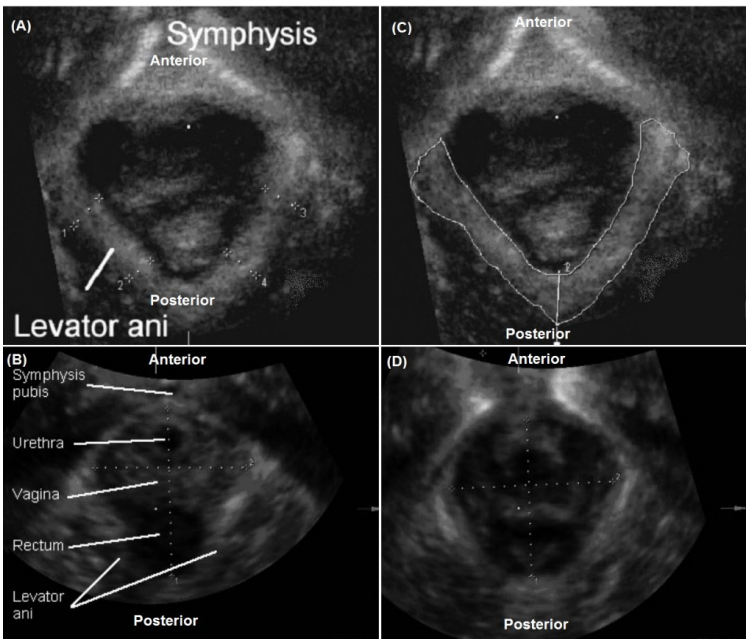

Figure 2.6 Oblique axial plane transperineal ultrasound image of the urogenital hiatus, the region of the female urogenital system bordered by the pelvic floor muscles. The top two images show the pubic symphysis and pubovisceral muscle, the iliococcygeus and puborectalis (a), with the pubovisceral muscle is outlined in (c). The bottom two images show the levator hiatus at rest (b) and at peak Valsalva (d). Reproduced with permission from [56].

and bladder neck angle at rest ($r = 0.292$) and peak Valsalva ($r = 0.209$). Additionally, their group observed significant negative correlations ($p<0.05$) between levator plate length and functional urethral pressure profiles ($r = -0.157$), and maximum urethral closure pressure ($r = -0.227$), as well as a correlation between changes in levator plate length and Valsalva leak point pressure ($r = -0.199$). In a separate study, Costantini et al. [57] measured changes in morphology of the anorectal angle to investigate the effects of vaginal birth on contractile strength of the levator ani muscles in the form of changes to anatomy and function of the PFMs. Comparing between three examinations performed prenatally, one week after delivery, and three months after delivery, Costantini et al. [57] found that the change in the angular magnitude of the anorectal angle during a PFM MVC was significantly less upon the third visit as compared to the first. While the meaning of these results are somewhat unclear, Costantini et al. [57] suggested that this measure was able to detect changes in anatomy and function of the pelvic floor after vaginal delivery.

In addition to urethral kinematics (Section 2.2.1.1), Constantinou's group [14], [45], [46], [71] also quantified the kinematics of the anorectal angle during coughing using dynamic TPUS. This was the first research using TPUS to quantify both the magnitude and direction of anorectal angle motion throughout an entire cough. Their analysis revealed significant differences between there cohorts of women without (N=22) and with (N=9) SUI. Data were averaged by synchronizing the maximum caudal displacement of the anorectal angle during the cough. This analytical approach yielded significant differences between cohorts were measured in peak values of anorectal angle displacements, velocities, and accelerations at and around the synchronization point (Table 2.2 and Table 2.3). Specifically, women with SUI did not exhibit the same initial antero-cranial displacement of the urogenital structures, thought to occur due to PFM contraction, as women without SUI. This is the only work to date that has reported on the differences between healthy women and women with SUI using full urogenital kinematic curves, rather than net displacements, and has contributed important information to our understanding of SUI. Additionally, there has been no investigation of anorectal angle kinematics during MVC or Valsalva tasks, excepting the single case report by Peng et al [45] which was a proof of concept illustration of their image analysis approach.

	Supine		**Standing**	
Mean ± SD	**Anterior-Posterior**	**Cranial-Caudal**	**Anterior-Posterior**	**Cranial-Caudal**
Displacement at Synchronization Point (cm)				
Continent	0.18 ± 0.05	-0.59 ± 0.04	0.01 ± 0.04	-0.40 ± 0.05
SUI	-0.21 ± 0.05	-1.00 ± 0.08	-0.88 ± 0.23	-1.17 ± 0.24
p-value	<0.0001	<0.0001	<0.0001	<0.0001
Velocity 0.5s Before Synchronization Point (cm/s)				
Continent	0.36 ± 0.09	-0.94 ± 0.07	0.12 ± 0.08	-0.68 ± 0.11
SUI	-0.15 ± 0.10	-1.34 ± 0.15	-1.31 ± 0.32	-1.86 ± 0.42
p-value	0.001	0.008	<0.0001	0.0003
Velocity 0.5s After Synchronization Point (cm/s)				
Continent	-0.11 ± 0.08	1.19 ± 0.06	0.20 ± 0.06	0.82 ± 0.09
SUI	0.55 ± 0.10	1.57 ± 0.14	1.19 ± 0.42	2.05 ± 0.57
p-value	<0.0001	0.005	0.0001	0.0004
Acceleration at Synchronization Point (cm/s^2)				
Continent	-2.61 ± 1.55	26.82 ± 2.06	3.16 ± 1.37	19.51 ± 2.47
SUI	5.90 ± 3.45	33.93 ± 3.32	7.28 ± 5.30	27.83 ± 8.17
p-value	0.01	0.07	0.28	0.20

Table 2.2 Values of anorectal angle kinematics in women with stress urinary incontinence (SUI) and without (continent) at or near the synchronization point (i.e. the maximum caudal anorectal angle displacement during a coughing task). Reproduced with permission from [14].

Mean ± SD	Anterior-Posterior	Cranial-Caudal	Resultant	Angle (°)
Peak Displacement (cm)				
Continent	0.18 ± 0.36	-0.63 ± 0.37	0.77 ± 0.36	285 ± 40
SUI	-0.20 ± 0.26	-1.01 ± 0.42	1.1 ± 0.40	260 ± 20
p-value	0.0038	0.0084	0.022	0.012
Peak Velocity Before Synchronization (cm/s)				
Continent	1.8 ± 0.95	-2.9 ± 1.5	NA	NA
SUI	-1.5 ± 0.66	-3.6 ± 1.0	NA	NA
p-value	<0.0001	0.10	NA	NA
Peak Velocity After Synchronization (cm/s)				
Continent	-1.3 ± 0.75	3.3 ± 1.4	NA	NA
SUI	2.2 ± 0.98	4.1 ± 1.5	NA	NA
p-value	<0.0001	0.085	NA	NA

Peak Acceleration (cm/s^2)	**Maximum**	**Minimum**	**Maximum**	**Minimum**		
Continent	15 ± 6.8	-18 ± 8.9	35 ± 18	-26 ± 12	NA	NA
SUI	24 ± 9.9	-21 ± 8.9	41 ± 13	-33 ± 8.6	NA	NA
p-value	0.015	0.16	0.20	0.092	NA	NA

Table 2.3 Peak values of anorectal angle kinematics in women with stress urinary incontinence (SUI) and without (continent) taken from curves averaged about a synchronization point (i.e. the maximum caudal anorectal angle displacement during a coughing task). Reproduced with permission from [46].

As mentioned above (Section 2.2.1.1), changes in levator plate length and motion of the anorectal angle are closely associated with PFM contraction. Huang et al.'s [35] work demonstrates the relationship between the anorectal angle and pressure changes in the lower urinary tract, as well as the anorectal angle's relationship to changes in the bladder neck position. While these are primarily weak correlations, this could potentially be due to the effects of connective tissues dispersing and altering forces generated by contraction of the PFMs. As well, Costantini et al. [57] and Constantinou's group [14], [45], [46], [71] showed that measures of the anorectal angle could be used to differentiate between patients pre- and post-vaginal delivery or between cohorts of women with and without SUI. While anorectal angle kinematics may correlate with PFM activity measured using EMG [50], [64], motion of the anorectal angle cannot be substituted for or used to infer PFM strength of a participant. Further, direction and magnitude of PFM force is altered by the effects of connective tissue and the structures of the urogenital system, so measures of anorectal angle kinematics must be considered in context. Motion of the anorectal angle does provide insight into PFM shortening and lengthening and the effects of those contractions on the urogenital system. One could also surmise that calculated accelerations of the anorectal angle, angular or otherwise,

may be proportional to resultant forces caused by PFM contraction, however this has not been proven. Logically, due to the anatomical significance of the anorectal angle (i.e. the point where the puborectalis wraps posteriorly around the rectum) and based on the evidence discussed here [35], [50], [57], [64], this landmark is likely the most appropriate urogenital landmark for quantitative observation of the impact of PFM activation in the midsagittal plane.

2.2.2 Healthy Urogenital Mechanics

2.2.2.1 Coughing Task

Women with SUI often leak urine when coughing, making this task extremely relevant to the study of the continence mechanism [4], [22], [28], [30], [72]. Coughing involves contraction of the diaphragm and abdominals [73], muscles at the anterior and cranial borders of the abdomen, which compress and displaces the internal organs, causing the IAP to increase up to 150cm H_2O (approximately 15kPa) [48]. In advance of this pressure increase, the PFMs appear to reflexively contract [74], likely in order to brake the downward acceleration of the pelvic organs [14], [48] and provide a firm surface against which the urogenital organs, especially the urethra, can be compressed to prevent urine leakage [46], [47]. Urine leakage during coughing may be associated with laxity of the pelvic floor [75]. Laxity of the PFMs and/or connective tissue could alter the force applied to the urethra due to the IAP – in magnitude, direction, or both – such that compression and displacement of the abdominal organs no longer prevents urine leakage [46], [47]. Based on this understanding of the internal biomechanics that accompany a cough, we can surmise that TPUS acquired from a healthy woman while coughing should show initial anterior motion of the anorectal angle due to reflexive contraction of the PFMs [42], [45], which precedes and limits postero-caudal displacement of the urethra (Figure 2.7) [14], [45], [46].

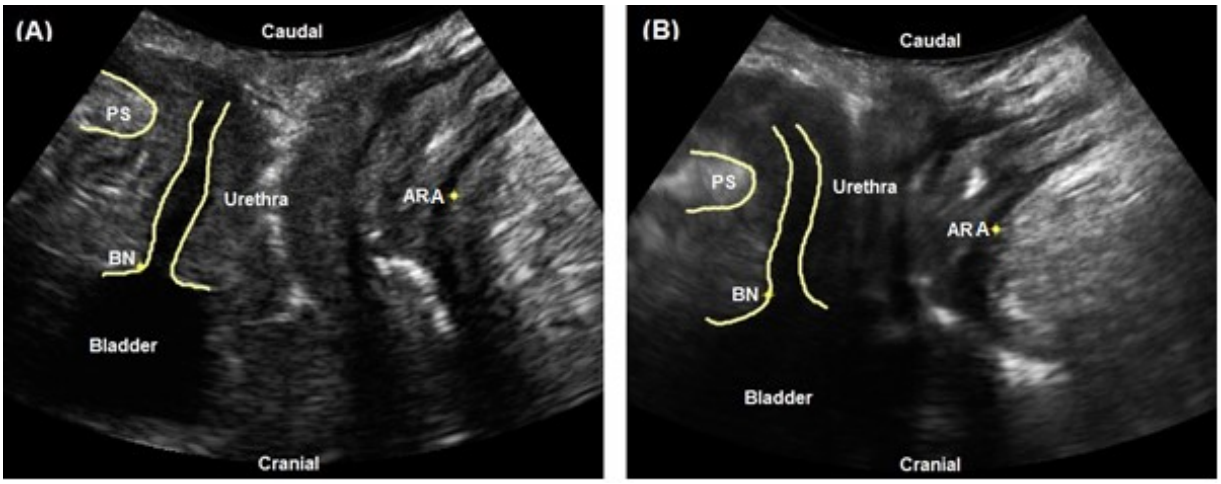

Figure 2.7 A sagittal plane ultrasound image of the female urogenital system at rest and peak of a coughing task, (A) and (B) respectively. The pubic symphysis (PS) displacement is indicative of probe motion, while posterocaudal displacement of the bladder neck (BN) and anorectal angle (ARA) relative to the PS occurs due to increased intra-abdominal pressure (IAP).

Analysis of coughing tasks from dynamic TPUS video has revealed three stages of urogenital motion in healthy women: initial PFM contraction, followed by urogenital organ descent, and then a relaxation and return of the organs to their initial positions (Figure 2.8) [14], [45], [46]. The initial contraction of the PFMs can be identified by the antero-cranial motion of the anorectal angle and bladder neck on TPUS (Figure 2.8a) [14], [45], [46]. Research has shown that the pressure increase in the distal urethra precedes the IAP increase at the beginning of a cough [74], suggesting that perhaps the PFMs and/or the urethral sphincters reflexively contract in advance of a cough. Further, Madill and McLean [76] identified no differences, between women with and without SUI, in speed of PFM contraction when coughing, suggesting that perhaps timing of the contraction and not the rate of contraction is the more relevant factor in maintaining continence. The organ descent seen in the second stage of the cough is characterized by a postero-caudal descent of the urogenital system (Figure 2.8b) [14], [45], [46] and occurs likely due to increased IAP exceeding the antero-cranial force of the, likely, pre-emptive PFM contraction. Lastly, the relaxation stage can be identified on TPUS video by the antero-cranial lift of the urogenital structures, returning the urogenital organs and tissues to their initial positions (Figure 2.8c) [14], [45], [46]. This lift is likely due to the decrease in IAP towards the end of the cough. In a healthy woman, the initial contraction of the PFMs, postero-caudal force generated by the IAP, and synergistic contraction of the urethral sphincter all combine to close the urethral lumen and prevent urine leakage. While it is generally

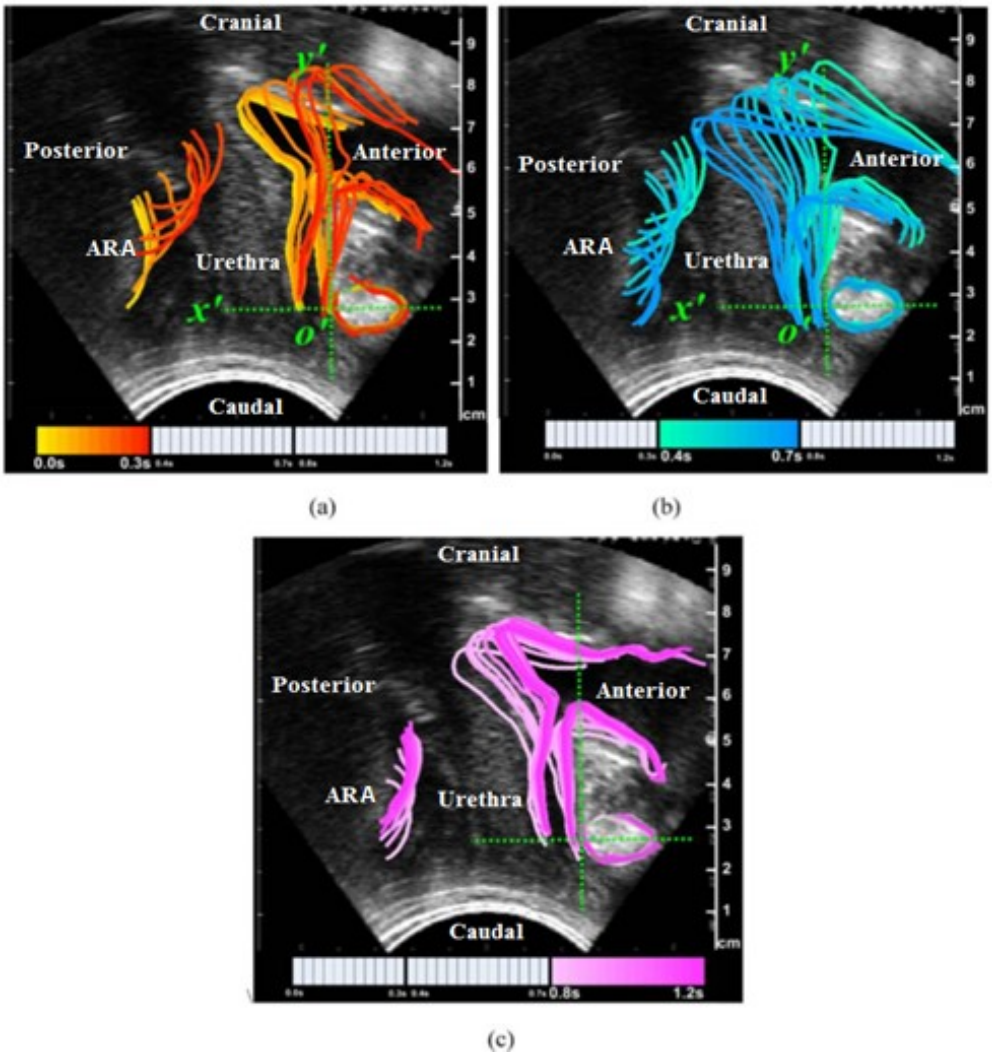

Figure 2.8 Motion of the anorectal angle (ARA) and urethra during a cough in a healthy female. The first phase of the task is show in (a); the second phase, in (b); and the third, in (c). The timing of the motion is shown by the color of the curves and the legend. Modified from with permission from [45].

held that the IAP compresses the urethral lumen against the taut pelvic floor to close the urethra [46], [47], this hypothesis has not been definitively validated in the literature and it is not exactly clear how sphincteric contraction contributes into this mechanism.

2.2.2.2 PFM Contraction

During a PFM MVC, a woman is asked to contract her PFMs to a maximal level while being imaged using TPUS. From TPUS video, qualitative assessment and quantitative measures of PFM MVCs can be made [28], [45], [77]. A PFM contraction is often described as a lift and squeeze around the urethra,

vagina, and rectum [21]. The success of a PFM MVC can be gauged by observation of the perineum; inward motion of the perineum indicates a correct MVC. Correct task performance, absent of the IAP increase and postero-caudal decent of the urogenital organs associated with a Valsalva maneuver, must be verified, as incorrect techniques can confound the motion [78]. Some women with SUI demonstrate poor PFM function, often observed using the MVC task, in comparison with healthy continent controls [79]. Midsagittal TPUS of a healthy patient performing an MVC visualizes the "lift" and the "squeeze" generated by the PFM contraction (Figure 2.9).

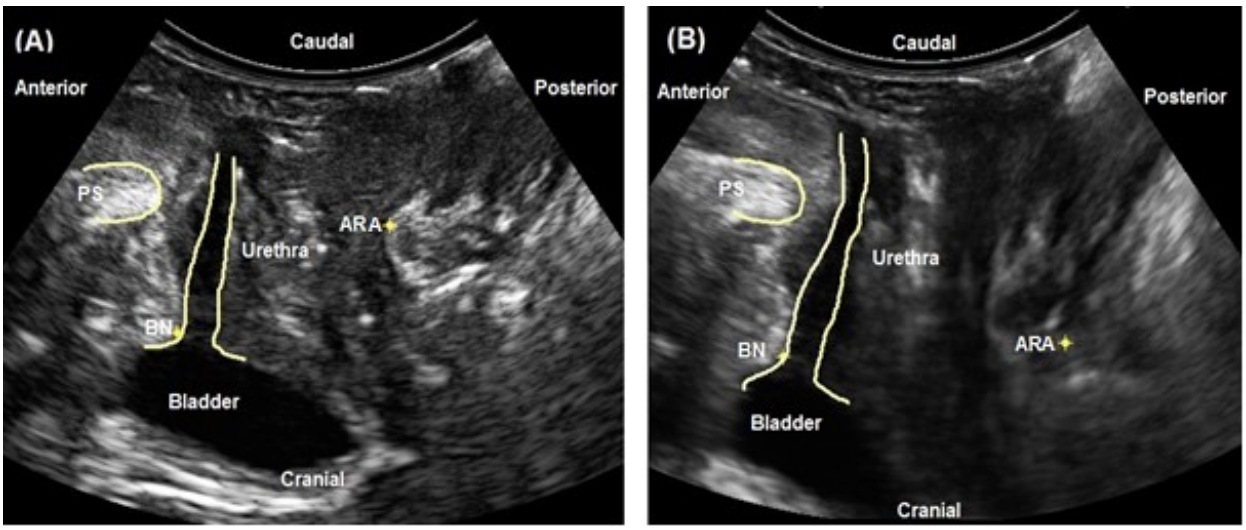

Figure 2.9 A sagittal plane ultrasound image of the female urogenital system at rest and peak maximum voluntary pelvic floor contraction, (A) and (B), respectively. The pubic symphysis (PS) displacement is indicative of probe motion, while the cranial bladder neck (BN) and anorectal angle (ARA) displacement occurs due to pelvic floor contraction.

Pelvic floor MVCs have been studied in great detail in continent women and the impact of a contraction on the urogenital anatomy can be described. A PFM contraction alters the anatomical relationships between the bladder base, urethra, and pubic symphysis [12]; including their relationship to the anorectal angle [45]. Motion of the urogenital system during a PFM MVC can be separated into two stages: the escalation of the contraction, followed by the relaxation of the muscles. A PFM contraction causes the pubococcygeus, puborectalis, and iliococcygeus to shorten, resulting in an antero-cranial lift of the pelvic floor [40], [45], [72]. In a healthy woman, this contraction generates antero-cranial motion of the anorectal angle and bladder neck as the contraction builds [12], [40], [45], [80], and postero-caudal descent as the PFMs relax (Figure 2.10) [45].

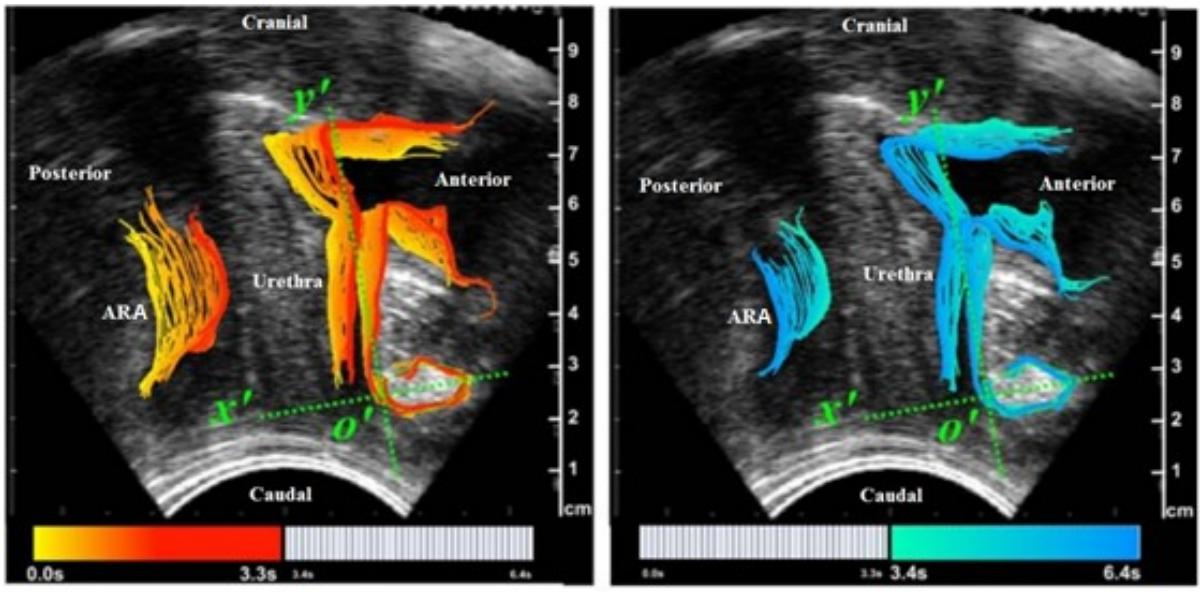

Figure 2.10 Motion of the anorectal angle (ARA) and urethra during a maximal voluntary contraction of the pelvic floor in a healthy female. The first half of the task is show in (a) and the second half is shown in (b). The timing of the motion is shown by the color of the curves and the legend. Modified with permission from [45].

2.2.2.3 Valsalva Manoeuver

The Valsalva maneuver is another important task in the study of incontinence [44], [45], [59]. Like a cough, a Valsalva involves a forced expiration against a closed gottis and contraction of the diaphragm and abdominal muscles [67]. This task generates a large increase in IAP [60] and is optimally performed against a relaxed pelvic floor [67]. Because the pelvic floor is responsible for supporting and stabilizing the urogenital organs, if the PFMs remain relaxed, a Valsalva causes descent of the pelvic organs, straining the pelvic floor muscles and connective tissues [50]. The effects of a Valsalva maneuver on pelvic organ descent and compliance of the pelvic floor may be extremely relevant to SUI [36], [60], [67]. Observing the urogenital system at rest and at peak Valsalva using TPUS visualizes the postero-caudal displacement of the urogenital system, specifically the anorectal angle, urethra, and bladder neck (Figure 2.11). In the absence of any confounding PFM contraction, the extent of bladder neck and urethral descent during Valsalva inform about the integrity of the pelvic floor connective tissues.

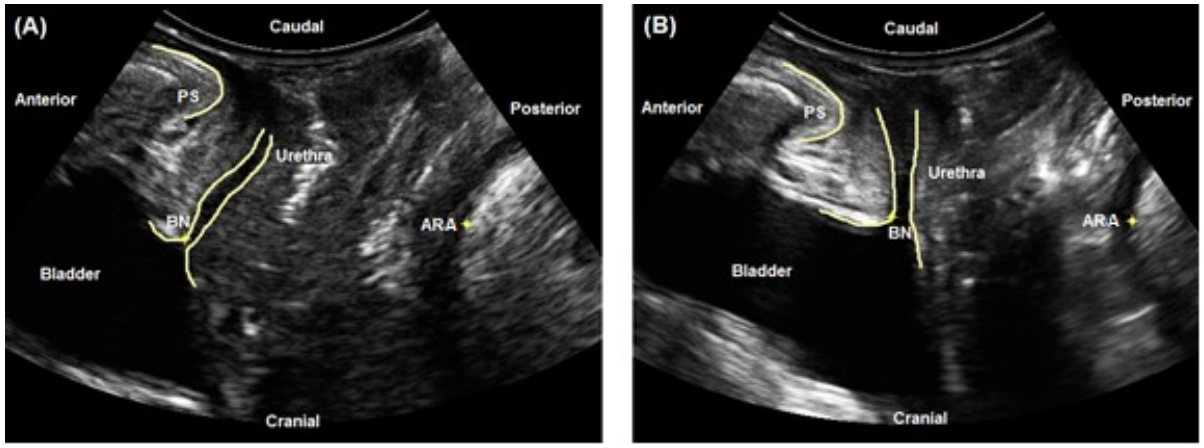

Figure 2.11 A sagittal plane ultrasound image of the female urogenital system at rest and peak Valsalva, (A) and (B), respectively. The pubic symphysis (PS) displacement is indicative of probe motion, while bladder neck (BN), and anorectal angle (ARA) caudal displacement occur due to increased intra-abdominal pressure again the relaxed pelvic floor.

Two stages of urogenital motion have been identified in a correctly performed Valsalva maneuver (Figure 2.12) [45]. During the first stage, the urogenital organs descend postero-caudally, presumably due to the increase in IAP against the relaxed pelvic floor. During the second stage of the task, the urogenital system ascends antero-cranially, likely as the IAP decreases and the organs return to their initial positions. TPUS imaging during Valsalva allows for the observation of maximal pelvic organ descent,

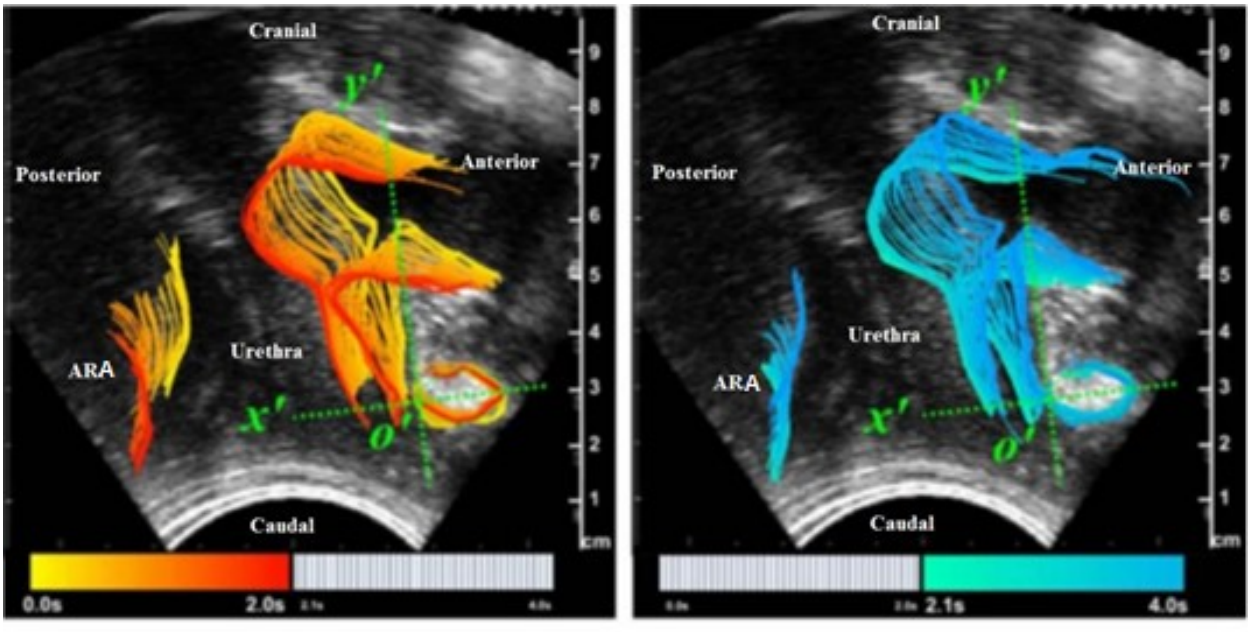

(a) (b)

Figure 2.12 Motion of the anorectal angle (ARA) and urethra during a Valsalva maneuver in a healthy female. The first half of the task is show in (a) and the second half is shown in (b). The timing of the motion is shown by the color of the curves and the legend. Modified with permission from [45].

ideally without a co-contraction of the levator ani confounding the results [67]. Studies comparing urogenital mechanics in women with and without SUI during Valsalva have yielded cut-offs in measures of urethral mobility [63] and changes in urethral morphology [62] associated with healthy urogenital mechanics that demonstrate high specificity and sensitivity in identifying women with SUI. The Valsalva maneuver is likely instrumental in developing a better understanding of the role of the urogenital connective tissues and their contributions to continence function.

2.2.2.4 Potential Confounders to Measures of Urogenital Mechanics

Gravity, bladder contents, and muscular co-activation can all act as potential confounders to urogenital mechanics measured using TPUS imaging. Depending on the position of the woman during imaging, different mechanical responses may be observed [14], [39], [47], [59]. In general, the supine or lithotomy positions appear to be the preferable standard for evaluating urogenital mechanics [59]; however, observing urogenital mechanics in a standing position may provide a more thorough understanding of urogenital mechanics under more functional circumstances, since most urine leakage occurs when women perform tasks in a sitting or standing position. The volume of urine in the bladder can also effect urogenital mechanics; lower measures of urethral and bladder mobility have been observed in women when the bladder is full compared to when it is empty [81]. Lastly, while there is a natural synergy between the abdominal muscles and the PFMs [82], 30% of women do not contract their PFMs correctly and instead recruit the abdominal muscles, gluteal muscles, and other muscles of the lumbopelvic region [67], [72], [78], [83], [84], which may confound measures of urogenital mechanics during functional tasks .

2.2.3 Urogenital Mechanics in SUI

In theory, SUI is thought to result from some combination of defects in the PFMs, pelvic fascia, and the urethral sphincters [11]–[17]. PFM dysfunction may arise from altered neurological or structural integrity, such that increased IAP may no longer result in force transmission that consistently closes the

urethral lumen and prevents urine leakage. Urethral hypermobility, likely caused by major defects in the connective tissues supporting the proximal urethra, is also thought to affect force transmission through the urogenital system and contribute to SUI [16]. While urethral sphincter dynamics are not well understood, their action likely contributes substantially to maintaining urinary continence and has been associated with increased vaginal closure force [17], PFM contractile strength [22], and elevation of the urethra [17].

In reality, there is little information available regarding the dynamic behavior of the female urogenital system in general, and in those with SUI, more specifically. This is likely due, in part, to the time-consuming task of manually processing dynamic ultrasound images, the complexity of automating the process, and the difficulty in taking accurate measurements across frames from TPUS data [37], [45]. The only studies of dynamic urogenital kinematics, performed by Constantinou's group [14], [45], [46], [71], revealed that, during a coughing task, women with SUI did not experience the initial antero-cranial lift of the anorectal angle and instead exhibited postero-caudal descent through the first half of the task. This motion may be attributable to a delayed or ineffective PFM contraction unable to counter the downward force generated by the increased IAP. Additionally, their results showed that, during a cough, the urethra tended to descend and ascend along a collinear trajectory in healthy women, but followed a more convoluted path with larger displacements at higher velocities in women with SUI [46]. These differences in urethral kinematics may be indicative of tissue damage in women with SUI, which results in a loss of urethral stability [15], [16].

While there are limitations to the work of Constantinou's group [14], [45], [46], [71] (Section 2.2.1.1), insight into the continence mechanism can still be gained by interpreting the outcomes of this research in the context of complimentary studies. For example, training PFM pre-contractions ("the Knack") before tasks known to cause increases in IAP can reduce urine leakage in some women [21], [85]. Research also shows that PFM pre-contraction reduces the peak descent of the bladder neck in nulliparous healthy

women during coughing tasks [58]. Taken together with dynamic urogenital tracking studies [14], [45], [46], we can postulate that the PFMs play a role in stabilizing the urethra and that delayed or ineffective PFM contraction during coughing could potentially result in urine leakage. Impaired PFM function could eliminate the first phase of urogenital motion seen during a cough (Section 2.2.2.1) and increase PFM and urethral descent, as seen in the literature [14], [45], [46]. PFM dysfunction can also have several underlying causes including neurological damage, muscle or connective tissue damage (micro or macro), altered kinesthetic awareness or atrophy, all of which could result in alterations to support and stabilization of the urogenital system. Robust measurements of urogenital kinematics may provide invaluable insight into PFM mechanics and the continence mechanism as well as other PFDs.

2.3 Transperineal Ultrasound Imaging

Over the past two decades, TPUS has become an ideal tool for measuring urogenital mechanics due to its non-invasive nature, the objective measures which it yields, and its reasonable correlation with traditional methods of pelvic floor assessment (i.e. palpation) [12]. Medical imaging of the pelvic floor provides quantitative data regarding anatomical morphology and function [45], [47], [50]. Currently, TPUS allows for 2D and 3D static and dynamic visualization of the urogenital system. The multiplanar structure and action of the PFMs makes 3D imaging techniques (e.g. MRI or 3D ultrasound) ideally suited to investigate the female urogenital system. Unfortunately, 3D imaging techniques cannot currently provide the temporal resolution necessary to track the dynamic motion of urogenital structures. While 2D TPUS is the current standard in the dynamic evaluation of the urogenital system [14], [45], 2D medical image analysis is complex and requires an understanding of not only female pelvic anatomy but also TPUS image acquisition [68], [86]. The basic principles behind ultrasound image acquisition and the validation of 2D kinematic measures made from TPUS video are discussed below.

2.3.1 Ultrasound Imaging of the Urogenital System

The term ultrasound refers to waves oscillating at frequency spectra above the range of human hearing (20kHz). Ultrasound probes (i.e. transducers) contain piezoelectric materials: materials that generate a voltage in response to an applied stress and vice versa. A voltage pulse applied to a piezoelectric material is equivalent to an impulse force and will cause the material to vibrate at its resonant frequency. The transducer is designed to generate bursts of ultrasonic energy, like a speaker, and then receive the sound waves reflected back, like a microphone. The reflected wave, or echo, will be attenuated depending on the acoustic properties and geometry of the reflective surface and the distance over which it was transmitted [87]. Thus, the change in the reflected sound wave with respect to the original sound wave can be used to build an ultrasound image.

At an interface between two tissues differing in echogenicity (i.e. acoustic properties), there will be a difference in contrast on the TPUS image [86]. Specifically, the behavior of a sound wave at a tissue interface is dependent upon the properties of the two media, including the speed of sound through each media (u), media density (ρ) and bulk modulus (E). These material properties affect a medium's acoustic impedance (Z), a factor of u and ρ; and acoustic reflectivity (i.e. the fraction of energy reflected) at the interface (R), a factor of Z [87]. Additionally, the sound wave will be modulated depending on: distance traveled; geometric spreading, reduction in amplitude over area; and attenuation. The concept of attenuation allows for the calculation of the half value layer, the distance travelled at the point when the amplitude has reduced by 50% [87]. Observing sample values of u, Z, R, and the half value layer for biological matter gives a better understanding of how certain materials will appear in TPUS images (Table 2.4).

In ultrasound images, highly echogenic (i.e. highly reflective) tissues appear in white; while anechoic (i.e. non-reflective) tissues appear in black. This difference in contrast makes ultrasound a useful tool for

Tissue	u (m/s)	Z (g/cm²·s)	Half Value Layer (cm)	Tissue Interface	R at Interface
Water	1496	1.49×10^5	1360	Air/Water	0.999
Fat	1476	1.37×10^5	3.8	Water/Fat	0.042
Muscle	1568	1.66×10^5	2.5	Water/Muscle	0.054
Brain	1521	1.58×10^5	2.5	Water/Brain	0.029
Bone	3360	6.20×10^5	0.23	Water/Bone	0.614
Air	331	4.13	1.1	Tissue/Air	0.999

Table 2.4 Acoustic properties of biological tissues at 1.0 MHz. Reproduced with permission from [87].

urogenital imaging because of the large variations in echogenicity of the different pelvic tissues (Figure 2.13). The bladder and urethra appear in black due to the anechoic nature of the fluid they contain: urine in the bladder and blood vessels that perfuse the urethral wall [86]. Depending on the anatomy of the woman being imaged, the section of pubic symphysis visualized may be the cartilage of the symphyseal joint, though sometimes cross-section of the lateral pubic bones is instead captured. Cartilage appears as a dull white, whereas bony regions appear as anechoic (i.e. black) with a hyperechoic (i.e. white) outline [86]. The vaginal walls usually collapse when empty and thus they are not normally visible on ultrasound images, while the rectum also collapses somewhat and is therefore not as clearly visible as the urethra. The hyperechogenic properties of muscle and fascia [86] make the cross-section of the puborectalis and accompanying connective tissue, as it loops around the posterior wall of the rectum forming the anorectal angle, relatively easy to identify [39]. Due to the high resolution images that can be obtained by modern TPUS, it has the potential to become a valuable clinical tool, allowing doctors and physiotherapists the capacity to measure the motion of the urogenital structures generated by PFM contraction during MVC and cough; or PFM relaxation, during Valsalva [72].

There are several additional factors that can impact TPUS images of the female urogenital system. Medical imaging frequencies range from 1MHz to 15MHz [87], though TPUS is usually ranges from 3.5MHz to 7MHz [39]. At higher frequencies, improved spatial resolution is observed, but imaging depth becomes limited [87]. Therefore, the frequency selection must be balanced between desired spatial resolution and the required depth of penetration. Wide image acquisition angles are ideal when imaging

the urogenital system in order to capture all necessary anatomical landmarks in the image frame. Ideally, clinicians would capture from the pubic symphysis to the coccyx or sacrum, eliminating some of the problems experienced during TPUS imaging in trying to maintain all relevant landmarks in view through dynamic tasks [14], [45]. Unfortunately, the view angles available using curvilinear surface probes, ideal for TPUS imaging, are limited to the range of 70° to 85°, and so researchers must settle for imaging from the pubic symphysis all the way to the anorectal angle. Thus, when imaging using a curvilinear probe, as is common in the assessment of stress incontinence [15], [19], [22], [60], [72], the acquisition angle is most often set to its maximum [15], which still may not be large enough to capture all relevant anatomical landmarks in some women.

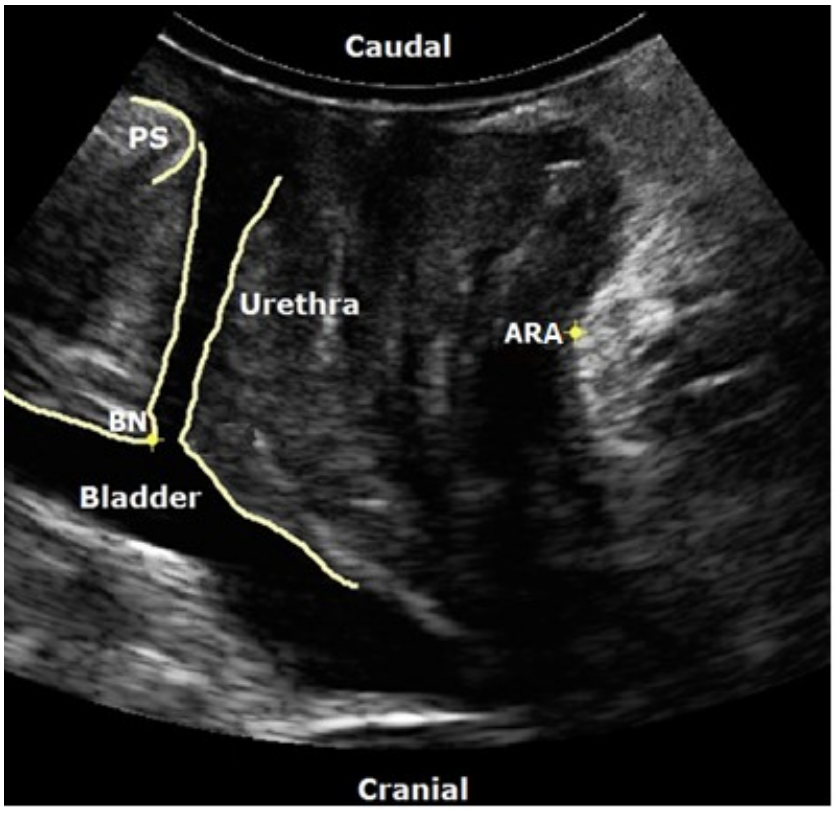

Figure 2.13 A two dimensional transperineal ultrasound image of the female urogenital system. The highly echogenic pubic symphysis (PS) and anorectal angle (ARA) can easily be seen while the anechoic nature of the bladder and urethra allow for easy identification as well. The bladder neck (BN), the anterior point where the urethra opens up to the bladder, can also be

When imaging the urogenital system, there are anatomical components in the more superficial region (e.g. the external urethral meatus), mid-depth (e.g. the PFMs), and deeper (e.g. the bladder neck and bladder) regions. The anisotropy of tissues also has implications in ultrasound image acquisition. A slight change in the angle of incidence of the ultrasound probe against the perineum can cause tissues to appear and disappear. As such, there is often an optimum angle of incidence for the probe which can be found by trial and error due to the natural biological variations in human physiology [86]. This tissue property helps clinicians to remain in a single plane during image acquisition, because any out of plane rotation causes disappearance of required anatomical landmarks. Additionally, during TPUS imaging the urogenital structures, shadows can be cast by anechoic (i.e. non-reflective) surfaces on anatomical structures beyond them in an image and these shadows can hide important landmarks required for image analysis [86]. For example, the pubic symphysis is a bony structure seen when imaging the urogenital system and is necessary for measurement and eliminating probe motion effects. In some patients and at some probe orientations, the pubic symphysis can cast a shadow on the urethra and/or bladder neck which are other structures of interest in many applications [22], [44], [66], [81]. Lastly, it should also be noted here that ultrasound images will appear inverted (
Figure 2.13) unless they have been rotated to match the orientation of an upright individual (Figure 2.10, Figure 2.12).

2.3.2 Reliability of Transperineal Ultrasound Measures

An early validation of TPUS imaging of the urogenital system was performed by Gordon et al [44] in 1989, who compared measures from TPUS to lateral chain urethrocystography. Twenty-one women were imaged in the supine position using TPUS. TPUS was used to image women, once with a catheter inserted into the urethra, and a second time with a chain inserted into the urethra. Women were also imaged using lateral chain urethrocystography: a lateral x-ray taken in the standing position with a chain placed in the urethra. Bladder neck descent was measured at rest and peak Valsalva with respect to the

pubic symphysis, the ideal reference point as it is the only bony landmark visible in TPUS images. Ultrasound measures were compared to measures from lateral chain urethrocystography, the gold standard at the time. Measures of bladder neck descent made from TPUS were similar to those made from urethrocystograms, using both the chain and the catheter methods. The authors noted the drawbacks of urethrocystography, including radiation exposure, patient motion and parallax (projection) artifacts, whereas TPUS was a safe alternative without the inherent error in measures caused by image projection. The authors concluded TPUS is a preferable tool for measuring bladder neck descent.

Expanding on this work, in 1992 Creighton et al [88] conducted a reliability study of measures of linear and angular displacement of the bladder neck taken from TPUS recorded during a Valsalva maneuver, as performed by Gordon et al. [44]. Six women were examined, each on three separate occasions. No significant differences were seen among repeated imaging sessions and the authors concluded that the results were reproducible within the context of the sample. While the results of this study were positive, there were several limitations associated with the study design. The low sample size limits the wide spread applicability and the method of statistical testing was not consistent with a robust assessment of reliability [89].

In a much larger study in 1995, Schaer et al [66] sought to assess the validity and reliability of measures taken from TPUS images. To establish between-rater reliability, 40 incontinent women were examined in the supine position, each by two separate observers, using TPUS. Between imaging sessions, intravesical pressures and bladder volumes were standardized for each patient using a pressure catheter and saline solution, respectively. To establish validity, 60 women were imaged in the standing position, using both TPUS and urethrocystography. Intravesical pressures were not standardized in the second stage of the study. In each stage, bladder neck position was measured at rest and peak Valsalva using an x and y coordinate system centered at the dorso-caudal margin of the pubic symphysis. Their results showed no significant differences between raters ($p<0.05$) and that measures taken using TPUS and

urethrocystogram were similar at rest. At peak Valsalva, however, there were significant differences ($p<0.05$) between measures of bladder neck position taken using TPUS and urethrocystography. The authors attributed this difference to inherent error in urethrocystogram images (e.g. parallax and superposition artifacts and unmonitored IAPs). Further, as the order of TPUS and urethrocystogram imaging sessions was not detailed and the IAP measures were not recorded, there may have been systematic bias introduced: a learning effect may result in higher IAPs being achieved in the second imaging session, thereby confounding the results. Regardless, as in Gordon et al [44], the findings of similar between-rater measures and comparable results at rest lead the authors to conclude that TPUS was valid with respect to urethrocystography, and is a reproducible tool for measuring bladder neck position. The authors also concluded that TPUS is superior to urethrocystography at peak Valsalva because it is not subject to the inherent error and risks associated with X-ray – yet no validation against a gold standard exists. Conclusions of reliability resulting from this study must be interpreted with caution as the authors did not complete a robust reliability analysis.

Reflecting on the work of Schaer et al [66], more recent research provides further insight into these results. TPUS probe motion during sagittal plane image acquisition has been shown to impact measures of urogenital kinematics [37]. Instantaneous visual feedback provided by TPUS allows clinicians to better maintain consistent probe orientation with respect to the patient, whereas this is not possible during X-ray imaging. At peak Valsalva, the motion of the pelvis itself (i.e. posterior pelvic tilt due to the "bearing down" task instruction) could cause changes in the orientation of the pubic symphysis, which do not appear to have been compensated for using urethrocystography. Further, Schaer et al [66] presented no quantitative method for alignment of the axes to the pubic symphysis and therefore differences between TPUS and urethrocystogram measures could be due to misalignment of these axes. With this perspective, it becomes clear that there are limitations inherent in measurements derived from both forms of biomedical imaging. TPUS appears to better represent the resting state and natural motions of the soft tissues of the urogenital system without the risks associated with more invasive procedures (i.e.

urethrocystography), and with the added benefit of instantaneous visual feedback allowing for real time image adjustment.

Following Schaer et al.'s [66] work, in 2001 Peschers et al [60] undertook a reliability study using similar methods. Absolute displacement of the bladder neck was measured in 20 nulliparous women on two occasions by two different examiners. Imaging was performed during cough and Valsalva tasks at standardized IAPs. The between-session measures differed by 1±2mm and 1±3mm during coughing and Valsalva, respectively, and measures showed excellent inter-rater reliability (ICC_{Cough}=0.956; $ICC_{Valsalva}$=0.99). While the statistical analysis in this study was the most robust analysis of these variables presented at this time, the methodological limitations regarding axis alignment were still present.

Measures of urogenital kinematics from TPUS have been found to be concurrently valid with respect to x-ray [66], [88] and also MRI and EMG [50], [57], [72], [90], and appear to have sufficiently adequate inter- [35], [39], [91] and intra-rater [19], [37], [39] reliability to be used in both research and clinical settings. TPUS may be an ideal tool to provide insight into important aspects of urogenital kinematics that may increase our understanding of SUI in women. Further work is needed in this area, as much of the research to date has not considered the problem of ultrasound probe rotation in the analysis of TPUS video.

2.3.3 The Problem of Ultrasound Probe Motion in Urogynecological Research

Gordon et al.'s [44] method, using the bony pubic symphysis as a reference point for the measurement of urogenital landmarks, has been used by several research groups and appears to have become the criterion standard in urogynecology research using TPUS [59]. This method has been used for dynamic image analysis [14] and in three-dimensional (volume) analysis [16]. Newly conceived TPUS measurements meant to better characterize SUI and other PFDs, are regularly being tested for validity and

reproducibility [13], [15], [68]. However, many of these measures are subject to error introduced by motion of the ultrasound probe with respect to the perineum if not considered during image analysis [14], [37], [45]. This problem has not been adequately addressed in the literature.

Reddy et al [37] were the first to consider the effects of probe motion relative to the patient and the potential error it introduces into kinematic analyses. Thirty women were imaged in standing position at rest, at peak Valsalva, at peak landmark excursion during coughing, and at peak PFM MVC. The pubic symphysis, often treated as a bony landmark in the literature, was used to track probe motion [92], with the assumption that its rigid nature makes its motion indicative of TPUS probe motion [14], [40]. The distance and angle of bladder neck displacement were measured with respect to the pubic symphysis. Errors in the measured distances and angles of bladder neck displacement specifically due to probe motion were found to be 28% and 18% during Valsalva, 33% and 22% during cough, and 28% and 87% during MVC, respectively. While these errors were notable, there were limitations to the methods chosen to track probe motion. Measurements were taken with respect to a Cartesian coordinate system centered at the posterocaudal margin of the pubic symphysis (Figure 2.14) however, the method of determining alignment of the coordinate system was not explicitly stated. In order to define the placement of a line (i.e. an axis) mathematically, two non-deforming reference points are required. However, Reddy et al [37] only defined a single point: the posterocaudal margin of the pubic symphysis. This methodology does not guarantee consistency between frames and so the measurements of error due to probe motion may be inaccurate.

In an effort to more accurately track probe motion, Peng et al [45] used more robust image processing techniques. Anatomical landmarks were identified in each frame using a semi-automated, reliable segmentation method [45], [71]. A global coordinate system (xoy) with origin at the bottom right corner of the frame and a local coordinate system (x'o'y') with origin at the posterocaudal margin of the pubic symphysis was established (Figure 2.15). By mathematically approximating the pubic symphysis as an

ellipse, its position and orientation could be calculated in the global coordinate system using least squares

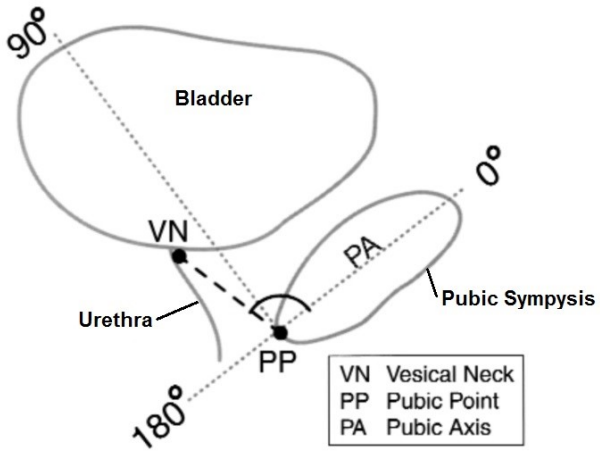

Figure 2.14 Measurement of bladder neck (vesical neck) with respect to the pubic symphysis according to the methods of Reddy et al [37]. Reproduced with permission.

estimation. In each frame, landmark positions were identified in the local coordinate systems (i.e. with respect to the pubic symphysis) and probe motion was tracked in the global coordinate system (i.e. displacement and rotation of the ellipse). Dimensions of the ellipse that approximated the pubic symphysis were averaged across all frames to account for the rigidity of the landmark. While there were strengths to this study, compensation for probe motion does not appear to have been conducted with respect to the true center of rotation. In-plane rotation of the ultrasound probe with respect the body during imaging may occur at the origin of the ultrasound generated by the TPUS probe (i.e. inside the

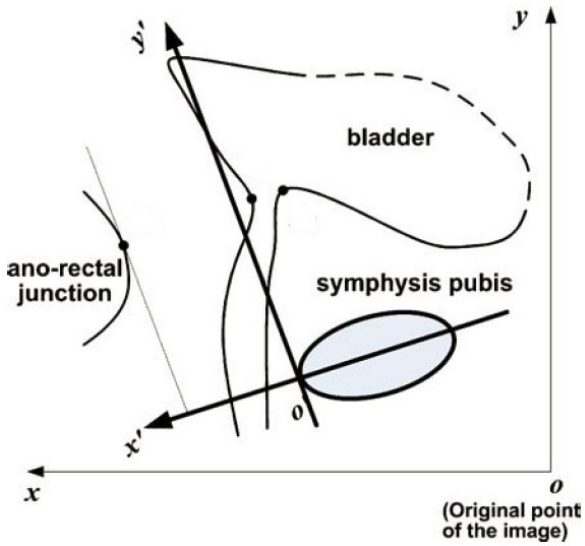

Figure 2.15 Cartesian coordinate system used by Peng et al [45] to track anatomical landmarks and compensate for probe motion.

ultrasound probe). If one wishes to model and compensate for this in-plane rotation, the true center of rotation must be investigated. As well, least squares estimation to calculate rotations and displacements without quantifying the quality of the fit introduces error into these measurements. Lastly, as noted previously, it is difficult to maintain the postero-caudal pubic symphysis and anorectal angle visible in the image during TPUS image acquisition and most often the entire pubic symphysis cannot be captured [91]. If the pubic symphysis is not completely visible, the accuracy of the algorithm is unknown.

Following this publication, Peng et al [14] continued with dynamic mapping of landmark trajectories by limiting in-plane probe rotation to ±5° using visual feedback from a Flock of Birds device during imaging, instead of attempting to compensate for this motion during image processing. This limited probe rotation was deemed acceptable by the researchers, but appears to have been an arbitrary limit set without any investigation into the actual mathematical effect of ±5° of in-plane probe rotation on landmark displacement measures from TPUS images. Translational probe motion was tracked using the postero-caudal margin of the pubic symphysis and measurements of anorectal angle displacement were taken with respect to the pubic symphysis. In addition to this, the authors applied a weighting factor, between

0.7 and 0.8, to the computed motion of the anorectal angle to compensate for soft tissue deformation, yet it is not clear how this weighting factor was derived. Although these studies presented a major improvement to previous methods used to study urogenital kinematics, this final iteration of the approach developed by Peng et al. [14] does not compensate for in-plane probe rotation. This, combined with the use of what appears to be an arbitrary weighting factor could add an unknown magnitude of error to the resulting trajectories.

Presently, there has been limited investigation into the effects of TPUS probe rotation and translation on measures of urogenital kinematics. Additionally, the time consuming and complex nature of dynamic, frame-by-frame TPUS analysis, a method providing large amounts of kinematic data, has likely limited its use [14], [45], [46]. In the decade since Peng et al.'s work [14] no other group has investigated the use of their algorithm and only one other conference abstract has reported an attempt to implement an alternative automated segmentation algorithm to measure urogenital kinematics [93]. There is a distinct gap in the literature regarding the effects of ultrasound probe rotation on TPUS measurements and in the use of software designed to allow larger amounts of dynamic TPUS video to be processed and presented. Innovations in methodology and software may reduce the time, effort, and specialized training needed for researchers to analyze and present kinematic data from TPUS and may enhance the clinical utility of this approach.

2.4 Summary

The PFMs, urethral support system, and the urethral sphincters are all integral to maintaining urinary continence in women. TPUS is a relatively new technology to be applied to the study of these structures. While there are many tools and methods available for obtaining data describing urogenital function, dynamic 2D TPUS non-invasively yields objective and reliable biomedical data. Additionally, TPUS acquired during MVC, cough, and Valsalva tasks is especially relevant to the female continence

mechanism. Unfortunately, processing dynamic TPUS is a time- and labor-intensive task and, until there has been sufficient research into the effects of in-plane TPUS probe rotation on measurements taken from ultrasound images, the time required to process or develop automated algorithms to allow for further interpretation is not justifiable.

Imaging healthy women has shown that PFM contractions should cause antero-cranial lift and then postero-caudal recovery of the pelvic organs; coughs will generate an initial reflexive antero-cranial lift, postero-caudal descent, and then antero-cranial recovery; and Valsalva maneuvers generate postero-caudal descent, and then antero-cranial recovery [45]. However, bladder volume, patient position, and other factors can influence these urogenital mechanics during dynamic imaging. In studies of coughing tasks, women with SUI demonstrate an absence of reflexive anterior lift, larger urethral displacements, and more convoluted paths of urethral displacement than their healthy, continent counterparts. Unfortunately, small sample sizes and complex and labor-intensive data processing have limited applicability of this approach in urogynecological research, leaving a large gap in the literature.

There has been extremely limited research into urogenital kinematics in women with and without SUI. Additionally, the only landmarks whose dynamic behaviors have been investigated are the anorectal angle and bladder neck. The literature has yet to include research into the dynamic behavior of other measurements and landmarks (e.g. the entire urethra, levator plate, etc.). Before this can be done, the effects of probe rotation on measurements taken from dynamic TPUS must be understood such that measurement error can be minimized. The use of urogenital kinematic analyses based on TPUS video will not gain popularity until the speed and efficiency of analysis has been improved. The aim of this thesis is to begin to address these issues. The first study, Chapter 3, presents the development and proof of concept for a semi-automated software to compensate for in-plane TPUS probe motion which automatically generates kinematic curves for key urogenital landmarks. Chapter 4 then presents a mathematical derivation detailing the impacts of in-plane probe rotation on measurements of landmark

motion made from TPUS. The contributions of these two studies are summarized in Chapter 5, which also highlights the next steps for this work. The work presented in this thesis is essential to move us toward our long-term goal of developing a clinically meaningful tool for the automated analysis of urogenital kinematics for use in research and clinical applications in urogynecology.

3 Refined Analysis of Sagittal Plane Transperineal Ultrasound to Calculate Urogenital Kinematics with Improved Accuracy

3.1 Abstract

Midsagittal plane, transperineal ultrasound (TPUS) allows for objective quantification of urogenital mechanics. Unfortunately, data processing methods currently in practice omit large amounts of information available in TPUS video regarding dynamic motion of the urogenital structures. This work details the development of UROKIN, a semi-automated software able to calculate kinematic curves representative of urogenital landmark motion. A proof of concept analysis, performed using UROKIN on TPUS video recorded from 20 women with and 10 women without stress urinary incontinence (SUI), is presented. TPUS data were collected during three trials of a maximum voluntary contraction of the pelvic floor muscles in all women. The anorectal angle and bladder neck were tracked while the motion of the pubic symphysis was used to compensate for the error incurred by TPUS probe motion during imaging. Kinematic curves of landmark motion were generated for each trial and curves were smoothed, time normalized, and averaged within groups. Kinematic data yielded by the UROKIN software showed statistically significant differences between women with and without SUI in terms of magnitude and timing characteristics of the kinematic curves depicting landmark motion. The results presented here provide insight into differences in pelvic floor muscle contraction mechanics between women with and without SUI. The UROKIN software offers improvements on methods described in the literature and provides unique capacity to further our understanding of urogenital biomechanics.

3.2 Introduction

Stress urinary incontinence (SUI), the leakage of urine with increased intra-abdominal pressure (IAP), can occur during everyday tasks such as coughing, sneezing, and laughing [3]. Approximately half of all women suffer from some form of urinary incontinence, half of which report symptoms of SUI [3]–[5].

SUI has been linked to high cumulative costs to health care systems around the world [8], [94], [95] and negatively impacts morbidity, mortality, quality of life, and psychosocial function [6], [9]. As the average age of the population increases, SUI prevalence is predicted to rise [10], yet this condition remains poorly understood and poorly managed.

During tasks involving physical exertion, there is a natural increase in IAP; the diaphragm descends and the abdominal muscles contract, causing a postero-caudal compression of the abdominal organs. These forces compress the bladder against the pelvic floor muscles (PFMs) and connective tissues [36], [46], [47], thereby increasing bladder pressure. In women with SUI, the bladder pressure can exceed the force holding the urethra closed, at which point urine leakage occurs. Biomechanically, SUI likely occurs due to concurrent failures in urethral sphincter function [11], [17], [22] , urethral support [15], [16], [22], and PFM mechanics [11], [14], [45], but the exact combination and interaction of these phenomena is not well understood. Currently diagnosis is made primarily through the report of symptoms [96] and no distinction is made regarding the underlying pathomechanics.

In order to investigate the pathomechanics associated with SUI and other pelvic floor disorders it is necessary to objectively quantify urogenital mechanics. Two-dimensional, dynamic, sagittal plane transperineal ultrasound (TPUS) is often used for this purpose, as it allows for objective, non-invasive measurement of the morphology of various urogenital landmarks at rest and provides adequate time and spatial resolution to study landmark motion during dynamic tasks (e.g. coughing, Valsalva maneuver). Using TPUS, the kinematics of the anorectal angle [14], [46], [71], urethra [15], [16], and bladder neck [14], [46] have been quantified and have been associated with PFM activity [35], [45], [57], urethral mobility [15], [16], and bladder support [45], [61], [97], respectively. Further, analysis of TPUS video clips captured during coughing tasks recently demonstrated differences in the kinematic curves of various urogenital landmarks between women with and without SUI [14], [45], [46]. Unfortunately, landmark motion detected from TPUS video is vulnerable to error caused by probe motion with respect to the

imaging surface (i.e. the perineum) and the underlying structures, particularly because there is only one rigid, non-deforming landmark. Out-of-plane probe motion (e.g. slight changes to the angle of incidence of the ultrasound probe) cause landmarks to disappear and reappear, making this motion easy to detect and avoid [86]. However, in-plane probe motion is more difficult to identify and can cause wide margins of error [37]. In-plane probe motion is often corrected during measurements by creating a local coordinate system in each TPUS image centered at the postero-caudal margin of the pubic symphysis [14], [16], [37], [66] which is, as noted above, the only rigid, non-deforming landmark. In order for this approach to be accurate, it requires consistent manual alignment of the coordinate system, and the validity of this methodology is unknown.

To improve on this methodology, Peng et al [45] incorporated automated segmentation of urogenital landmarks on TPUS video. In their methods, the pubic symphysis was mathematically modelled as an ellipse and a coordinate system was subsequently constructed, based on the orientation of the modeled pubic symphysis. The motion of various urogenital landmarks was calculated with respect to this coordinate system. In a subsequent publication, Peng et al [14] limited in-plane probe rotation during image acquisition to ±5°, assuming that error incurred by this minimal rotation would be negligible. In fact, the effects of in-plane ultrasound probe rotation during image acquisition on measures of urogenital kinematics have, to our knowledge, not been investigated in the literature. While the methods of Peng et al [14], [45] provide marked improvements over manual orientation of the coordinate system [37], [59], [98], there are still many issues that need to be addressed. First is the difficulty of maintaining the complete mid-sagittal profile of the pubic symphysis in the frame during image acquisition. In particular, women with elongated pelvic floors, such as those with pelvic organ prolapse and those with obesity, create a distinct challenge. With the inherent limitations on the view angles of the curvilinear ultrasound transducers that are often used for this type of imaging, it is sometimes impossible to keep even a small margin of the pubic symphysis visible in the imaging frame while also visualizing the other relevant landmarks needed for measurement, such as the anorectal angle. The result is that only a small portion of

the pubic symphysis is visible on all frames acquired throughout the task. The impact of using only a small margin of the pubic symphysis on automated segmentation of TPUS images is currently unknown. Further, the error associated with such an automated segmentation algorithm when applied to TPUS images is unknown and no approach has been presented to mitigate this potential error. Lastly, the impact of probe rotation on measurement error in the context of studying urogenital kinematics is not known.

To better understand the biomechanical factors associated with SUI, valid and reliable measurements are required. TPUS is a potential solution, having demonstrated high levels of reliability in measuring peak excursion of urogenital landmarks [44], [58], [66]. However, for researchers to draw meaningful conclusions about urogenital pathomechanics, the computation of full urogenital kinematic curves is necessary and these curves must be valid and reliable. The purpose of this study was to develop a semi-automated software, UROKIN, to compensate for in-plane probe motion during TPUS imaging in order to provide a valid means of quantifying urogenital kinematics in the sagittal plane using 2D ultrasound imaging. Here, we present the UROKIN software that has been designed for this purpose, and the results of an analysis performed on TPUS video collected from 20 women with SUI and 10 healthy controls to demonstrate the potential utility of the software.

3.3 Methods

3.3.1 Software Development

All computational methods were implemented using MATLAB 2015b (Mathworks, Natick, MA, USA). The user first loads a dynamic 2D TPUS video into UROKIN. Using the UROKIN interface, the user scans through the frames of the TPUS video and selects a frame in which the posterior margin of the pubic symphysis is easily visible to set as the reference frame. In the reference frame, the user traces the visible portion of the posterior margin of the pubic symphysis (Figure 3.1). This profile of the pubic symphysis is then duplicated across all frames of the video and maximally aligned with the posterior

margin of the pubic symphysis, as seen by the user, using the translation and rotation tools incorporated into the UROKIN interface.

Once the pubic symphysis has been identified in all frames, UROKIN automatically generates a coordinate system in each frame using the most postero-caudal point on the profile of the pubic symphysis (Figure 3.2). This coordinate system in the reference frame is defined as the global coordinate system (GCS), while the coordinate systems in all other frames are each termed local coordinate systems (LCSs). At this point, UROKIN automatically constructs a transformation matrix for each frame using the unit vectors of GCS (I,J,K) and of each frame's LCS (i,j,k), as in Equation (3.1), where (p,q) represents the x and y distances between the origins of the GCS and LCS. Using the transformation matrix, any point in a given frame can be converted from the LCS to the GCS according to Equation (3.2), where (x',y') represents the position of a given point in the LCS, (x,y) represents the position of the same point in the GCS, and TR refers to the transformation matrix.

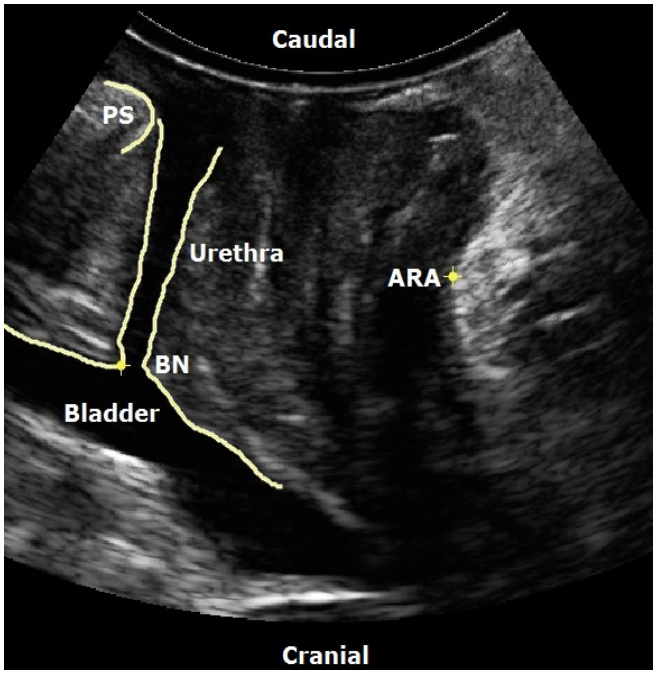

Figure 3.1 Identification of the pubic symphysis (PS), anorectal angle (ARA), bladder neck (BN), and urethra on a sagittal plane transperineal ultrasound image.

$$TR = \begin{bmatrix} i \cdot I & i \cdot J & p \\ j \cdot I & j \cdot J & q \\ 0 & 0 & 1 \end{bmatrix} \tag{3.1}$$

$$\begin{bmatrix} x \\ y \\ 1 \end{bmatrix} = \begin{bmatrix} i \cdot I & i \cdot J & p \\ j \cdot I & j \cdot J & q \\ 0 & 0 & 1 \end{bmatrix} \begin{bmatrix} x' \\ y' \\ 1 \end{bmatrix} \tag{3.2}$$

$$GCS = TR \quad LCS$$

At this point, the user can trace or mark all relevant landmarks in the TPUS video (e.g anorectal angle, bladder neck, urethra) using the UROKIN interface. It should be noted here that the anorectal angle was treated only as a point landmark, not as an angular measure. As such, the linear kinematics of the anorectal angle were tracked and not the angular kinematics. UROKIN then converts all landmarks to the GCS, thereby eliminating any error incurred by in-plane probe motion. Linear and angular displacements, velocities, and accelerations are automatically calculated in the GCS and all trajectories are automatically smoothed using a low pass, effective fourth order, zero phase Butterworth filter (dual pass, zero phase, 2nd order effective 4th order) with the cut-off frequency equal to the image acquisition rate of the TPUS machine. The smoothing is performed in order to eliminate noise introduced into the kinematic curves by the manual landmark identification process.

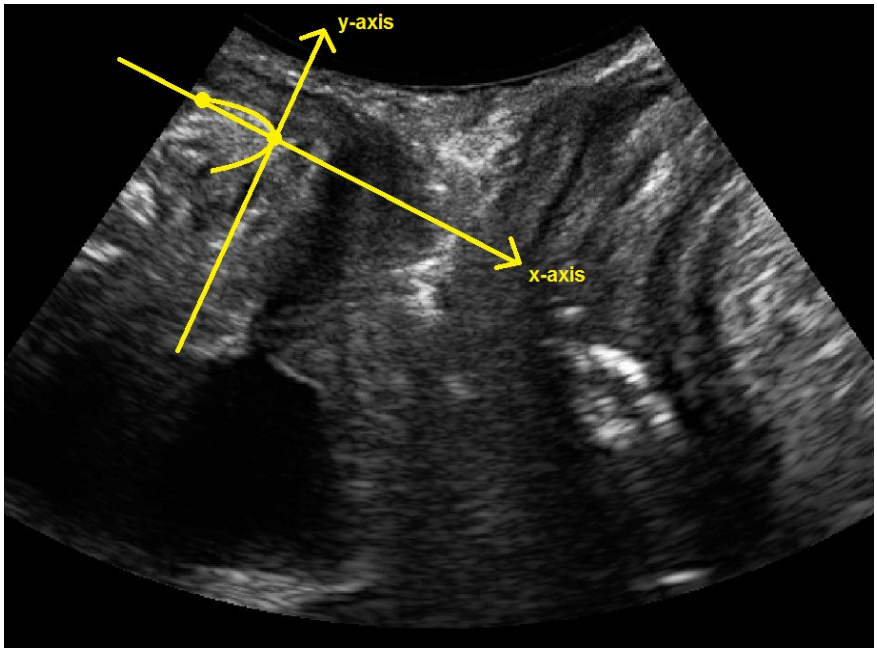

Figure 3.2 UROKIN's automatic generation of a coordinate system constructed using a user-identified profile of the posterior margin of the pubic symphysis. The x-axis intercepts the end and midpoint of the profile while the y-axis runs perpendicular to the x-axis and intercepts the midpoint of the profile.

The linear and angular displacements of all variables are calculated according to Equation (3.3) for the case of the linear displacement of the anorectal angle from time (1) to time (i) (Figure 3.3). In this scenario, the anorectal angle displacement at time (i) is represented by $ARA_{disp}(i)$, while the anorectal angle's position at times (1) and (i) are represented by vectors v(1) and v(i), respectively. Velocities and accelerations are taken as the first and second time derivatives of the displacement, respectively.

$$ARA_{disp}(i) = v(i) - v(1) \tag{3.3}$$

While the kinematics of all point variables (e.g. anorectal angle and bladder neck) are presented for the purposes of this chapter, UROKIN also calculates the kinematics of other variables describing urogenital kinematics and morphology, including: the length of the levator plate, the distance from the postero-caudal pubic symphysis to the anorectal angle; the displacement of the anterior and posterior margins of the urethra running from the levator plate to the bladder neck; the displacement of six equidistant points on the urethral midline, based on the urethral mobility profile of Shek and Dietz [16]; the distance between the bladder neck and the pubic symphysis; and the perpendicular distance between the levator plate line and the bladder neck. The kinematic data generated by UROKIN are exported into an Excel sheet or can be saved and merged with other participant data for the purposes of batch analysis. Additionally, UROKIN is able to automatically write a new video file with the relevant landmarks permanently saved in each frame for later reference.

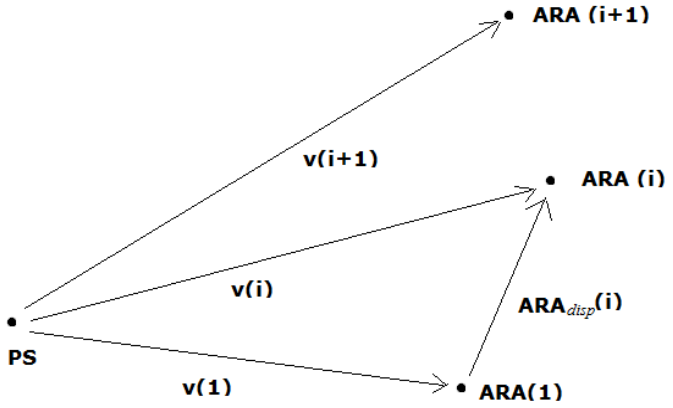

Figure 3.3 Calculation of landmark displacement for the anorectal angle (ARA) with respect to the midpoint on the posterior trace of the pubic symphysis, i.e. the origin of the global coordinate system(GCS), at time (i). The X-Y positions of the ARA in the GCS are represented at times (1), (i), and (i+1) by ARA(1), ARA(i), and ARA(i+1), respectively. The vectors v(1), v(i), and v(i+1) represent the position of the ARA in the GCS at times (1), (i), and (i+1). $ARA_{disp}(i)$ is then the displacement of the ARA at time (i).

3.3.2 Experimental Protocol

To test the software, a secondary analysis of data from an ongoing study was performed. The study was approved by the University of Ottawa Health Science and Sciences and the Queen's University Health Sciences and Affiliated Teaching Hospitals' Research Ethics Boards. Women over the age of 18 who presented to a local obstetrician/gynecologist reporting symptoms of SUI, and who were on a waiting list for mid-urethral sling surgery were recruited through local hospitals in Kingston and Ottawa, Canada. Healthy women over the age of 18 years and with no history of urogenital signs or symptoms were recruited from the local community to serve as a control group. The criteria for exclusion from both groups were: fecal incontinence, pregnancy or within the first post-partum year, pelvic organ prolapse greater than ICS POP-Q stage II [70], any posterior compartment prolapse, the use of medications known to increase or relieve incontinence, known neurological or connective tissue disorders, and known or suspected detrusor muscle instability. Symptomatic participants completed a 3-day bladder diary [99] to assess the frequency, amount and circumstances surrounding incidents of urine leakage over three consecutive days representative of normal activities, and filled out the ICIQ-FLUTS questionnaire to assess self-reported lower urinary tract symptoms [96].

Volunteers who met the screening criteria underwent a clinical exam administered by a registered physical therapist. Participants underwent a standardized 30-minute pad test to confirm the presence and severity or absence of urinary incontinence, whereby an increase in pad weight of >2g over the duration of the test was deemed to indicate urine leakage [22]. Women then undressed from the waist down, covered their lower body with a sheet and positioned themselves in a supine position on an examination table. A digital palpation exam followed, which included sensory and reflex testing to rule out undiagnosed neurological impairment involving the perineum, and palpation to rule out evidence of any pelvic mass. PFM strength and function were scored using the Modified Oxford Scale and PERFECT scheme, respectively [100]. Next, ultrasound images were acquired transperineally using a GE Voluson-i ultrasound system (GE Healthcare Austria GmbH & Co OG, Zipf, Austria) in 2D real-time B-mode using

a curvilinear probe (RAB 4-8 MHz). The probe was covered with ultrasound gel, a condom was stretched over it, and more gel was placed on top. Imaging was performed after bladder emptying and with participants in the supine position, with their hips slightly abducted and flexed approximately 30°, their knees flexed approximately 30°, and their feet resting flat on the examination table. The transducer was placed transperineally with the main transducer axis oriented in the mid-sagittal plane and the acquisition angle set to its maximum of 85°. As a part of a larger protocol, the physical therapist captured dynamic TPUS video of three repetitions of a MVC of the PFMs. MVCs were conducted with verbal encouragement by the physiotherapist while observing visual feedback from the TPUS in real time. Participants were encouraged to continue to increase the level of contraction until the physiotherapist no longer observed motion of the anorectal angle or urethra on the ultrasound image for a period of at least one second, at which time the participant was instructed to relax. MVCs were followed by a minimum of 90s rest before the next repetition or task. Visual feedback from the TPUS machine was monitored by the physiotherapist during imaging to ensure the presence of the antero-cranial motion associate with MVC of the PFMs.

3.3.3 Data Analysis

Two novice users, with no specific background in urogynecology or image processing, were trained to use the UROKIN software. User 1 processed 57 TPUS videos capturing 10 SUI and 9 control participants performing three trials each of a PFM MVC task. User 2 processed a group of 60 TPUS videos capturing the same 10 SUI patients as previously processed, along with 10 more SUI patients, each acquired while participants performed the three trials of the PFM MVC task. The users processed the videos as outlined in Section 3.3.1. The data containing the linear and angular kinematic curves of all possible variables were retained for bulk analysis, performed using Matlab.

The initial phase of the data analysis involved time normalization so that data could be averaged across trials and participants. As there was no precedent for time normalizing urogenital kinematic curves

obtained from MVC data captured using TPUS, the time normalization process was modelled after the data alignment protocol used on urogenital kinematic curves obtained during coughing by Constantinou's group [14], [46]. In these studies [14], [46], the linear kinematic motion of each landmark was decomposed into the (x) and (y) Cartesian coordinates, representing the anterior-posterior and the cranial-caudal motion of a given landmark, respectively. Constantinou's group initially aligned all variables using the peak caudal displacement for each trial and participant [46]; however, in subsequent studies, they began aligning all graphs based on the maximum caudal displacement of the anorectal angle [14]. As a PFM MVC involves a cranial lift of the PFMs, rather than the caudal displacement seen during a coughing task [45], we could not directly apply this approach. Additionally, our data were collected as a part of an ongoing study such that the file duration of the TPUS video capture had not been optimized for this purpose – specifically we did not capture the relaxation phase after the contraction. As such, we chose to time normalize based on the length of the levator plate line, which is thought to characterize the contraction of the PFMs in the sagittal plane [42], [64], [72]. All tasks were time normalized from rest (t1), determined by taking the maximal levator plate length measured during the first half of the video clip, up to 90% of the minimal levator plate length (t2) achieved throughout the MVC task. The 90% peak was selected to omit the higher levels of variability observed in the position of soft tissue landmarks at the point of maximal levator plate shortening due to directional changes in landmark motion occurring as the levator plate nears its point of maximal shortening and, subsequently, the PFMs relax.

Root mean square error (RMSE), was used to quantify the between-rater variability for each variable calculated, as in Equation 3.4, where R1(i) represents an average measure across three trials for patient number (i) as calculated by data from the first rater, R2 represents an average measure across three trials patient (i) as calculated by data from the second rater, and n is the total number of patients. Pooled standard deviations (SD), was then used to quantify the biological variability across all patients for each variable calculated, as in Equation 3.5, where $SD_{R1}(i)$ represents the SD across three trials for patient number (i) as calculated by data from the first rater, $SD_{R2}(i)$ represents the SD across three trials for

patient number (i) as calculated by data from the second rater, and n is the total number of patients. Using these calculations, RMSE and pooled SD were found across all relevant variables for the data from the 10 women with SUI that were processed by both users to quantify the between-rater variability and biological variability, respectively. Comparing these values between users, we determined that the inter-user reliability was acceptable as compared to the biological variability, which allowed us to pool the data from the ten participants with SUI processed by User 1 and the ten participants with SUI processed by User 2. This yielded data from a total of 20 women with SUI and 9 women without SUI who served as control participants.

$$RMSE = \sqrt{\frac{\sum_{i=1}^{i=n}(R1(i) - R2(i))^2}{n}} \tag{3.4}$$

$$Pooled\ SD = \frac{\sum_{i=1}^{i=n}\sqrt{\frac{(SD_{R1}(i)^2 - SD_{R2}(i)^2)}{2}}}{n} \tag{3.5}$$

Time-normalized curves for the relevant variables were averaged across the three trials for each participant and the kinematic peaks and their timing were extracted. Peaks and peak-timings were then averaged across each group and standard error values were calculated. The time-normalized curves generated for each participant were averaged across each group (SUI and control). Standard error bands were calculated along the length of the curves. Peaks and their timing were tested for normality using the Shapiro-Wilk parametric hypothesis test of composite normality. The magnitude and timing of kinematic peaks recorded from the SUI and control group data were compared using a Student's t-test, in the case of data showing parametric distributions, and using a Wilcoxon rank sum test, in the case of data showing non-parametric distributions ($\alpha = 0.05$). All variables were tested for correlation with PFM strength, measured with the Modified Oxford Scale using Spearman's rho ($\alpha = 0.05$).

3.4 Results

Demographic and clinical assessment data are shown in Table 3.1. There were no significant differences between women with and without SUI in terms of age or body mass index (BMI), however women with SUI had significantly higher parity than those without SUI ($p<0.01$). The control group demonstrated greater PFM strength on the Modified Oxford Scale ($p<0.0001$) and higher overall PFM function score using the PERFECT scheme ($p<0.001$).

	Control (N=9)	**SUI (N=20)**
Age (years)	38.0 ± 3.4	46.8 ± 2.4
BMI (kg/m^2)	22.5 ± 0.9	26.1 ± 1.2
Parity	0.8 ± 0.4*	2.5 ± 0.3*
ICIQ – FLUTS	NA	22.8 ± 1.8
PFM Strength (0-5)	4.4 ± 0.1*	3.0 ± 0.1*
PFM Function (0-35)	18.6 ± 1.0*	13.7 ± 0.7*

Table 3.1 Results of the demographic and clinical assessment are displayed showing averages and standard errors for age, body mass index (BMI), pelvic floor muscle (PFM) strength (Modified Oxford Scale), ICIQ - FLUTS scores [96], and PFM function (PERFECT scheme) [100]. Significant differences ($p<0.05$) are indicated by *.

For the ten participants with SUI whose data were processed by both software users, a comparison of between-user variability, characterized by RMSE, and biological variability characterized by pooled standard deviation (SD), is shown for each relevant kinematic variable in Table 3.2. On average, the variability between users was less than 18% of the biological variability seen across participants.

Landmark	**Variable**	**Direction**	**RMSE (mm)**	**Pooled SD (mm)**
ARA	**Displacement (mm)**	**Anterior-Posterior**	0.34	2.38
		Cranial-Caudal	0.84	2.16
	Acceleration (mm/s^2)	**Anterior-Posterior**	5.88	32.13
		Cranial-Caudal	8.09	35.84
BN	**Displacement (mm)**	**Anterior-Posterior**	0.07	1.17
		Cranial-Caudal	0.09	0.93
	Acceleration(mm/s^2)	**Anterior-Posterior**	2.41	20.26
		Cranial-Caudal	2.47	11.92

Table 3.2 Comparison of between-rater variability and biological variability between patients, represented by root mean square error (RMSE) and pooled standard deviation (SD), respectively, for the anorectal angle (ARA) and bladder neck (BN) anterior-posterior and cranial-caudal displacements and accelerations from 0% to 90% of the peak of a maximum voluntary contraction (MVC). The three trials each for 10 participants were used to generate mean kinematic curves for each landmark. Ultrasound videos were processed once each by User 1 and User 2.

Figure 3.4 and Figure 3.5 show a comparison of the kinematic curves resulting from User 1 and User 2 tracking the anorectal angle and bladder neck in the same sample of ten women with SUI. The average between-rater difference in displacements over time was 0.85 ± 0.34 mm and 0.11 ± 0.030 mm for the anorectal angle and bladder neck, respectively. The average between-rater difference in peak acceleration over time was 3.8 ± 9.4 mm/s^2 and 2.4 ± 2.6 mm/s^2 for the anorectal angle and bladder neck, respectively.

Kinematic curves, averaged across three trials, for an MVC task performed by a single participant with no history of SUI are shown decomposed into the anterior-posterior and cranial-caudal displacements and accelerations of the anorectal angle, showing the identification of the peak of each respective motion, in Figure 3.6. The kinematic peaks and the timing of the peak anorectal angle and bladder neck motion, averaged across the SUI group and the healthy control group, are shown in Table 3.3. The anterior and cranial peaks were determined as shown in Figure 3.6. No significant differences were found between groups in the posterior or caudal kinematic peaks or timings. The control group demonstrated significantly higher peak anterior displacement of the anorectal angle ($p<0.01$) and significantly later timing of the peak cranial displacement of the anorectal angle ($p<0.01$). Peak cranial displacement of the bladder neck was also found to be significantly higher in the healthy control group ($p<0.05$). Peak anterior displacement ($\rho=0.65$, $p<0.001$), timing of the peak cranial displacement ($\rho=0.48$, $p<0.01$), peak anterior acceleration ($\rho=0.39$, $p<0.05$) of the anorectal angle all correlated moderately and positively with PFM strength. Bladder neck kinematics did not correlate with PFM strength.

The anorectal angle and bladder neck kinematics computed over the MVC task are shown in Figure 3.7 and Figure 3.8. Visual inspection of these figures suggests that the control group, as a whole, appears to demonstrate higher anterior displacement of the anorectal angle during the task. The control group also appears to demonstrate a cranial displacement of the anorectal angle that lasts significantly longer than that of the SUI group. When the peak cranial displacement of the anorectal angle occurs in the control group, the anorectal angle is already descending in the SUI group. As well, the anterior-posterior and

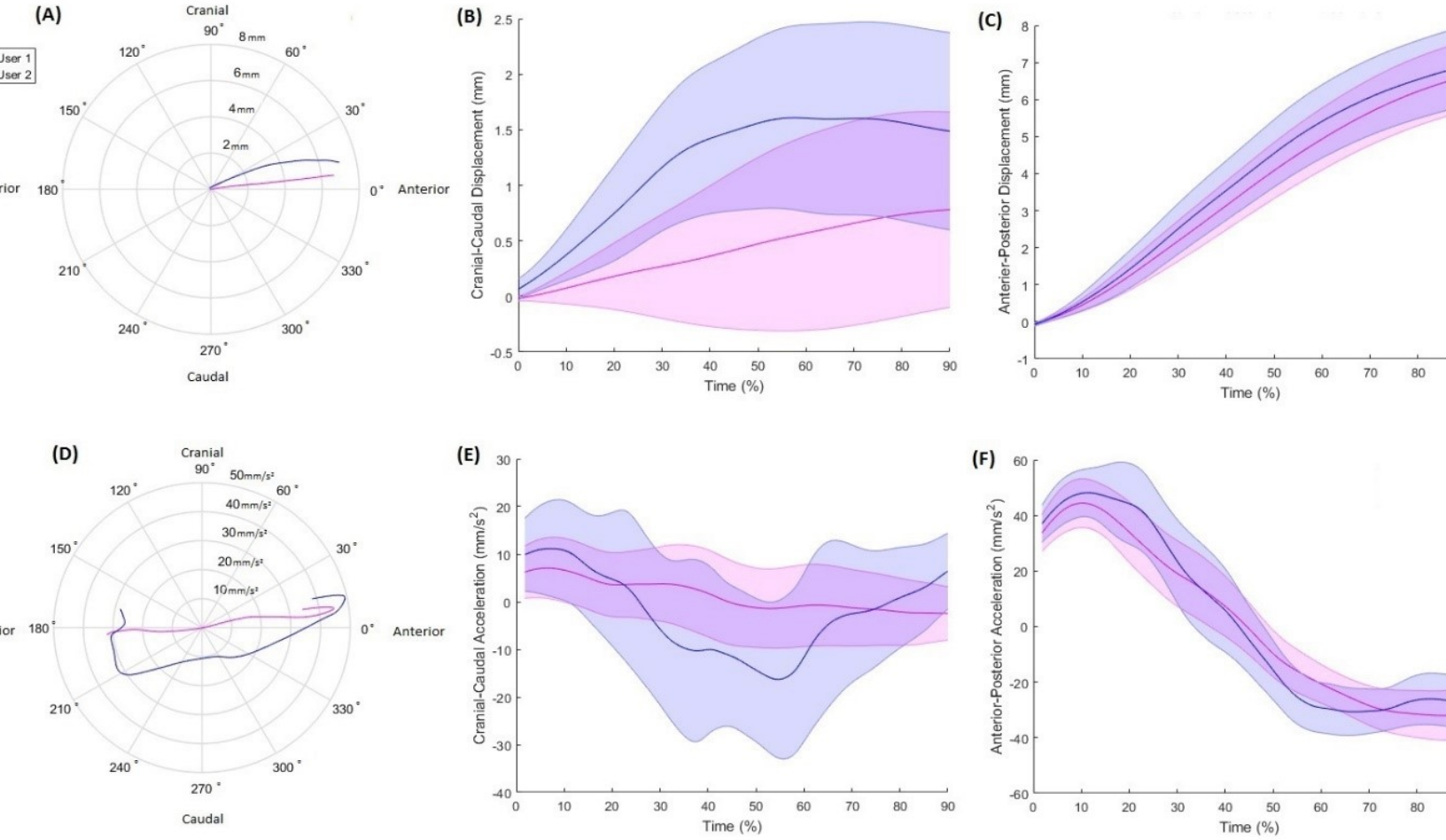

e 3.4 Preliminary between-rater comparison of the UROKIN software output tracking anorectal angle kinematics in ten women with SUI while they performed maximum
tary contractions of their pelvic floor muscles. Data are shown from the beginning of the task to 90% of the peak shortening of the levator plate. All videos were proces
o different users, indicated by purple (User 1) and blue (User 2) output. Polar plots show the average displacements (A) and accelerations (B), across the sample for the
ctal angle. Cranial-caudal displacements (B) and accelerations (E) and the anterior-posterior displacements (C) and accelerations (F) are also presented as mean curves w
ard error bands for the data as processed by each user.

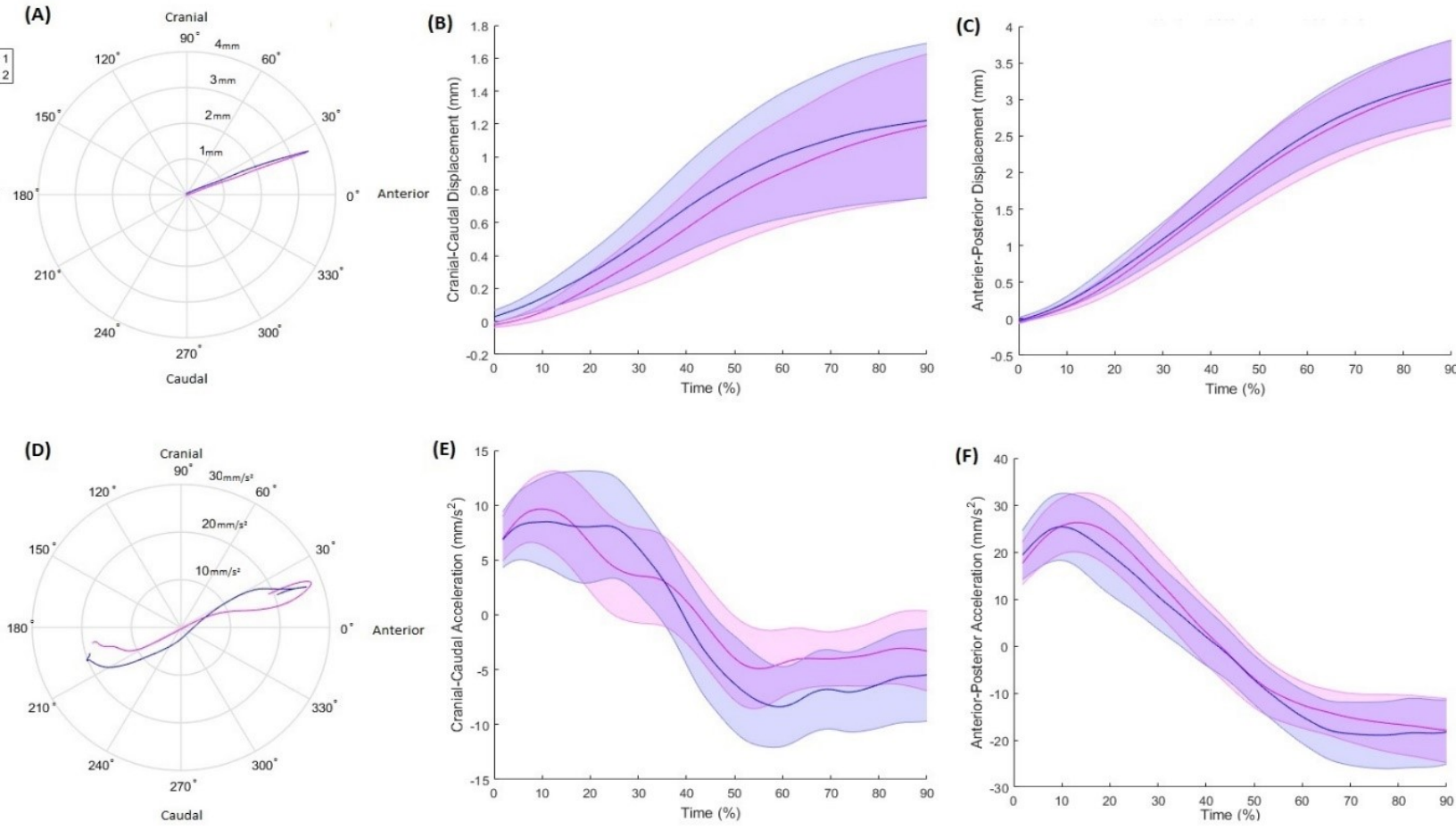

.5 Preliminary between-rater comparison of the UROKIN software output tracking bladder neck kinematics in ten women with SUI while they performed maximum y contractions of their pelvic floor muscles. Data are shown from the beginning of the task to 90% of the peak shortening of the levator plate. All videos were processe different users, indicated by purple (User 1) and blue (User 2) output. Polar plots show the average displacements (A) and accelerations (B), across the sample for the neck. Cranial-caudal displacements (B) and accelerations (E) and the anterior-posterior displacements (C) and accelerations (F) are also presented as mean curves with d error bands for the data as processed by each user.

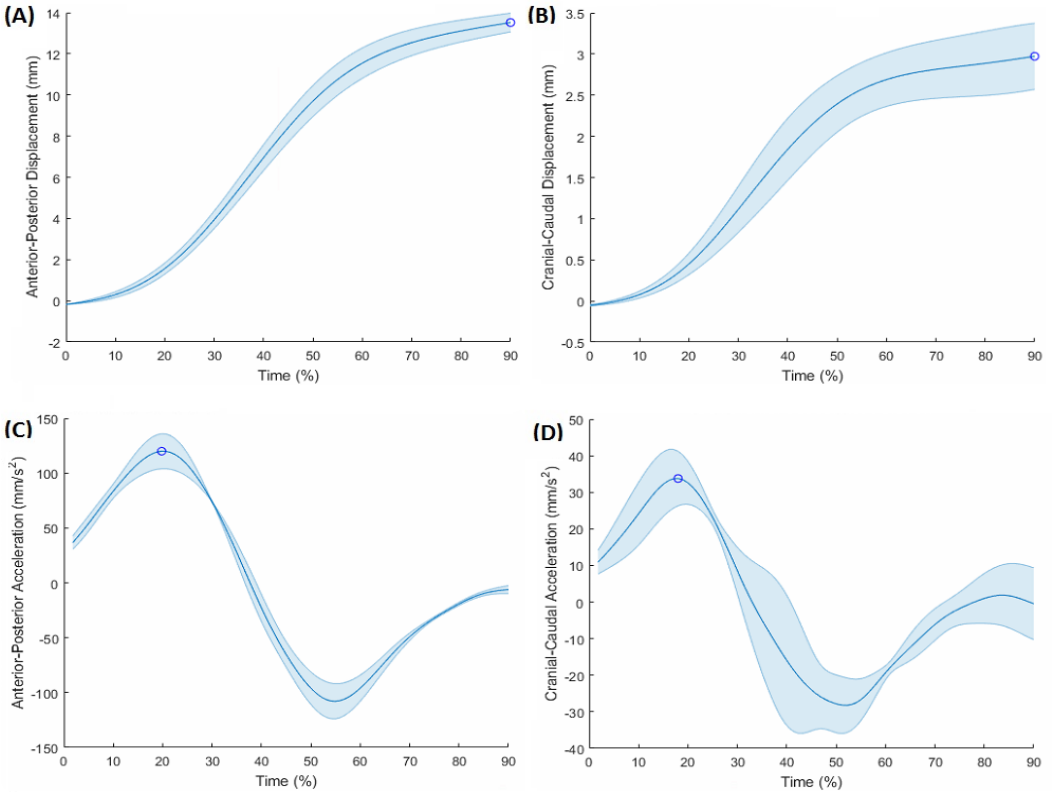

Figure 3.6 A sample of the decomposed kinematic data derived from the motion of the anorectal angle in a healthy female participant performing a maximum voluntary contraction (MVC). Anterior-posterior displacement (A) and acceleration (C) and cranial-caudal displacement (B) and acceleration (D) are shown from 0 to 90% of the peak of levator plate shortening.

		Variable		Control (N=9)	SUI (N=20)	Spearman's Rho
ARA	Displacement	Anterior-Posterior	Peak (mm)	12.0 ± 0.9*	7.6 ± 0.7*	0.65 $^{\Psi}$
			Timing (%)	90.0 ± 0.0	90.0 ± 0.0	NA
		Cranial-Caudal	Peak (mm)	2.5 ±0.5	2.2 ± 0.4	0.30
			Timing (%)	77.0 ± 8.7*	55.8 ± 7.1*	0.48$^{\Psi}$
	Acceleration	Anterior-Posterior	Peak (mm/s^2)	96.0 ± 20.0	57.8 ± 6.4	0.39 $^{\Psi}$
			Timing (%)	17.6 ± 3.0	18.1 ± 2.1	0.09
		Cranial-Caudal	Peak (mm/s^2)	30.6 ± 8.5	29.9 ± 5.3	0.19
			Timing (%)	23.1 ± 4.8	31.4 ± 6.1	-0.04
BN	Displacement	Anterior-Posterior	Peak (mm)	5.0 ± 0.7	4.0 ± 0.5	0.30
			Timing (%)	90.0 ± 0.0	88.8 ± 1.1	-0.08
		Cranial-Caudal	Peak (mm)	2.4 ± 0.6*	1.4 ± 0.3*	0.27
			Timing (%)	78.5 ± 9.9	75.3 ± 5.2	0.03
	Acceleration	Anterior-Posterior	Peak (mm/s^2)	45.1 ± 9.5	32.2 ± 4.6	0.17
			Timing (%)	21.3 ± 4.4	14.1 ± 2.1	0.32
		Cranial-Caudal	Peak (mm/s^2)	21.8 ± 4.6	13.5 ± 2.3	0.14
			Timing (%)	20.2 ± 4.3	17.0 ± 3.7	0.17

Table 3.3 Peak and timing of the anorectal angle (ARA) and bladder neck (BN) displacements and accelerations in the anterior-posterior and cranial-caudal directions during a maximum voluntary pelvic floor muscle contraction performed by women with and without (control) stress urinary incontinence (SUI). Kinematic data are presented from 0% to 90% of the maximum shortening of the levator plate. Spearman's rho measures the correlation between the given variable and the manually assessed pelvic floor muscle (PFM) strength across all participants. Significant group differences are indicated by * and significant correlations with PFM strength are indicated by $^{\Psi}$.

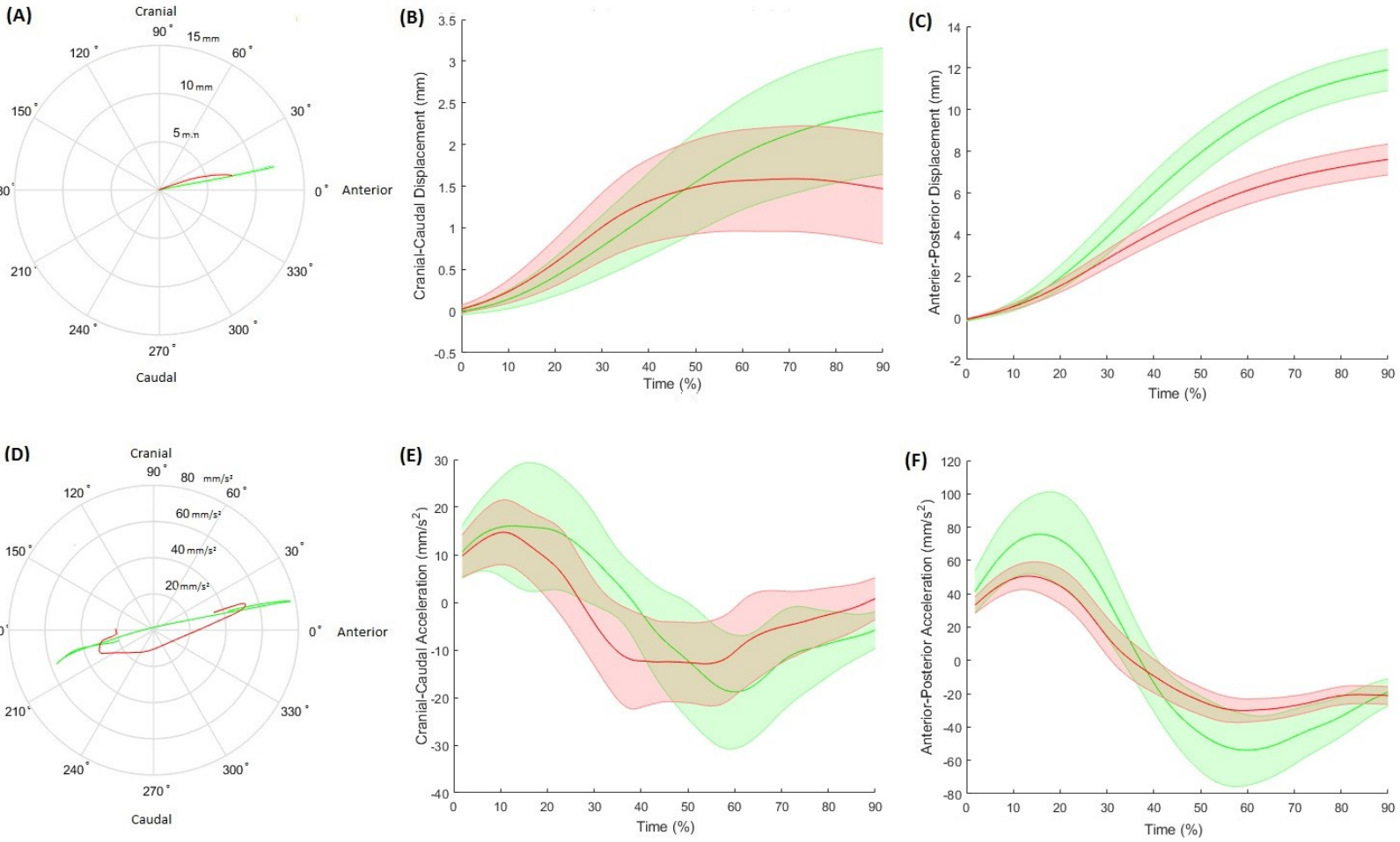

Preliminary analysis by the UROKIN software comparing anorectal angle kinematics in 20 SUI patients (red) and 10 healthy control participants (green), during voluntary contractions of the pelvic floor muscles from 0% to 90% of the peak of the contraction. Polar plots compare the average displacements (A) and ns (B) of the anorectal angle in the sagittal plane. Cranial-caudal displacements (B) and accelerations (E) and the anterior-posterior displacements (C) and ns (F) show the decomposed kinematics of the bladder neck. Shaded bars show standard error.

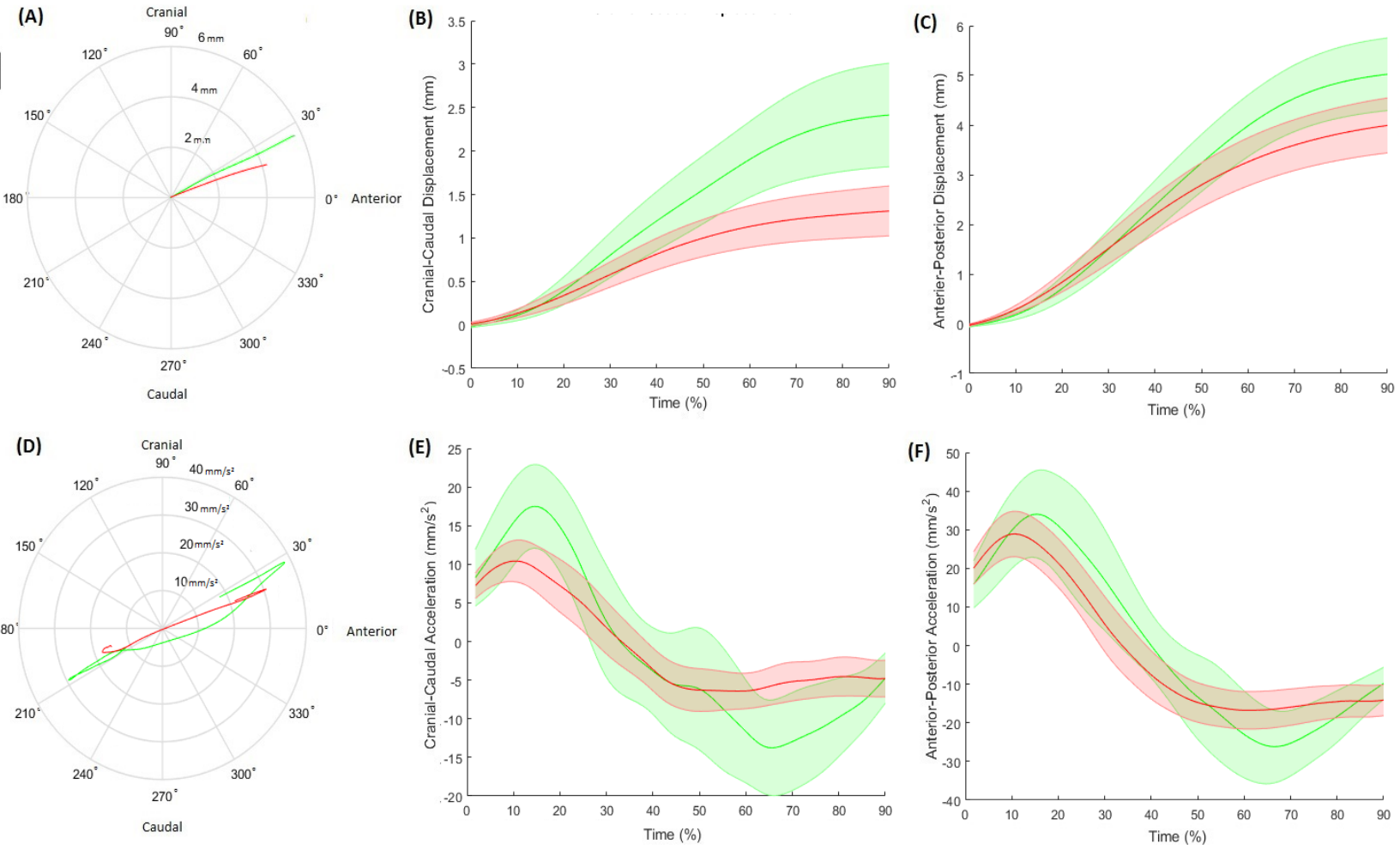

3 Preliminary analysis by the UROKIN software comparing bladder neck kinematics in 20 SUI patients (red) and 10 healthy control participants (green), during maximum contractions of the pelvic floor muscles from 0% to 90% of the peak of the contraction. Polar plots compare the average displacements (A) and accelerations (B) of the eck in 2D. Cranial-caudal displacements (B) and accelerations (E) and the anterior-posterior displacements (C) and accelerations (F) show the decomposed kinematics of er neck. Shaded bars show standard error.

cranial-caudal accelerations of the anorectal angle appear to be slightly out of phase in the SUI group when compared to the control group. The control group appear to also exhibit higher cranial displacement of the bladder neck and out of phase acceleration profiles when compared to the SUI group.

3.5 Discussion

The UROKIN software allows users to investigate urogenital morphology and kinematics in the sagittal plane while improving upon the limitations of previous works and providing robust kinematic data that are necessary to answer complex questions about urogenital biomechanics. UROKIN is capable of generating data that can be used to detect significant differences in urogenital kinematics among different patient populations. This software allows for time normalization of kinematic curves across trials and patients, such that phase and amplitude characteristics of the curves may be investigated. The preliminary analysis presented here suggests that outcomes generated by the software have the capacity to discriminate between women with and without SUI when they perform PFM MVCs. Although only data for PFM contractions are presented here, UROKIN may be useful in evaluating urogenital kinematics during a wide range of tasks including coughing, Valsalva maneuvers and more. The results of this study provide support for continued research using UROKIN.

The inter-rater variability outcomes from the UROKIN software, when used to analyze an MVC task performed by women with SUI, and when characterized by RMSE, was less than 18% of the biological variability, characterized by the pooled SD. The high between-user agreement in outcomes resulted in variability far less that reported in the only other algorithm to calculate dynamic profiles of urogenital mechanics during coughing [14], [45], [71]. Based on Peschers et al [40], we calculated the minimum detectable change (MDC) in bladder neck decent during coughing (MDC=1.8mm) and Valsalva (MDC=2.5mm) tasks in nulliparous, continent women. While our data represent bladder neck and anorectal angle displacements observed during a different task (ie. MVC), the between-user RMSE for

both of these landmarks fell well below the MDC values calculated from Peschers et al [40]. Though this is not a thorough reliability analysis, for the purposes of this work the between-rater reliability was deemed satisfactory, allowing us to pool data analyzed by two different users to increase our sample size of women with SUI to n = 20. An essential next step with the software is to complete a comprehensive between- and within-user reliability analysis on outcomes generated by the UROKIN software.

Displacements of urogenital landmarks, measured using TPUS, have been used to provide insight into PFM function in men and women [50], [64], [101] and have contributed to our understanding of the PFMs as a structural support mechanism, primarily limiting urethral displacement, and thereby enabling the force transmission necessary for complete urethral closure [21], [36], [46], [47], [58], [85]. Relative to women with SUI, our control group demonstrated larger anterior displacement and longer duration of rise in cranial displacement in the anorectal angle during the contraction, and higher cranial displacement of the bladder neck. The differences in peak amplitudes of anterior anorectal angle displacement and cranial bladder neck displacement between women with and without SUI were larger than the between-rater variability and the biological variability for the respective variable (i.e. RMSE and pooled SD, respectively) in both cases. Further, these findings were consistent with the significantly higher PFM strength in the control group relative to the women with SUI, measured by manual assessment. These results may reflect that the PFMs of the women in the control group may have more capacity to alter the bladder neck trajectory in the absence of increased IAP, potentially facilitating the greater urethral and bladder stability exhibited by the control group. The significant differences in urogenital biomechanics exhibited by the women with SUI confirm suggestions throughout the literature that women with SUI have lower PFM strength and/or altered PFM control in comparison with healthy controls [14], [46], [49], [79], [102]. In contrast, however, while aspects of anorectal angle kinematics correlated significantly with PFM strength, there was no correlation between bladder meck motion and PFM strength. This is likely because connective tissue also plays a large role in stabilizating the bladder and urethra. The only studies of sagittal plane urogenital kinematics, to date, have shown that women with SUI experience

posterior descent of the anorectal angle during the first half of a coughing task whereas healthy controls demonstrate an anterior displacement [14], [45], [46], [71]. The findings of these studies suggest that women with SUI may have difficulty overcoming the downward forces caused by the increased IAP generated during coughing [46]. Reduced PFM strength or altered PFM control may be implicated. During a cough, concurrent contraction (descent) of the diaphragm and abdominal muscles causes an increase in IAP that is not present during a PFM MVC. Regardless, our results are complementary to those reported by Constantinou's group [14], [45], [46], [71]. In the SUI group, the PFMs appear to be unable to achieve and maintain the cranial displacement throughout the first 90% of the MVC, as evidenced by the significantly earlier timing in peak cranial displacement of the anorectal angle with respect to the control group. From approximately 70% to 90% of the MVC, the women with SUI appear to be still actively contracting their PFMs (i.e. shortening the levator plate), yet while the anorectal angle continues to displace anteriorly, it has also begun to descend caudally, which is not the case in the control group. Additionally, women with SUI exhibited significantly less cranial displacement in the bladder neck with respect to the controls. Taken together, these results suggest that the capacity to generate and maintain a cranial displacement of the pelvic structures during PFM contraction may be an important feature in the pathomechanics of SUI.

While the kinematic curves presented here are only artifacts, not an exact measure, of the PFM MVC, the differences in urogenital mechanics observed between the SUI and control groups may indicate differences in strength, neuromuscular control, and/or morphology between groups. Although palpation is not the ideal means of evaluating PFM force generating capacity [12], [98], women with SUI exhibited weaker PFMs than the women in the control group. Additionally, PFM strength was moderately correlated with the magnitude of the anterior displacement and acceleration of the anorectal angle, as well as the timing of the peak cranial displacement of the anorectal angle. The literature has suggested that some women with SUI demonstrate differences in motor control compared to women without SUI. Specifically, they appear to co-contract their abdominal muscles during PFM MVCs [58], [82], [101],

which would raise the IAP and could consequently limit the cranial displacement of the anorectal angle and bladder neck. It is important to remember that differences in the motion of the anorectal angle and bladder neck during PFM contraction may be equally influenced by connective tissue morphology. For example, levator avulsion or connective tissue infiltrates may limit the extent of the anterior displacement of the anorectal angle during PFM contraction.

Although definitions vary, the PFMs consist of the levator ani and the coccygeus muscles [48]. The levator ani, in turn, consist of three muscular components, the paired puborectalis and pubococcygeus muscles, whose contraction result primarily in anterior motion of the urogenital structures, and the iliococcygeus muscles, whose contraction result primarily in a cranial displacement of the urogenital structures. Weakness or damage to the puborectalis and/or pubococcygeus muscles, seen in approximately 15% of parous urogynecological patients [103], could explain the significantly lower anterior displacement of the anorectal angle exhibited among women with SUI in this study. Damage to the iliococcygeus muscle is less likely to occur due to childbirth [104], [105], and more likely occurs due to repetitive or sustained straining loads, such as would occur in women with obesity, chronic cough, or those who routinely perform high impact exercise activities. Therefore, the group differences in the timing and magnitude of the cranial displacement of the anorectal angle and bladder neck, respectively, are not likely attributable to parity, but potentially may be attributable to neuromuscular or connective tissue damage sustained both during pregnancy and throughout the lifespan. Further investigation is needed to understand the differences in urogenital kinematics demonstrated between women with and without SUI, and among different subgroups of risk factors. With the UROKIN software now developed, such investigations are possible.

As with any research, there are some limitations to this methodology. Inter- and intra-user reliability of the UROKIN software must be formally established using intra-class correlation coefficients and Bland-Altman analysis before the clinical and research utility of the software is known. Such analyses are

beyond the scope of the present chapter but are necessary prior to establishing UROKIN as a clinical or research tool. Additionally, although the UROKIN software corrects for in-plane probe rotation using a co-ordinate system established based on the location and orientation of the pubic symphysis before the start of any motion, the rotation actually occurs about a point inside the TPUS probe rather than the pubic symphysis (Chapter 4). This modification will be incorporated into future versions of the UROKIN software. As well, there is currently some concern with aligning coordinate systems in which calculations are made to anatomically relevant and consistent coordinate systems across TPUS videos. This is a common problem and we are currently working to further improve our methods.

The inherent limitations on time and spatial resolution of 2D dynamic ultrasound also cannot be ignored. Further, shadows cast across a TPUS image drastically reduce the user's ability to identify urogenital landmarks. While we saw high levels of preliminary inter-rater reliability, the users reported difficulty with visual identification of landmarks in many cases. The use of low-pass filtering to smooth kinematic curves is able to mitigate minor between-frame variability in landmark identification and positioning, however it is not a complete solution. Three-dimensional TPUS video would provide a more comprehensive visualization and vastly increase the amount of data available to ensure correct identification of soft tissue landmarks. Unfortunately, limitations on both time and spatial resolution are even more severe for 3D TPUS imaging. Newer systems would likely yield more reliable results due to improved image quality and the UROKIN software can easily be modified to perform analysis of 3D urogenital kinematics.

The user-input required to generate outcomes using the UROKIN software makes it very time- and labor-intensive in its current form. Beyond the improvements required in centering and orienting coordinate systems, future work will focus on determining the minimum sampling rate required to generate kinematic curves of urogenital landmarks, in order to optimize efficiency and avoid aliasing. Our current data set will be useful for this purpose; however, we must also analyze images acquired during cough

tasks, which likely result in higher frequency components in the kinematic data than those produced during a PFM MVC and Valsalva tasks. An obvious future step is also to incorporate methods for automated landmark detection, which is essential if the UROKIN software is to be clinically useful. Lastly, it is important to remember that SUI is a multifactorial disorder that requires data from many different sources to provide a complete explanation of the associated pathomechanics. Results from data processed using the UROKIN software are unlikely to be useful in isolation and should be interpreted in the context of other evaluations including intravaginal dynamometry, urethral sphincter pressure generating capacity, as well as subjective and objective measures of incontinence severity.

The UROKIN software provides us with the capacity to gain significant insight into PFM mechanics and continence system mechanics more broadly, as well as insight into other conditions such as pelvic organ prolapse, conditions such as urinary retention, chronic constipation and dyspareunia, associated with an overactive pelvic floor [106], and even postural control [107]. Research has shown that underlying morphological or pathomechanical factors may be relevant in the selection of successful interventions for women with SUI. SUI patients exhibiting strong PFMs and urethral hypermobility are less likely to benefit from PFM training [28], [108]. Additionally, women with smaller urethral cross-sectional areas are less likely to see improvement with mid-urethral sling insertion [29] and would perhaps be more likely benefit from PFM training or the use of urethral bulking agents [30]. A better understanding of urogenital kinematics throughout dynamic tasks may provide insight needed to better direct course of treatment in certain cases.

Regardless of current limitations, the UROKIN software allows for complete analysis of 2D urogenital kinematics and can identify significant differences between healthy women and women with SUI. Further, the UROKIN outcomes are logical in the context of published clinical findings. The UROKIN software yields improved functionality for more complex analysis than has been used to date to aid in our understanding of urogenital biomechanics. If UROKIN is deemed to have acceptable reliability, we plan

to make it available as an open source software to provide a consistent tool for researchers to use to analyze dynamic, sagittal plane TPUS images.

4 In-plane probe rotation during transperineal ultrasound: How much is too much?

4.1 Abstract

Transperineal ultrasound (TPUS) allows for dynamic measurement of urogenital kinematics and morphology, which are essential to our understanding of continence mechanics. However, ultrasound probe rotation during dynamic image acquisition may incorporate error into these measurements. The purpose of this work was to identify factors influencing the error incurred in measures of urogenital kinematics by in-plane TPUS probe rotation. TPUS probe motion was mathematically modelled and found to be dependent on: r, the radius of rotation; Θ, the in-plane angular rotation of the TPUS probe; and α, the angular deviation between the anatomical coordinate system and an arbitrary reference coordinate system in which error was calculated. In a group of 12 healthy women and 20 women with stress urinary incontinence, average measures of r ranged from 35 to 70 mm and average measures of α ranged from 320° to 350°, depending on the continence status, anatomy, and position of the participant during imaging, and on the task being performed. Moreover, in a single healthy female, Θ was found be up to 20° during imaging depending on the latter three factors. Variables r and Θ were found to be more influential on the magnitude of error than α. Researchers using measures of urogenital mechanics from TPUS should be aware of these sources of error and attempt to limit or compensate for them where possible.

4.2 Introduction

Transperineal ultrasound (TPUS) imaging is gaining popularity as a tool for quantifying female and male urogenital function and morphology [11], [22], [39], [42], [44], [57], [66], [68], [80], [88]. Using dynamic TPUS, measurements can be made from video acquired during tasks relevant to urogenital function, such as landmark motion generated by maximal pelvic floor muscle (PFM) contractions [39],

[50], [58], [72], [91], coughing [39], [60], [72], [88], and Valsalva manoeuvers [35], [39], [44], [50], [57], [60], [66], [88], [91]. These measurements, mainly involving anorectal angle, bladder neck, and urethral trajectories, can also be used to generate kinematic curves for the investigation of the pathomechanics associated with complex and multifactorial pelvic floor disorders [14], [45], [46], [65], [71], [109], [110]. However, dynamic image acquisition involves the use of an unrestricted TPUS probe, held against the perineum by a skilled technician to capture ultrasound video of an unrestrained patient while he or she performs a dynamic task. This approach provides many opportunities for motion of the patient with respect to the probe, or vice versa, which incorporates unknown error into the measurements taken from the resulting TPUS image frames.

The extent of anorectal angle, bladder neck, and urethral excursion measured in the sagittal plane during functional tasks may provide valuable information regarding PFM function and the integrity of the connective tissues. For example, the urethral mobility profile has been used to characterize changes in the extent of urethral excursion on Valsalva maneuver observed after childbirth [16], presumably as the result of acute soft tissue strain. Similarly, the extent of bladder neck descent during Valsalva maneuvers has been suggested as a measure to define pelvic floor integrity in women [16]. Changes in levator plate length and anorectal angle position during coughing have been correlated with urethral closure pressure [35], and have demonstrated differences in the urogenital mechanics of women with and without SUI [14], [46]. Yet, potential errors in these measurements incurred by in-plane probe rotation have not been adequately addressed in the literature.

One of the first reported uses of TPUS to evaluate urethral kinematics was by Gordon et al. [1] in 1989 who measured bladder neck descent during Valsalva maneuvers performed by women with urinary incontinence [44]. To combat the problem of a limited view angle combined with only a single rigid landmark in the image frame, the pubic symphysis, measurements of bladder neck position were taken with respect to the pubic symphysis at rest and at peak Valsalva effort to demonstrate the efficacy of

TPUS as a tool for evaluating urogenital function. In this analysis, the pubic symphysis, a secondary cartilaginous joint between the lateral pubic bones, was treated as a rigid body and became the origin of a coordinate system used for taking measurements of various urogenital landmarks. In 1995, this method was refined by Schaer [66]: a centerline was drawn longitudinally along the pubic symphysis to form an x-axis while a perpendicular line intercepting the postero-caudal margin of the pubic symphysis formed a y-axis (Figure 4.1). The authors reported that the use of a consistent coordinate system could minimize error caused by in-plane TPUS probe motion and would allow for valid comparisons across tasks and between patients. This method has been applied by several researchers in the two decades since its publication [35], [36], [39], [42], [66], [80], [111]. Unfortunately, there is inherent error in measurements made using this methodology. Because it is difficult if not impossible to capture the entire pubic symphysis in the image frame along with all other urogenital landmarks needed for evaluations, defining the locations of these longitudinal and vertical axes with respect to the pubic symphysis can be difficult. Variability in the shape and symmetry of the pubic symphysis, low image resolution, particularly during dynamic tasks, and human error in the manual identification of these points further complicate this process.

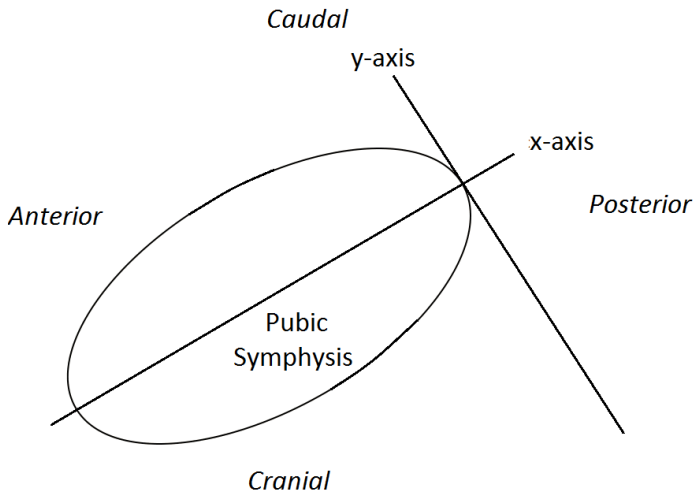

Figure 4.1: Graphical representation of Shaer et al's [66] methodology for standardizing the position and orientation of the pubic symphysis between image frames. The pubic symphysis is approximated by an ellipse with a longitudinal centerline drawn as the x-axis. The y-axis is drawn perpendicular to the x-axis and intersects the postero-caudal margin of the pubic symphysis. Orientation of the cranial, caudal, anterior, and posterior directions are shown in italics.

In 2001, Reddy et al [37] used Schaer et al's methodology [66] to investigate whether probe motion, during TPUS image acquisition, with respect to the patient had a significant effect on the calculated excursions of urogenital landmarks during dynamic tasks. From a sample of 10 primiparous, continent women and 10 women with incontinence, they estimated that probe motion with respect to the person caused 28%, 33%, and 37% error in the magnitude of bladder neck displacement during Valsalva, cough, and PFM contraction, respectively, when tasks were performed in standing. Even with the methodical approach employed by Reddy et al [37], the limitations of Schaer et al's work [66] still apply in this case. As well, these error values were never validated, leaving unknown levels of uncertainty in measurements taken using this method. The validation and optimization of measures of urogenital kinematics in the sagittal plane is essential if such data are to be used clinically or in research.

In 2007, Peng et al [14] used an electromagnetic tracking system to monitor probe motion during image acquisition while women performed coughing tasks in supine and in standing. Peng et al [14] stated that with the probe rotation limited to 5° in all planes, there was no need to track or compensate for error caused by probe rotation during image capture. However, there was no justification or explanation given for this claim. In subsequent studies, Peng et al [14] proceeded to omit any compensation for probe rotation and simply measured the positions of urogenital landmarks of interest (mainly the bladder neck, urethra, and anorectal angle) with respect to the postero-caudal margin of the pubic symphysis similarly to the approach outlined by Schaer [3].

Despite these seminal works, which have outlined and greatly improved methods for evaluating urogenital biomechanics, there has been limited methodical investigation into the effects of in-plane TPUS probe rotation on measures of urogenital kinematics. Thus, the purposes of this work are to (1) characterize the mathematical error induced in measurementss of urogenital kinematics taken from 2D TPUS videos captured during dynamic tasks, (2) investigate biological variability of parameters found to influence error (Experiment 1), and (3) demonstrate, through a single case study, how the magnitudes of

these parameters might impact the error in measures of urogenital kinematics in women (Experiment 2). This work provides a basis for understanding the extent of measurement error that results from in-plane probe rotation during TPUS image acquisition and processing, and will enable users to make more informed decisions regarding the processing of data from TPUS images and video.

4.3 Methods

4.3.1 2D Model of In-Plane Probe Rotation

In constructing a mathematical model to calculate the theoretical error incurred by in-plane probe rotation, the point about which the pelvis (i.e. the pubic symphysis) rotates during image acquisition must be defined. Theoretically, this center of rotation would exist at the origin of the ultrasound wave emission, though in reality waves are emitted along the entire surface of the probe. In the case of 2D imaging using a curvilinear probe, the situation is simplified and the center of rotation can be assumed to exist at some point along the main transducer axis inside the head of the ultrasound probe. Further, in a 2D TPUS image acquired using a curvilinear probe, this origin can be theoretically extrapolated by extending the edges of the ultrasound image until they converge (Figure 4.2). The scale that is provided in a standard ultrasound image can then be used to calculate the distance of various urogenital landmarks in a TPUS image frame relative to this center of rotation.

Knowing the theoretical point about which in-plane probe rotation occurs and using the postero-caudal margin of the pubic symphysis as a reference point, a 2D model of in-plane ultrasound probe rotation can be developed. The postero-caudal margin of the pubic symphysis and the center of rotation define the x-axis, while the y-axis runs perpendicular to the x-axis, intercepting the center of rotation to form the origin of this arbitrary reference coordinate system (Figure 4.3A). The pubic symphysis, the center of rotation, and an arbitrary urogenital landmark are sufficient to model in-plane probe rotation (Figure 4.3B).

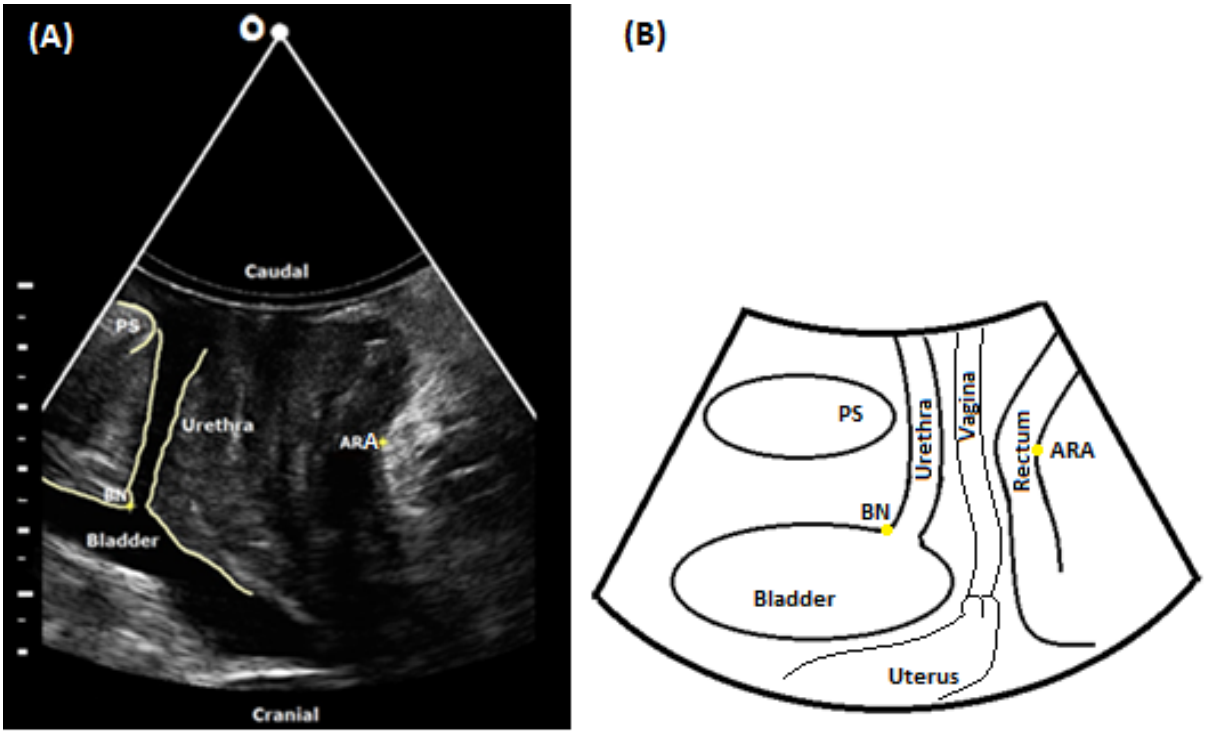

Figure 4.2: Manual extrapolation of the edges of a 2D mid-sagittal plan transperineal ultrasound image (A) to converge at the theoretical center of rotation (O) and (B) a schematic showing midsagittal anatomy of the female urogenital system. The pubic symphysis (PS), anorectal angle (ARA), and bladder neck (BN), urethra and bladder are shown on both images, while the vagina, rectum, and uterus are only identified on (B). Distance between ticks on scale is 5mm.

If Figure 4.3B represents the initial position of the pubic symphysis, P1, and an arbitrary landmark, L1, then their final position, after in-plane probe rotation of Θ degrees and unknown soft tissue deformation have occurred, can be defined as P2 and L2, respectively (Figure 4.4). This model assumes that the pubic symphysis rotates about a theoretical fixed center of rotation located inside the ultrasound probe at a fixed radius, r, from the origin of this arbitrary reference coordinate system to the postero-caudal margin of the pubic symphysis. Using this model, the displacement of the arbitrary landmark can be calculated, accounting for probe rotation: the pubic symphysis moves to position P2(rsinΘ,rcosΘ), while probe rotation and soft tissue deformation together cause the landmark to move to position L2(c,d)). Conversely, if probe rotation is assumed to be negligible, the pubic symphysis would then remain at P1(r,0) while the arbitrary landmark would move to position L2(c,d)).

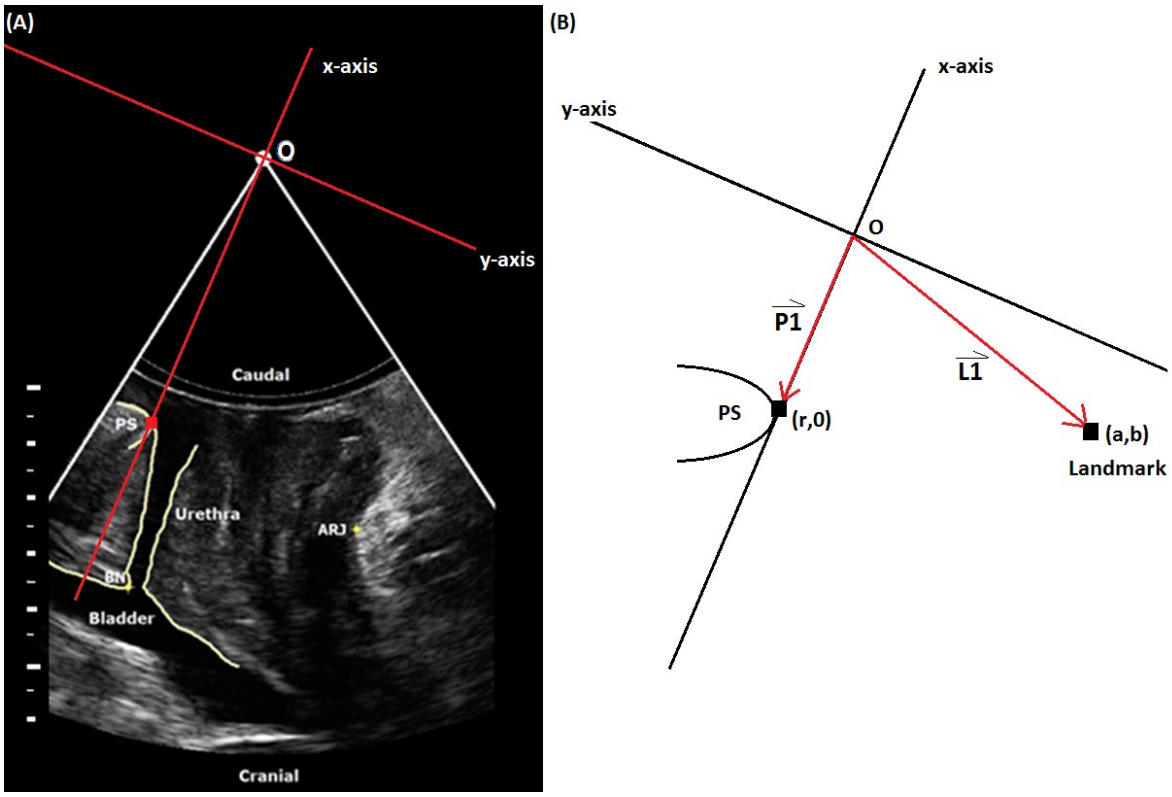

Figure 4.3: The coordinate system used to model in-plane probe rotation is established using the theoretical center of rotation (O) and the postero-caudal margin of the pubic symphysis (PS), indicated by the red square, to construct the x-axis, while the y-axis intercepts the center of rotation (A). In-plane probe rotation can be modelled using O and the postero-caudal margin of the PS, indicated by a black square, located at a distance, r, along the x-axis, to define a coordinate system (B). The motion of any arbitrary anatomical landmark, marked by a black square at position (a,b) can be tracked from one frame to the next. The position of the postero-caudal margin of the PS is represented by vector P1(r,0) and the position of the arbitrary landmark is indicated by vector L1(a,b).

Equation 4.1 shows the calculated error associated with in-plane probe rotation, where vectors represent the position of the soft tissue landmark with respect to the pubic symphysis, initially (P_{Li}), the end position neglecting probe rotation (P_{Lf}), and the end position while incorporating the effects of probe rotation (P_{Lfrot}). Vectors Δd_L and Δd_{Lrot} represent the displacement of the landmark from its initial to final position, neglecting and including in-plane probe rotation, respectively. The error between the landmark displacement calculated with and without including the effects of in-plane probe rotation is represented by E_X and E_Y in the x- and y-directions, respectively.

Measures of urogenital morphology and kinematics reported in the literature are often taken using a coordinate system aligned with the anatomical planes [16], [22], [37], [66]. In the derivation presented

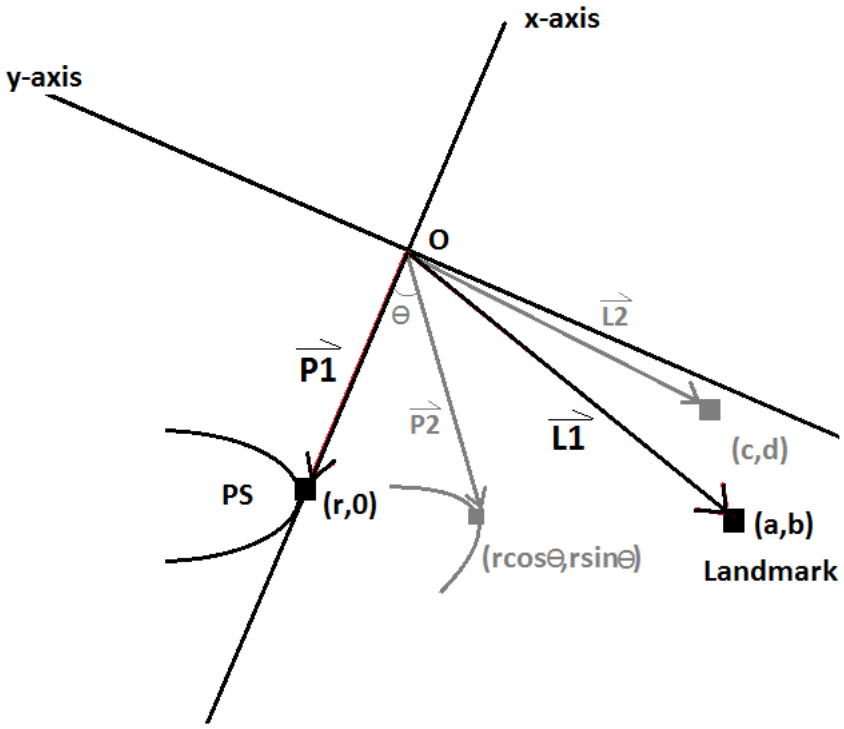

Figure 4.4: Initial positions of the pubic symphysis (PS) and a landmark of interest are shown in black, initially represented by the vectors P1(r,0) and L1(a,b), respectively. The final positions, after in-plane probe rotation about O, are shown in grey, and are represented by the vectors P2(rsinΘ,rcosΘ) and L2(c,d), respectively. This model assumes that the individual's pubic symphysis moves about the center of rotation (O), inside the ultrasound probe, at a fixed radius.

$$\overrightarrow{P_{Li}} = \overrightarrow{L1} - \overrightarrow{P1} = \begin{bmatrix} a-r \\ b \end{bmatrix}$$

$$\overrightarrow{P_{Lf}} = \overrightarrow{L2} - \overrightarrow{P1} = \begin{bmatrix} c-r \\ d \end{bmatrix}$$

$$\overrightarrow{P_{Lf_{rot}}} = \overrightarrow{L2} - \overrightarrow{P2} = \begin{bmatrix} c-r\cos\theta \\ d-r\sin\theta \end{bmatrix}$$

$$\overrightarrow{\Delta d_L} = \overrightarrow{P_{Lf}} - \overrightarrow{P_{Li}} = \begin{bmatrix} c-a \\ d-b \end{bmatrix}$$

$$\overrightarrow{\Delta d_{L_{rot}}} = \overrightarrow{P_{Lf_{rot}}} - \overrightarrow{P_{Li}} = \begin{bmatrix} c-a+r(1-\cos\theta) \\ d-b-r\sin\theta \end{bmatrix}$$

$$Error = \begin{bmatrix} E_X \\ E_Y \end{bmatrix} = \overrightarrow{\Delta d_{L_{rot}}} - \overrightarrow{\Delta d_L} = \begin{bmatrix} r(1-\cos\theta) \\ r\sin\theta \end{bmatrix} \quad (4.1)$$

here, however, there is an angular deviation (α) between the arbitrary reference coordinate system, in which theoretical error has been calculated, and a coordinate system of anatomical significance (Figure 4.5). By applying a 2D rotation of α degrees, the theoretical error incurred by in-plane probe rotation is converted to an anatomically significant coordinate system (4.2, 4.3), where (E_X, E_Y) represents the theoretical error in the original, arbitrary reference coordinate system and (E_{Xa},E_{Ya}) represents the theoretical error in the anatomical coordinate system. Alternatively, the effects of α and Θ can be expressed in terms of r and two functions in the x- and y-directions (K_x,K_y). From this model, it is apparent that the theoretical error due to in-plane probe rotation is a function of: r, the distance between

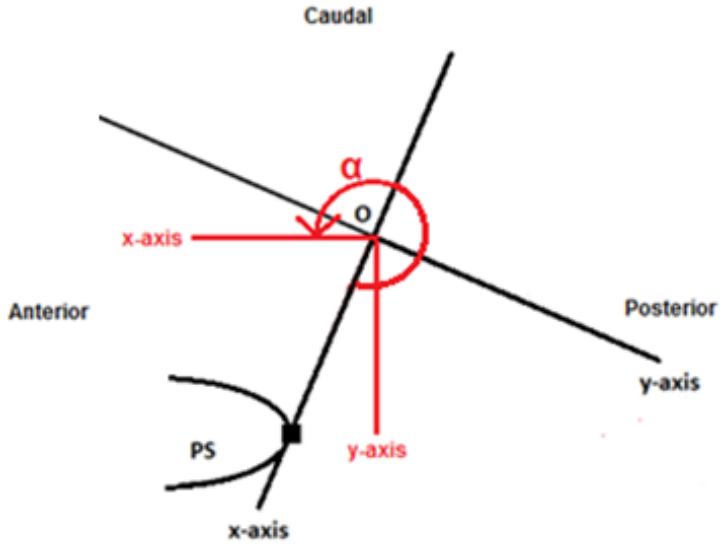

Figure 4.5: The angular deviation (α) between the coordinate system in which displacements of urogenital landmarks are measured (red) and the coordinate system in which error incurred by in-plane ultrasound probe rotation is calculated. Measures of urogenital kinematics are taken in a coordinate system aligned to the pubic symphysis (PS) with the positive ex-axis aligned to the anterior direction and the positive y-axis aligned to the cranial direction x-axis, such that the measures have anatomical meaning [42].

$$\begin{aligned}\begin{bmatrix} E_{Xa} \\ E_{Ya} \end{bmatrix} &= \begin{bmatrix} \cos\alpha & -\sin\alpha \\ \sin\alpha & \cos\alpha \end{bmatrix} \begin{bmatrix} E_X \\ E_Y \end{bmatrix} \\ &= \begin{bmatrix} \cos\alpha & -\sin\alpha \\ \sin\alpha & \cos\alpha \end{bmatrix} \begin{bmatrix} r(1-\cos\theta) \\ r\sin\theta \end{bmatrix} \\ &= \begin{bmatrix} r(1-\cos\theta)\cos\alpha - r\sin\theta\sin\alpha \\ r(1-\cos\theta)\sin\alpha + r\sin\theta\cos\alpha \end{bmatrix} \\ &= \begin{bmatrix} rK_{Xa}(\alpha,\theta) \\ rK_{Ya}(\alpha,\theta) \end{bmatrix}\end{aligned} \quad (4.2)$$

the theoretical center of rotation and the postero-caudal margin of the pubic symphysis, where coordinate systems for measuring urogenital kinematics are traditionally centered [14], [16], [37], [45], [66]; Θ, the magnitude of in-plane probe rotation; and α, the angular deviation between the arbitrary reference coordinate system and the anatomical coordinate system. Further, the absolute error (or magnitude of error) incurred due to probe rotation, E_{Ma}, can be expressed, as in Equation 4.3. The calculation of absolute error yields an expression which is greatly simplified from the directional expression of error and in which the only factors impacting error are r and Θ. It should be noted that, as our group and others often take measures only in terms of lengths, displacements, and other kinematic variables, there is no need to incorporate the translational deviation between the arbitrary reference and anatomical coordinate systems into this derivation. In order to perform a case analysis of error incurred by in-plane probe rotation, motion capture was conducted concurrently with TPUS imaging.

$$\begin{aligned} E_{m_a} &= \sqrt{(r(1-\cos\theta)\cos\alpha - r\sin\theta\sin\alpha)^2 + (r(1-\cos\theta)\sin\alpha + r\sin\theta\cos\alpha)^2} \\ &= \sqrt{r^2(1-\cos\theta)^2(\cos^2\alpha+\sin^2\alpha) + r^2\sin^2\theta(\cos^2\alpha+\sin^2\alpha)} \\ &= \sqrt{2r^2(1-\cos\theta)} \\ &= \sqrt{4r^2\sin^2(\frac{\theta}{2})} \\ &= 2r\sin(\frac{\theta}{2}) \end{aligned} \tag{4.3}$$

4.3.2 Experiment 1

TPUS image data from 20 women with stress urinary incontinence (SUI) and 12 women with no signs or symptoms of urogenital disorders were randomly selected from our database. These data had been acquired for the purposes of two ongoing studies which included the use of TPUS data for the purposes of developing strategies to measure urogenital kinematics. Approval was granted by the University of Ottawa Health Sciences and Science Research Ethics Board and the Queen's University Health Sciences

and Affiliated Teaching Hospitals' Research Ethics Board. All women provided written informed consent prior to participating. Women with SUI were recruited from surgical wait lists for mid-urethral sling surgery through local hospitals and physiotherapy clinics in Kingston and Ottawa, Canada. Women without any urogenital symptoms were recruited from the local Ottawa community using word-of-mouth and recruitment flyers. All women were over the age of 18. The exclusion criteria for both studies were current or recent pregnancy (within six months), symptoms of fecal incontinence, pelvic organ prolapse beyond stage II on the pelvic organ prolapse quantification scheme (POP-Q) [70], the use of medications known to increase or alleviate symptoms of incontinence, the presence of known neurological impairments, connective tissue disorders, or detrusor muscle instability.

A research physiotherapist trained in TPUS imaging and pelvic floor physiotherapy, and with six years of experience, conducted all clinical examinations and image acquisition. Participants underwent a clinical urogynecological exam, which included palpation and sensory and reflex testing to rule out the presence of pelvic masses and/or sensory alterations affecting the spinal segmental dermatomes from S2 to S4, then had their PFM strength assessed using the Modified Oxford Scale (MOS, [100]) and their PFM tone assessed using a seven point scale [98]. Patients were also trained by the physiotherapist on how to correctly perform PFM contraction, Valsalva maneuvers, and maximal effort coughs using intravaginal palpation and visual inspection of the perineum [78]. Additionally, symptomatic participants underwent a standardized pad test to confirm the presence of SUI and if the pad weight gain after the test was less than 2g, they were excluded from participating [22].

Ultrasound imaging was performed after women emptied their bladders. The physiotherapist prepared the ultrasound probe by covering it in ultrasound gel, placing a latex-free condom over the probe head, and then applying more gel over the condom. Ultrasound images were acquired using a GE Voluson-i ultrasound system (GE Healthcare Austria GmbH & Co OG, Zipf, Austria) in 2D real-time B-mode using a 3D curvilinear probe (8-4MHz). Women were initially in the supine position with their hips slightly

abducted and flexed approximately 30°, their knees flexed approximately 30°, and their feet resting flat. The transducer was placed transperineally with the main transducer axis oriented in the mid-sagittal plane and volume acquisition angle was set to its maximum of 85°. Before data acquisition began, the physiotherapist, again, verified that the participants could perform a correct PFM contraction, evidenced by an antero-cranial displacement of the anorectal angle, and a correct Valsalva maneuver, evidenced by an postero-caudal displacement of the anorectal angle, using instantaneous visual feedback from the TPUS. The physiotherapist then captured dynamic TPUS video of three repetitions each of a maximum voluntary contraction (MVC) of the PFMs, a maximum Valsalva manoeuver (MVM), and a maximal effort cough. The participants then moved to a standing position with a plinth raised in line with their posterior-superior iliac crest to minimize postural sway. The participant repeated three repetitions each of the MVM and cough tasks in standing while the physiotherapist captured TPUS video. All tasks were conducted with standardized verbal encouragement by the physiotherapist while also observing visual feedback from the TPUS screen. Women were encouraged to increase the intensity of the MVCs and MVMs until the physiotherapist observed no further change in landmark motion for at least for one second. All tasks were followed by a minimum of 60s rest between repetitions.

4.3.3 Experiment 2

During one 2D TPUS imaging session, a healthy female with no history of urogenital dysfunction, who was already participating in Experiment 1, consented to be instrumented with a motion capture device (3D Guidance trakSTAR, Ascension Technology Corporation, Milton, VT, USA) and to have the investigator (C.C.) present during data collection. After the physical exam, the investigator was invited into the assessment room to instrument the ultrasound probe and the participant with a 3D electromagnetic tracking system in order to track the 3D positions and orientations of the ultrasound probe and the participant. A single sensor was placed on the lateral face of the ultrasound probe so as not to interfere with the physiotherapists hand position during TPUS imaging. The local x-axis of the probe sensor was aligned with the main transducer axis, such that in-plane probe rotation during mid-sagittal

plane imaging would occur in the local xy-plane about its local z-axis. A second sensor was then placed on the female patient's left anterior-superior iliac spine (ASIS), identified by the investigator using manual palpation, in order to monitor the motion of her pelvis, and, as such, the motion of the pubic symphysis during imaging. The local z-axis of this sensor was aligned to the probe sensor's local z-axis. This alignment provided instantaneous feedback on the sensor positions in a global coordinate system (GCS). Three dimensional positions and yaw/pitch/roll angles of the sensors in the GCS were digitally sampled at 240Hz. With these sensors in place, the participant performed the protocol as described above (Section 4.3.2).

4.3.4 Data Processing

4.3.4.1 Motion Capture Data

Custom Matlab software (The MathWorks^{TM}, Natick, MA, USA) was used to process the motion capture data. All position and orientation data were first down-sampled to 30Hz. The yaw/pitch/roll angles were used to build the rotation matrix for each data point in order to transform from the global coordinate system (GCS) to the local coordinate system (LCS) of each sensor. These rotational matrices were then used to build a new rotational matrix that converted the pelvic LCS to the probe LCS as in Equation 4.4, where vector X_G represents a GCS vector, R_{pelvis} represents the rotational matrix that transforms from the GCS to the LCS of the pelvic sensor, vector $X_{Lpelvis}$ represents a vector LCS of the pelvic sensor, R_{probe} represents the rotational matrix that transforms from the GCS to the LCS of the probe sensor, vector X_{Lprobe} represents a vector in the LCS of the probe sensor, and R_{new} represents the rotational matrix that transforms the LCS of the pelvic sensor to the LCS of the probe sensor. In this way, the yaw/pitch/roll angles of the pelvis with respect to the probe could be calculated where the roll angle (i.e. Θ from 4.1), represents the in-plane angular displacement of the TPUS probe (Θ) during image acquisition.

$$\begin{aligned} \overrightarrow{X_G} R_{pelvis} &= \overrightarrow{X_{L\,pelvis}} \\ \overrightarrow{X_G} R_{probe} &= \overrightarrow{X_{L\,probe}} \\ \overrightarrow{X_{L\,pelvis}} R_{new} &= \overrightarrow{X_{L\,probe}} \\ R_{new} &= (R_{pelvis})^{-1} R_{probe} \end{aligned} \tag{4.4}$$

4.3.4.2 TPUS Data

TPUS video analysis was conducted offline using ImageJ (version 1.49; http://imagej.nih.gov) software. With the understanding that that the perineum is composed of soft tissue and that the pressure of the TPUS probe upon the perineum may vary during image acquisition, a maximal and minimal r value were measured for all TPUS videos. The TPUS video was visually scanned to identify the frame in which the postero-caudal margin of the pubic symphysis sat the most cranially, or furthest from the theoretical center of rotation, and then scanned again to identify the frame in which the pubic symphysis sat the most caudally, or closest to the theoretical center of rotation. In each frame, two lines were drawn along the edges of the ultrasound image to extrapolate the theoretical center of rotation as in Figure 4.2. The investigator then identified the postero-caudal margin of the pubic symphysis and measured the distance between this point and the center of rotation in each of the two frames to yield a maximal and minimal radius (i.e. r from Equation 4.1). Additionally, the coordinates of the theoretical center of rotation and the position of the postero-caudal margin of the pubic symphysis were used to calculate the angular deviation between the arbitrary reference coordinate system and the anatomically significant coordinate system (α) for the purposes of quantifying the error incurred by in-plane probe rotation in the x- and y-directions. The anatomically significant coordinate system was assumed to have a horizontal x-axis. This process was repeated for all tasks performed by all participants in supine and in standing.

All statistical analyses were conducted using Matlab 2015b (Mathworks, Natick, MA, USA). For the TPUS data collected from women with and without SUI (Experiment 1), measured values of r were

compared between groups and within groups between positions (i.e. standing vs. supine). Data were first tested for normality using the Shapiro-Wilk parametric hypothesis test of composite normality. Data showing parametric distributions were compared using a student's t-test, while data showing non-parametric distributions were compared using Wilcoxon rank sum test (alpha = 0.05). Between-group comparisons were conducted using unpaired t-tests, while within-group comparisons were conducted using paired t-tests. Group, position, and task difference for α were tested using a three-way ANOVA.

For the TPUS data acquired during the motion capture (Experiment 2), maximal excursion (i.e. displacements) of the anorectal angle and bladder neck were measured for each task. Net displacements from rest to maximum excursion were calculated as in [42], where the vector describing the change in levator plate length is recognized as a measure of the displacement of the anorectal angle. The peak value of Θ during each task, and the values of r_{max} and α at r_{max}, r_{min} and α at r_{min} were used to calculate peak values of error (in mm) in the x- and y-directions, as in Equation 4.3, for this specific case. In order to understand how error incurred due to in-plane probe rotation compared to the measured values for urogenital landmark displacement, error was expressed as a percentage of landmark displacement for each landmark.

4.4 Results

4.4.1 Experiment 1

Randomly selected TPUS data records included twelve healthy women with no history of urogenital signs or symptoms (age = 41±13 years; body mass index (BMI) = 22±3 kg/m^2; Parity = 1±1 child) and twenty women with SUI (age = 47±11 years; BMI = 26±5 kg/m^2; Parity = 3±1 child). Measurements of r and α are presented in Table 4.1. The groups demonstrated significant differences in terms of BMI ($p<0.05$) and parity ($p<0.001$). Between-group and between-position (i.e. standing vs. supine) effects were seen in the measures of r_{min} and r_{max} for many of the tasks. In many cases, women with SUI

exhibited higher measures of r than those without SUI ($p<0.05$, Table 4.1) and measures of r were higher in standing than in supine for both groups ($p<0.05$, Table 4.1).

Task	r_{min} (mm)		r_{max} (mm)	
	SUI	Control	SUI	Control
Cough Supine	$43 \pm 3^{*\Psi}$	$40 \pm 3^{*\Psi}$	$51 \pm 4^{\Psi}$	$47 \pm 5^{\Psi}$
Cough Standing	$55 \pm 6^{*\Psi}$	$48 \pm 5^{*\Psi}$	$60 \pm 6^{*\Psi}$	$53 \pm 6^{*\Psi}$
MVM Supine	$43 \pm 4^{\Psi}$	$41 \pm 5^{\Psi}$	$51 \pm 6^{\Psi}$	$48 \pm 6^{\Psi}$
MVM Standing	$57 \pm 6^{*\Psi}$	$50 \pm 4^{*\Psi}$	$63 \pm 7^{*\Psi}$	$53 \pm 8^{*\Psi}$
MVC Supine	42 ± 4	40 ± 5	43 ± 4	41 ± 5

Table 4.1 Measures of radius of rotation in women with (N=20) and without stress urinary incontinence (SUI; N=12).The distance between pubic symphysis (PS) and theoretical center of rotation (r) was measured. Maximum values of r (r_{max}) were measured in the video frame in which the PS appeared most cranial. Minimum values of r (r_{min}) were measured in the video frame in which the PS appeared most caudal. Mean (± standard deviation) is presented for each group and task. Significant differences between groups (SUI vs Control) are indicated by * and significant differences within groups, between positions (i.e. supine vs. standing position) are indicated by $^{\Psi}$.

There were no differences in α by group, task, or position (Table 4.2).

Task	α at r_{min} (°)		α at r_{max} (°)	
	SUI	Control	SUI	Control
Cough Supine	337 ± 7	330 ± 5	339 ± 8	339 ± 6
Cough Standing	330 ± 6	331 ± 5	332 ± 7	336 ± 7
MVM Supine	338 ± 8	330 ± 6	336 ± 8	338 ± 7
MVM Standing	330 ± 6	327 ± 4	329 ± 6	329 ± 5
MVC Supine	336 ± 7	331 ± 6	337 ± 7	336 ± 5

Table 4.2 The angular deviation between the anatomical and arbitrary reference coordinate systems (α) were measured in a group of women with stress urinary incontinence (SUI, n = 20) and a group of women with no urogenital signs or symptoms (Control, n = 12) at maximum values of r (r_{max}), the distance between pubic symphysis (PS) and theoretical center of rotation, and at minimum values of r (r_{min}). Mean (± standard deviation) is presented for each group and task.

4.4.2 Experiment 2

The data for this experiment were acquired from a single healthy, nulliparous female volunteer (age 23; BMI 22.3 kg/m^2) who had no history of urogenital signs or symptoms. Table 4.3 shows the maximum and minimum observed r measured during each task, r_{max} and r_{min}, respectively. Additionally, values of α were measured at r_{max} and r_{min}, peak values of Θ were measured during each task, and the error incurred by probe rotation was calculated at r_{max} and r_{min} in the anatomical coordinate system (Table 4.3).

Task	Values at r_{min}		Values at r_{max}		Θ_{Pk} (°)	Error at r_{min}			Error at r_{max}		
	r (mm)	α (°)	r (mm)	α (°)		E_{Xa} (mm)	E_{Ya} (mm)	E_{Ma} (mm)	E_x (mm)	E_y (mm)	E_{Ma} (mm)
Cough Sup	37.0	324.9	41.6	330.1	2.4	0.9	1.2	1.5	0.9	1.5	1.7
Cough St	42.5	329.1	45.0	334.5	5.1	2.1	3.1	3.7	1.9	3.5	4.0
Valsalva Sup	37.2	325.0	40.2	330.6	11.6	4.9	5.7	7.5	4.7	6.6	8.1
Valsalva St	46.8	327.7	48.5	326.5	15.8	8.3	9.8	12.9	8.8	10.0	13.3
MVC Sup	36.0	332.3	37.5	333.8	3.7	1.1	2.0	2.3	1.1	2.1	2.4

Table 4.3 Parameters effecting error measured during transperineal ultrasound imaging. Data was collected from a single participant performing coughing and Valsalva tasks in supine (Sup) and standing (St), and pelvic floor muscle maximum

voluntary contractions (MVC) in supine. The distance between the pubic symphysis and the transperineal ultrasound (TPUS) probe was measured at its maximum (r_{max}) and minimum (r_{min}) during each task. Angular deviation between the anatomical and arbitrary reference coordinate systems (α) was measured at r_{min} and r_{max}, and peak in-plane angular displacement of the TPUS probe (Θ_{pk}) was also measured during each task. These values were used to calculate error in the anatomical Cartesian coordinate system (E_{Xa} and E_{Ya}) and the absolute error (E_{Ma}) incurred by probe rotation, in mm, for each task.

TPUS video from the same patient was analyzed to yield the peak excursion of the anorectal angle and bladder neck, during each task in the x- and y-directions of the anatomical coordinate system (Figure 4.5). Table 4.4 shows these measures along with the error calculated at r_{max} and r_{min}, expressed as a percentage of respective landmark excursion, each in the x and y directions of the anatomical coordinate system.

	Anorectal Angle						**Bladder Neck**					
	ARA_{disp} (mm)		**Error at r_{min}**		**Error at r_{max}**		**BN_{disp} (mm)**		**Error at r_{min}**		**Error at r_{max}**	
Task	**D_{Xa} (mm)**	**D_{Ya} (mm)**	**E_{Xa} (%)**	**E_{Ya} (%)**	**E_{Xa} (%)**	**E_{Ya} (%)**	**D_{Xa} (mm)**	**D_{Ya} (mm)**	**E_{Xa} (%)**	**E_{Ya} (%)**	**E_{Xa} (%)**	**E_{Ya} (%)**
Cough Sup.	-4.4	20.3	29.1	4.3	34.5	4.1	-3.7	-7.6	34.6	11.4	41.1	11.0
Cough St.	4.2	1.2	78.0	144.6	86.5	125.6	13.6	-9.5	24.3	18.7	27.0	16.3
Valsalva Sup.	2.3	10.4	285.3	35.1	323.9	31.2	15.0	-6.2	43.6	59.2	49.5	52.6
Valsalva St.	17.6	-0.7	66.5	753.7	68.3	817.0	9.7	-8.3	121.0	64.1	124.1	69.5
MVC Sup.	-11.8	26.1	17.7	3.9	18.6	3.8	-1.6	1.4	131.5	71.7	138.6	70.6

Table 4.4 Peak excursions and error for the anorectal angle and bladder neck were measured in the anatomical x-direction (D_{Xa}) and the anatomical y-direction (D_{Ya}) and are expressed in mm. Error incurred by probe rotation, measured at the maximal and minimal sagittal distance between the pubic symphysis and the transperineal ultrasound (TPUS) probe, r_{max} and r_{min}, respectively, are expressed as a percentage of ARA and BN excursion in the anatomical x- and y-directions (E_{Xa} and E_{Ya}).

Using the data presented in Table 4.4, the absolute displacement of the anorectal angle and bladder neck were calculated in order to quantify the absolute error incurred by probe rotation as a percentage of landmark displacement at r_{max} and r_{min} (

	Anorectal Angle					**Bladder Neck**				
Task	**ARAdisp**	**Error at rmin**		**Error at rmax**		**BNdisp**	**Error at rmin**		**Error at rmax**	
	DMa (mm)	**EMa (mm)**	**EMa (%)**	**EMa (mm)**	**EMa (%)**	**DMa (mm)**	**EMa (mm)**	**EMa (%)**	**EMa (mm)**	**EMa (%)**
Cough Sup.	20.7	1.5	7.4	1.7	8.4	8.4	1.5	18.3	1.7	20.6
Cough St.	4.4	3.7	85.1	4.0	90.2	16.6	3.7	22.6	4.0	24.0
Valsalva Sup.	10.6	7.5	70.3	8.1	76.1	16.2	7.5	46.2	8.1	50.0
Valsalva St.	17.6	12.9	73.0	13.3	75.6	12.7	12.9	101.0	13.3	104.6
MVC Sup.	28.6	2.3	8.1	2.4	8.4	2.1	2.3	109.2	2.4	113.7

Table 4.5).

	Anorectal Angle					**Bladder Neck**				
Task	**ARA_{disp}**	**Error at r_{min}**		**Error at r_{max}**		**BN_{disp}**	**Error at r_{min}**		**Error at r_{max}**	
	D_{Ma} (mm)	**E_{Ma} (mm)**	**E_{Ma} (%)**	**E_{Ma} (mm)**	**E_{Ma} (%)**	**D_{Ma} (mm)**	**E_{Ma} (mm)**	**E_{Ma} (%)**	**E_{Ma} (mm)**	**E_{Ma} (%)**
Cough Sup.	20.7	1.5	7.4	1.7	8.4	8.4	1.5	18.3	1.7	20.6

Cough St.	4.4	3.7	85.1	4.0	90.2	16.6	3.7	22.6	4.0	24.0
Valsalva Sup.	10.6	7.5	70.3	8.1	76.1	16.2	7.5	46.2	8.1	50.0
Valsalva St.	17.6	12.9	73.0	13.3	75.6	12.7	12.9	101.0	13.3	104.6
MVC Sup.	28.6	2.3	8.1	2.4	8.4	2.1	2.3	109.2	2.4	113.7

Table 4.5 Absolute displacement and error for the anorectal angle (ARA) and bladder neck (BN), were calculated in mm. Absolute error (E_{Ma}) incurred by probe rotation, at the maximal and minimal sagittal distance between the pubic symphysis and the transperineal ultrasound (TPUS) probe, r_{max} and r_{min}, respectively, is expressed as a percentage of absolute excursion of the ARA and BN.

Group averages and standard deviations, combined with the single case study data presented here, show that α ranges from approximately 320° to 350° (Table 4.1), r ranges from approximately 35mm to 70mm (Table 4.1), and, in the single-patient data collection, Θ ranged from approximately 0° to 20° (Table 4.3), depending on the task. With the understanding that in-plane probe rotation, Θ, can occur in the positive or negative direction, the range of Θ can be expanded from -20° to +20°. Using these ranges, surface plots of the functions K_{Xa} and K_{Yx} can be used to visualize the impacts of changes in Θ and α on error in the x- and y-direction measures taken (Figure 4.6). The magnitude of the K function, at given values of Θ and α, will act as a multiplier on the measured r value (see Table 4.1).

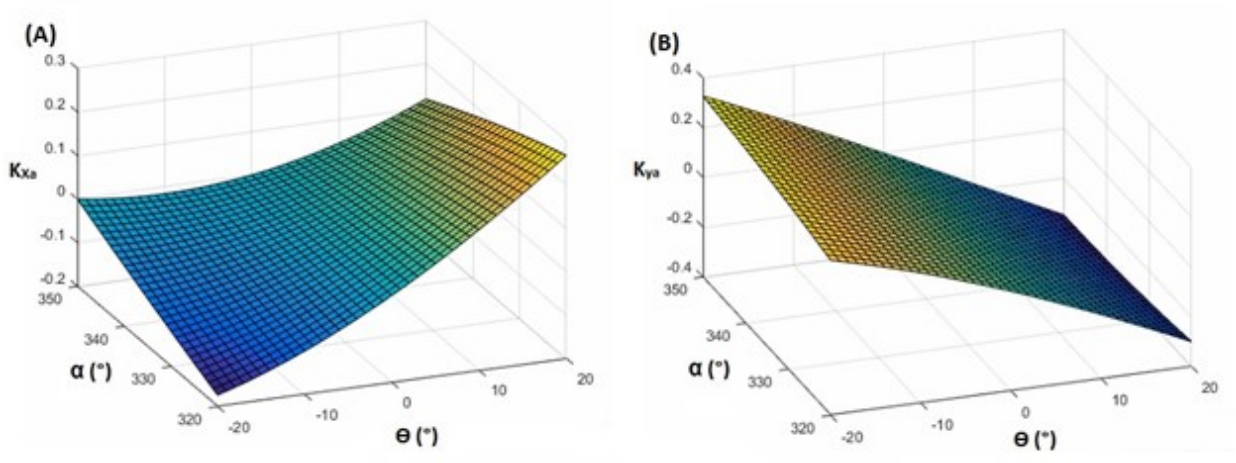

Figure 4.6: Error incurred by in-plane transperineal ultrasound (TPUS) probe rotation in (A) the anatomical x-direction (K_{Xa}, antero-posterior) and (B) the anatomical y-direction (K_{Ya}, cranial-caudal) are expressed as functions of angular deviation between the anatomical and arbitrary reference coordinate systems (α) and peak in-plane angular displacement of the TPUS probe (Θ), with color moving from darker to lighter as the value of the K function increases. Ranges of α and Θ are based on the experimental data presented in Table 4.1, Table 4.3, and Table 4.4.

Further, because the magnitude of error or absolute error incurred by in-plane probe rotation is a factor of r and Θ alone, a surface plot can be used to characterize this error (in mm), as in Figure 4.7. This figure

provides a visualization of how the error incurred by in-plane probe rotation changes with each of its independent variables, r and Θ.

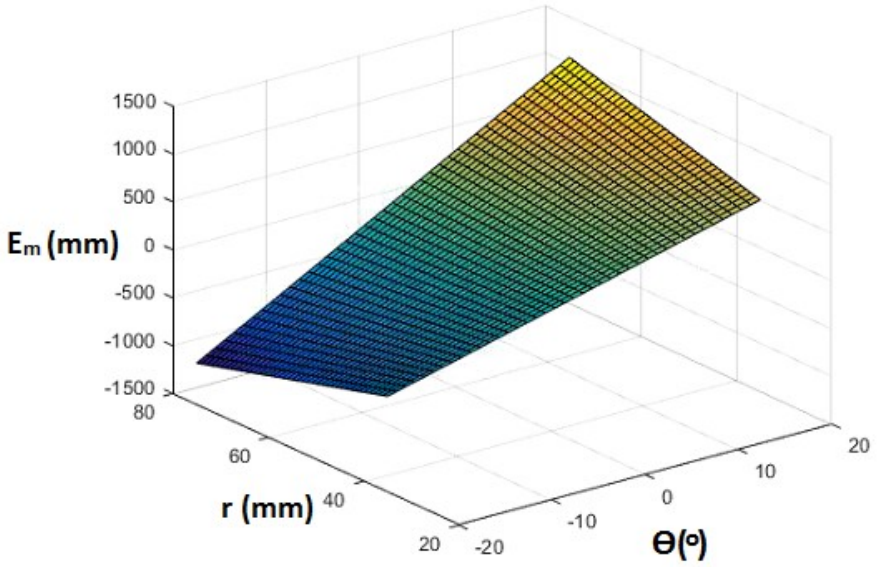

Figure 4.7 The absolute error, incurred by in-plane transperineal ultrasound (TPUS) probe rotation (E_m), in millimeters, is expressed as a function of the radius about which this rotation takes place (r) and peak in-plane angular displacement of the TPUS probe (Θ), with color moving from darker to lighter as the value of the value of E_m increases. Ranges of r and Θ are based on the experimental data presented in Table 4.1 and Table 4.4

4.5 Discussion

This work aimed to characterize the error incurred in sagittal plane measures of urogenital kinematics taken from TPUS images due to in-plane rotation of the ultrasound probe during image acquisition. Additionally, we aimed to generate a set of error values that can be expected during dynamic tasks commonly investigated using TPUS. The mathematical analysis performed here demonstrates that the error incurred by in-plane probe rotation is a factor of not only the in-plane angular displacement of the TPUS probe (Θ), but also of the radius about which the in-plane rotation occurs (r) and the angular

deviation between the anatomical coordinate system in which measures are taken and the arbitrary reference coordinate system used to derive expressions of error (α). The error incurred by in-plane probe rotation can also be expressed an absolute value, in which case it is a factor of only r and Θ. In a group of women, the measured r can vary from 35 to 70 mm and α can vary from 320° to 350°, depending on the task being performed, the continence status of the woman, and the position in which the TPUS images are acquired. An additional case analysis showed that peak Θ can vary by almost 20° in a healthy female depending on the position and on the task. As well, Θ and α can be absorbed to create the functions K_{Xa}, K_{Ya}, which are multiplied by r to produce the magnitude of error in the x- and y-direction, respectively. Depending on the continence status of the woman being imaged, and the task being performed, K_{Xa} and K_{Ya}, can vary between approximately -0.2 to 0.3 and -0.4 to 0.4, respectively, resulting in errors ranging from 4% to over 100% of peak landmark excursion in the x- and y- directions. As an absolute value, the error incurred by in-plane probe rotation can be quite high, depending on the anatomical morphology of the women being examined, the task being performed, and the magnitude of in-plane probe rotation. These results have widespread implications for researchers using measures of urogenital kinematics [14], [65], [93] or net displacements of urogenital landmarks [42], [43], [50] to characterize healthy and pathological urogenital biomechanics.

Based on data from a sample of women with (n=20) and without (n=12) SUI, both minimum and maximum r values during a task are larger when images are captured in standing compared to supine. Measurements in the literature have shown that the bladder neck sits significantly more cranially in the supine position as compared to the standing position [22]. Additionally, vaginal closure forces, vaginal resting pressure, and bladder pressure are significantly higher in standing than in supine [112], [113]. These results have been attributed to the increased IAP in the standing position due to the effects of gravity on the internal organs. The r defined in the current study reflects the distance measured in the sagittal plane between the postero-caudal margin of the pubic symphysis and the center of rotation within the TPUS probe. With this in mind, the consistently larger distance between the pubic symphysis and the

TPUS probe observed in the standing position with respect to the supine position could also be attributed to the same phenomenon. Between a supine and a standing position, the caudal excursion of the pubic symphysis should be minimal due to the bony nature of this landmark. However, in the standing position, gravitational forces causes the urogenital organs to sit more caudally in the body, resting more heavily on the PFMs which function to support the internal organs [47], presumably leading to the significantly higher vaginal resting pressure in standing position [113]. The results here combined with information from the literature may suggest that in the standing position the soft tissue of the perineum actually sits more caudally with respect to the pubic symphysis, leading to a higher r in the standing position with respect to the supine position. Additionally, in the standing position the technician may not be holding the TPUS probe as firmly against the perineum as when the patient is in the supine position due to the effects of gravity and the added difficulty of capturing TPUS in standing rather than supine [58]. Knowing that the measured r contributes substantially to the magnitude of error, researchers should attempt to minimize this value, somewhat, by ensuring that the ultrasound probe is placed firmly against the perineum throughout data collection. Beyond this, r will be mainly a function of a woman's anatomy and cannot be controlled.

The differences in the r values measured across the different tasks may also be attributable to the different urogenital biomechanics associated with each task. During a coughing task, there is an increase in IAP as the diaphragm and the abdominals contract. Similarly, during a Valsalva maneuver, "bearing down" is achieved by a conscious increase in IAP generated by the patient. In contrast to this, a PFM MVC involves a lift and squeeze around the urethra, vagina, and rectum [72]. With this in mind, it then follows that the higher maximum r values measured during coughing and Valsalva tasks with respect to the MVC task, each in the supine position, for both the control and the SUI women, could be attributed to the increased IAP generated during the former two tasks. Conversely, minimum measures of r did not differ between tasks in supine or in standing for either group. During coughing and Valsalva tasks, increased IAP could result in the descent of urogenital tissues and the perineum thereby increasing the value of r

towards the peak of the task. This would result in r_{min} likely occurring at rest. However, the MVC involves a "lift and squeeze" [21]; antero-cranial motion of the PFMs [45] combines with concurrent abdominal contraction [82] which, while having a clear impact on the urogenital structures [45], may not result in any significant lift occurring at the perineum in the supine position. As such, our results showing similar values of r_{min} across each group for the standing tasks and, separately, for the supine tasks, appear to be logical. It should be noted, however, that an MVC performed in standing may not necessarily yield similar r_{min} values to either standing coughing or Valsalva maneuvers. The significantly higher r values in the SUI group as compared to the control group, especially in standing, may be the result of the differences between groups in terms of BMI and parity. Further investigation is required to understand the nature of this difference.

Mathematically, the variable α may change depending on TPUS probe orientation, pressure of the probe on the perineum, the anatomy of the participant, and potentially other factors. It does not appear to vary between cohorts, tasks or positions, yet it is still an essential element in the calculation of the error associated with urogenital kinematic analysis if we are to consider landmark excursions in terms of their x- and y-components. As such, measures of α were collected simply to investigate biological variability of this parameter and differences between groups, positions, and tasks were not tested. Further, all factors that could impact the value of α may also impact the magnitude of either r or Θ. With this in mind, α may be mathematically dependant on either r or Θ, or potentially both. As such, it may be more reasonable to consider landmark excursions as absolute values with an angular direction in order to eliminate the effects of the α on the error incurred by in-plane probe rotation.

Tasks performed in standing yielded larger Θ values than the corresponding task performed in supine. This may be attributable to the difficulty associated with imaging women in the standing position rather than supine [58]. Specifically, the technician must hold the ultrasound probe securely against the perineum, but move with the perineum if there is any motion – which takes strength, skill, and co-

ordination that is not required when imaging in supine. Further, the technician often purposely rotates the probe in order to keep the pubic symphysis and the anorectal angle visible in the image frame as these landmarks move apart. The values of in-plane probe rotation measured in the coughing task, in both standing and supine, were in line with those reported by Peng et al [14]. The coughing and MVC tasks performed in supine generated the lowest magnitudes of probe rotation, whereas the Valsalva task performed in standing yielded the highest Θ. This could be as a result of the combined straining effort and the increased IAP that characterize a Valsalva, combined with the added difficulty of capturing TPUS images in the standing position. During a properly performed Valsalva maneuver, the increased IAP, perineal descent, and straining effort from the patient could all contribute to increased motion during the task which could result in higher Θ values. While data from a single participant are not adequate to draw generalized conclusions, the results here suggest that researchers taking measures of urogenital kinematics from TPUS images must be aware of the potential for probe motion depending on the task being performed, the position of the woman, and her continence status.

The K functions were devised to act as multipliers on r for the quantification of error in the x- and y-directions (Figure 4.6), whereas the nature of absolute error incurred by in-plane probe rotation allows for the complete visualization of this phenomenon as a factor of its independent variables (Figure 4.7). While positive and negative Θ values will affect the direction of the error differently, the absolute error function (Figure 4.7) best describes the effects of Θ and r on error. Where there is no probe rotation ($\Theta = 0$), the error function will be zero regardless, while in situations where $\Theta \neq 0$ changes in α and r can have marked effects on the directional and absolute error. Regardless of the direction of in-plane probe rotation, higher values of Θ will yield higher magnitudes of error. With this in mind, and with an understanding that our ability to control for variations in r and α may be limited, at this point researchers should focus on minimizing Θ and should consider expressing measures of landmark excursion as absolute values with an angular direction as opposed to expressing measures in anatomic or Cartesian co-ordinates.

Considering these results, it is clear that larger values of r and Θ will inherently lead to higher error in measures, however if the measures being taken are small to begin with (e.g. caudal displacement of the anorectal angle during a Valsalva performed in standing by a woman with a healthy pelvic floor) then error quickly explodes to a higher percentage of the measure itself, and the measure no longer has clinical value. Though the motion capture data collected during the various tasks were not synchronized to the TPUS video, the data suggest that professionals using TPUS images as a basis for measuring urogenital landmark excursion should do so with caution. Additionally, while some groups have implemented a manually aligned coordinate system to minimize the error incurred due to probe rotation [16], [37], [66], if the coordinate system is misaligned by even a few degrees (e.g. MVC supine), depending on the task, the error resulting from this misalignment can be quite large. With this understanding of TPUS image analysis and the results present here, the much lower magnitudes of error presented by Reddy et al [37] may in reality have been calculated compensating only for probe motion, but not for probe rotation. It should also be noted that depending on the task and the biomechanics in a given patient, general trends can be expected. Healthy control patients tend to exhibit more stability in their urogenital organs and thus lower displacements during tasks such as Valsalva and coughing [11], [14], [36], [71]. As such, the impacts of error caused by in-plane probe rotation will likely be higher in healthy women during coughing and Valsalva due to the small magnitudes of the measures being taken. Additionally, in MVC tasks, women with weaker PFMs who exhibit lower levels of soft tissue deformation [12] will be more likely to yield higher magnitudes of error in measures taken from TPUS.

While this work provides valuable insight into the effects of in-plane probe rotation on measures taken from TPUS images, there are several inherent limitations, the most prominent of which is sample size. This work is meant to present a mathematical model that allows for error calculation and a single case analysis showing the potential effects of error in a specific data collection. As such, data from a single patient do not necessarily represent population effects. Although there is obvious need for follow-up

work with a larger sample size, the results of this single case analysis suggest that there is a need to develop strategies to limit the parameters contributing to error in measures taken from TPUS. Additionally, our motion capture was not synchronized to the TPUS image acquisition. While the data collection was carefully controlled by the investigator (C.C.), there is potential that peak values for Θ may have occurred slightly before or after image acquisition rendering the values non-representative of probe rotation during the actual data collection. Use of an ultrasound system that can be triggered externally will provide further insight and should be used in subsequent studies. The alignment of the anatomically significant coordinate system with the horizontal, regardless of orientation of the pubic symphysis must also be acknowledged as another limitation. Lastly, as explained in the methods section, modelling the origin of ultrasound wave omission in the sagittal plane as a single point may be an oversimplification of the situation. Despite these limitations, the mathematical model and data presented here serve the intended purpose: to inform of the potential for error in a method used by many researchers around the world.

This study demonstrates that error in measures of sagittal plane urogenital kinematics incurred due to in-plane TPUS probe rotation varies depending on the dynamic task being performed, the continence status, the position, and the anatomy of the patient. Additionally, higher levels of in-plane probe rotation will yield a higher magnitude of error. In the standing position and during tasks involving increases in IAP or straining, researchers can expect the impacts of this error to be potentially quite large. Additionally, the smaller the expected measures, the larger the impact of error due to in-plane probe rotation will be. In the case of researchers using manually aligned coordinate systems, misalignment of the coordinate system can also impact measures in the same way as in-plane probe rotation. Moving forward, researchers are advised to either monitor and compensate for in-plane probe rotation when taking measures from TPUS video, or to employ visual feedback monitoring in-plane probe rotation during image acquisition, such that the technician can limit probe rotation to a range deemed acceptable by the research team based on the expected magnitude of landmark motion.

5 Discussion

There are critical gaps in the literature in terms of our understanding how TPUS probe motion influences the calculation of sagittal plane urogenital kinematics and the validity of these measures. This work aimed to (1) develop a semi-automated software (UROKIN) that compensates for in-plane TPUS probe motion and calculates kinematic curves of relevant urogenital landmarks, and (2) characterize and quantify the error incurred in measures of urogenital system kinematics due to in-plane TPUS probe rotation. The results presented within this thesis have achieved these aims and show tremendous promise for UROKIN as a valuable tool, able to answer relevant clinical and research questions.

5.1 Summary of Results

The development of the UROKIN software is described in Chapter 3. TPUS video captured from twenty women with SUI and nine women with no history of SUI while they performed three repetitions of a PFM MVC task in a supine position were used to complete preliminary testing of the UROKIN software. Specifically, two users processed the same 30 TPUS videos, three PFM MVC trials each from ten women with SUI, and the between-user variability, reported using RMSE, was found to be well below the biological variability among the women. As such, we were able to pool videos processed by the two users, to generate complete kinematic curves for all women in the sample. The output of the UROKIN algorithm was able to distinguish both timing and amplitude differences in the kinematic curves of anorectal angle and bladder neck motion between women with and without SUI. Specifically, from normalized, ensemble-averaged curves; we found that the anorectal angle exhibited a lower peak anterior displacement and an earlier peak in cranial displacement in women with SUI, while the same group demonstrated significantly lower cranial motion of the bladder neck, as compared to the healthy control group. All of these variables correlated significantly with PFM strength measured using manual digital palpation.

In developing a mathematical model to characterize the impact of in-plane TPUS probe rotation on measures of urogenital kinematics in the sagittal plane, error incurred in measures of urogenital landmark displacement by in-plane probe rotation was found to be a factor of: r, the distance from the postero-caudal margin of the pubic symphysis to the theoretical mid-sagittal origin of the TPUS probe; and Θ, the magnitude of in-plane ultrasound probe rotation. Additionally, when considering the directional impact of error in its x- and y- components, a third variable contributed to error incurred in measures of landmark excursion: α, the angular deviation between the anatomical coordinate system and an arbitrary reference coordinate system oriented with the x-axis running from the postero-caudal pubic symphysis to the theoretical origin of the TPUS probe. In the derivation for directional error presented, the expression is simplified such that r acts as a multiplier on K, a function of Θ and α. Plots of the K function demonstrate that the value of K in the x-direction, y-direction, and as an absolute value varied to a larger degree with changes in Θ than with changes in α. When error was considered as an absolute value, a simple expression could be used in which r and Θ acted as the independent variables and absolute error could be visualized as a 3D surface plot (Figure 4.7). Using ultrasound image data from women with and without SUI, average values were found to range from 35mm to 70mm for r, and from 320° to 350° for α. In a case analysis on a healthy female, values of Θ were found to vary between 0 and 20°. All of these values are dependent on the continence status of the woman, the task being performed, and the position of the woman during image acquisition. Tasks in the standing position were found to yield higher r and Θ values than in supine, likely due to the confounding influences of postural control and inherent difficulty stabilizing the probe surface firmly against the perineum using consistent pressure. Between tasks, Valsalva maneuvers were found to yield the highest values of Θ among all tasks in both the standing and supine positions, likely because the clinician must deliberately rotate the probe in order to keep relevant anatomical landmarks in view. During Valsalva maneuvers, clinicians must also adjust the amount of pressure applied by the probe on the perineum as it descends, which may affect magnitudes r and Θ. Based on the analysis presented, error in measures of urogenital landmark displacement can vary from

4% to over 100% of the measure depending on the task, the position of the patient, and the landmark being traced.

5.2 The UROKIN Software

The UROKIN algorithm provided extremely positive results in our proof of concept. Our initial reliability evaluation of UROKIN software outcomes yielded an average between-user variability, characterized by RMSE, of less than 5% of the mean between-user difference in kinematic outcomes computed for a coughing task, identified by Peng et al.'s algorithm [45], [71]. Admittedly urogenital landmark motion observed during PFM MVCs may have less between-participant variability than what is observed during coughing, however this level of between-user variability is also much smaller than the biological variability we observed in our sample. These results provide justification for completing a thorough reliability analysis on kinematic outcomes computed for different urogenital landmarks and throughout different tasks.

The UROKIN algorithm was able to identify significant differences between women with and without SUI in both time and amplitude characteristics of the urogenital landmark kinematic curves. The findings of this study are complimentary to the only other results presented in the literature thus far. During coughing, women with SUI were observed to initially experience a caudal decent of the anorectal angle, perhaps indicative of a difficulty in the PFMs ability to overcome downward forces generated by the increase in IAP [14], [46]. Our women with SUI demonstrated lower anterior motion and a lower and earlier peak in cranial motion of the anorectal angle, as well as less cranial motion of the bladder neck compared to the control group. These results suggest that, although the women with SUI were actively contracting their PFMs, as evidenced by the shortening of the levator plate, the cranial aspect of their contraction ends prematurely. This may suggest that the women with SUI experience difficulty generating and maintaining the lifting component of the PFM contraction, which may translate to less

stability of the urethra seen during coughing [14], [46]. The outcomes of this work provide sufficient evidence that this line of investigation is worth pursuing, and that once the reliability of UROKIN has been established, we can proceed to investigate larger samples of women performing different tasks in different positions.

5.3 The Effects of In-Plane Probe Rotation

The mathematical model of in-plane probe rotation showed that r, and Θ are all relevant to the magnitude of error, while a third factor, α, is relevant to directional error. This finding was in line with our expectations. The independent variables r and Θ appear to have the most prominent effect on the magnitude of error. The variable α appears to be dependent on variety of factors including an individual woman's anatomy, probe pressure, probe orientation, and other factors, making it difficult to control. Higher values of r measured in the standing position support evidence in literature that the bladder neck [22] rests more caudally and that forces in the caudal portion of the urogenital system are higher in the standing position than in supine [113], presumably due to the weight of the abdominal and pelvic contents resting on the pelvic floor, and the increased IAP generated by the abdominal muscle contraction required for postural stability. As expected, our results suggest that the entire perineum rests more caudally in standing compared to supine, leading to an increased distance between the pubic symphysis and the ultrasound probe (ie. our r value) when TPUS images are acquired in standing. Additionally, the measured values of r generally tended to be higher in the SUI group with respect to the control group. This may be due to the significantly higher BMI of the SUI group, which has been linked to increased IAP and increased urethral mobility [18]. Unfortunately, there is little to be done during image acquisition to mitigate the impact of r or α. The imaging technician should ensure that the TPUS probe is resting firmly against the perineum, without causing pain, but beyond this, r and α are factors of the patient's anatomy and cannot be closely controlled.

There is little research presented in the literature investigating the magnitudes of probe rotation during sagittal TPUS imaging. The values presented in Chapter 4 during the coughing task were in line with the ±5° of probe rotation observed by Peng et al. who also investigated a coughing task [14]. Beyond this, there is no published literature providing estimates of probe rotation measured during the acquisition of TPUS video during Valsalva or MVC tasks. Although we recorded probe motion during imaging in only one woman, we observed higher magnitudes of probe rotation during the Valsalva maneuver compared to PFM MVC or coughing. This is likely due to the nature of the Valsalva maneuver itself, in that it requires a woman to increase her IAP and relax the pelvic floor – causing the urogenital structures to move postero-caudally in the mid-sagittal plane. The descent of the perineum itself, which was observed in our sample, may alter the orientation of the TPUS probe, potentially increasing magnitudes of probe rotation. We observed higher magnitudes of probe rotation in the standing position with respect to supine. It is well known that imaging in standing can impact the stability of the TPUS transducer [58], however PFM mechanics do vary from the supine to the standing position [22], [113], [114]. As such, it is necessary for researchers to consider how these factors may impact TPUS acquisition in standing and thus influence outcomes. Tracking and minimizing the magnitude of Θ during image acquisition would minimize error incurred in computations of urogenital kinematics by TPUS probe rotation.

5.4 Contributions to the Literature

The literature review completed at the outset of this study identified significant gaps with respect to the limitations of TPUS as it has been used in research to date, the validation of software designed to take measures of urogenital kinematics, and urogenital kinematic measures themselves. The mathematical model of in-plane probe rotation presented here has quantified a previously uninvestigated phenomenon. Using this derivation and measures detailed here, we now have a better understanding of the impacts of patient anatomy, probe design and orientation, and in-plane probe rotation on the measures being taken. For those who do not compensate for the effects in-plane probe rotation, the evidence here suggests that

this variable may be worth monitoring and limiting. For those who already compensate for the effects in-plane probe rotation in their analyses, the effects of small rotations on their results can be quantified. The UROKIN algorithm has demonstrated improvements upon some of the previous limitations in the literature, provides promising preliminary evidence of acceptable inter-user reliability, and was able to distinguish urogenital kinematic differences between continent women and women with SUI. While there are still many improvements to be made, this body of work has eliminated some of the uncertainty associated with TPUS of the urogenital system and has provided a unique solution in the form of UROKIN.

5.5 Future Work

Although the research presented in this thesis has made valuable contributions to knowledge, there is much room for improvement. In terms of the UROKIN software, angular rotations in the algorithm, currently calculated with respect to the pubic symphysis, must be updated to incorporate what we have learned through the error analysis presented in Chapter 4. In-plane probe rotation should be compensated for with respect to the theoretical origin of the ultrasound probe. The method of tracing the pubic symphysis to generate a local coordinate system for each video, while generally in line with the anatomical directions, is not perfectly aligned between patients or trials. Finding a way to align coordinate systems consistently between TPUS videos will improve the validity of these measures. Further, the two users of the software who processed images for this study have suggested many improvements which will be implemented to speed up data processing. These two users are currently participating in a formal reliability analysis which we are hoping to present in the near future. As well, we have completed the pilot testing to assess the validity of the UROKIN algorithm and will present this in future works.

The use of the UROKIN software, in its current form, is very time consuming. One video, that is one trial of one MVC task, can take upwards of 6 hours to process. An obvious direction for this research is to incorporate automated segmentation into the UROKIN algorithm. The last group to employ automated segmentation of urogenital structures in sagittal TPUS video analysis, published their algorithm in 2006 [45] and there have been many breakthroughs in image analysis since then. Once we have refined UROKIN based on the results of this thesis, we are next planning to optimize the sampling rates by performing an in-depth frequency analysis of kinematic curves obtained using the UROKIN algorithm.

5.6 Conclusion

While there is still much to be done, the mathematical derivation and the UROKIN software presented in this thesis have yielded essential additions to the literature. This formulation of error and investigation into its contributing factors will provide researchers with information required to better understand research involving the motion of urogenital landmarks. As well, the initial development and testing of the UROKIN software has provided the exciting capacity to investigate the kinematics of urogenital mobility and morphology. This software will be instrumental in future investigation into the continence mechanism, SUI and many other PFDs. Continued work to further develop the UROKIN software is definitely warranted, and has the capacity to change how we evaluate and intervene to improve continence function in women – thus having a major impact on both their health and quality of life.

6 References

[1] I. Nygaard, M. D. Barber, and K. Burgio, "Prevalence of symptomatic pelvic floor disorders in US women," *J. Am. Med. Assoc.*, vol. 300, no. 11, pp. 1311–1316, 2008.

[2] A. H. MacLennan, A. W. Taylor, D. H. Wilson, and D. Wilson, "The prevalence of pelvic floor disorders and their relationship to gender, age, parity and mode of delivery," *BJOG An Int. J. Obstet. Gynaecol.*, vol. 107, no. 12, pp. 1460–1470, 2000.

[3] W. S. Reynolds, R. R. Dmochowski, and D. F. Penson, "Epidemiology of stress urinary incontinence in women," *Curr. Urol. Rep.*, vol. 12, no. 5, pp. 370–376, 2011.

[4] M. Bettez, L. M. Tu, K. Carlson, J. Corcos, J. Gajewski, M. Jolivet, and G. Bailly, "2012 update: Guidelines for adult urinary incontinence collaborative consensus document for the Canadian Urological Association," *J. Can. Urol. Assoc.*, vol. 6, no. 5, pp. 354–363, 2012.

[5] D. Taylor and M. Weir, "The Self-reported Prevalence and Knowledge of Urinary Incontinence and Barriers to Health Care-Seeking in a Community Sample of Canadian Women," *Am. J. ...*, vol. 3, no. 5, pp. 97–102, 2013.

[6] J. Perera, D. S. Kirthinanda, S. Wijeratne, and T. K. Wickramarachchi, "Descriptive cross sectional study on prevalence, perceptions, predisposing factors and health seeking behaviour of women with stress urinary incontinence," *BMC Womens. Health*, vol. 14, no. 1, p. 78, 2014.

[7] C. Chaliha, "Postpartum bladder dysfunction," *Rev. Gynaecol. Perinat. Pract.*, vol. 6, no. 3–4, pp. 133–139, 2006.

[8] "The Impact of Incontinence in Canada A Briefing Document for Policy-Makers," no. December, 2014.

[9] P. Abrams, A. P. Smith, and N. Cotterill, "The impact of urinary incontinence on health-related quality of life (HRQoL) in a real-world population of women aged 45-60 years: Results from a survey in France, Germany, the UK and the USA," *BJU Int.*, vol. 115, no. 1, pp. 143–152, 2015.

[10] J. M. Wu, A. F. Hundley, R. G. Fulton, and E. R. Myers, "Forecasting the prevalence of pelvic floor disorders in the U.S. women: 2010 to 2050," *Obstet. Gynecol.*, vol. 114, no. 6, pp. 1278–1283, 2009.

[11] J. O. L. DeLancey, J. M. Miller, R. Kearney, D. Howard, P. Reddy, W. Umek, K. E. Guire, R. U. Margulies, and J. A. Ashton-Miller, "Vaginal Birth and De Novo Stress Incontinence," *Obstet. Gynecol.*, vol. 110, no. 2, Part 1, pp. 354–362, Aug. 2007.

[12] H. P. Dietz, S. K. Jarvis, and T. G. Vancaillie, "The assessment of levator muscle strength: A validation of three ultrasound techniques," *Int. Urogynecol. J. Pelvic Floor Dysfunct.*, vol. 13, no. 3, pp. 156–159, 2002.

[13] C. Lewicky-Gaupp, J. Blaivas, A. Clark, E. J. Mcguire, G. N. Schaer, J. Tumbarello, R. Tunn, and J. O. L. Delancey, "' The cough game ' : are there characteristic urethrovesical movement patterns associated with stress incontinence?," *Int. Urogynecology J. Pelvic Floor Dysfunction2*, vol. 20, pp. 171–175, 2009.

[14] Q. Peng, R. C. Jones, K. Shishido, and C. E. Constantinou, "Ultrasound evaluation of dynamic responses of female pelvic floor muscles.," *Ultrasound Med. Biol.*, vol. 33, no. 3, pp. 342–52, 2007.

[15] A. Pirpiris, K. L. Shek, and H. P. Dietz, "Urethral mobility and urinary incontinence," *Ultrasound Obs. Gynecol*, vol. 36, pp. 507–511, 2010.

[16] K. L. Shek and H. P. Dietz, “The urethral motion profile: a novel method to evaluate urethral support and mobility.,” *Aust. N. Z. J. Obstet. Gynaecol.*, vol. 48, no. 3, pp. 337–42, 2008.
[17] D. M. Morgan, W. Umek, K. E. Guire, H. K. Morgan, A. Garabrant, and J. O. L. DeLancey, “Urethral sphincter morphology and function with and without stress incontinence.,” *J. Urol.*, vol. 182, no. 1, pp. 203–209, 2009.
[18] D. J. Osborn, M. Strain, A. Gomelsky, J. Rothschild, and R. R. Dmochowski, “Obesity and female stress urinary incontinence,” *J. Urol.*, vol. 82, no. 4, pp. 759–763, 2013.
[19] D. Howard, J. O. L. Delancey, R. Tunn, and J. A. Ashton-Miller, “Racial Differences in the Structure and Function of the Stress Urinary Continence Mechanism,” *Obstet. Gynecol.*, vol. 95, no. 5, pp. 713–717, 2000.
[20] D. H. Thom, S. K. van den Eeden, A. I. Ragins, C. Wassel-Fyr, E. Vittinghof, L. L. Subak, and J. S. Brown, “Differences in prevalence of urinary incontinence by race/ethnicity.,” *J. Urol.*, vol. 175, no. 1, pp. 259–64, 2006.
[21] K. Bø, “Pelvic floor muscle training is effective in treatment of female stress urinary incontinence, but how does it work?,” *Int. Urogynecol. J. Pelvic Floor Dysfunct.*, vol. 15, no. 2, pp. 76–84, 2004.
[22] L. McLean, K. Varette, E. Gentilcore-Saulnier, M.-A. Harvey, K. Baker, and E. Sauerbrei, “Pelvic floor muscle training in women with stress urinary incontinence causes hypertrophy of the urethral sphincters and reduces bladder neck mobility during coughing,” *Neurourol. Urodyn.*, vol. 32, no. 8, pp. 1096–1102, Nov. 2013.
[23] K. L. Noblett, A. McKinney, and F. L. Lane, “Effects of the incontinence dish pessary on urethral support and urodynamic parameters,” *Am. J. Obstet. Gynecol.*, vol. 198, no. 5, pp. 1–5, 2008.
[24] A. Jain, F. Majoko, and O. Freites, “How innocent is the vaginal pessary? Two cases of vaginal cancer associated with pessary use,” *J. Obstet. Gynaecol. (Lahore).*, vol. 26, no. 8, pp. 829–830, Jan. 2006.
[25] D. P. Hay, W. L. Martin, and F. J. Darne, “Potentially dangerous complication of an ineffective shelf pessary,” *J. Obstet. Gynaecol.*, vol. 19, no. 6, p. 669, 1999.
[26] E. J. McGuire, “Urethral bulking agents.,” *Nat. Clin. Pract. Urol.*, vol. 3, no. 5, pp. 234–5, 2006.
[27] C. C. G. Chen, S. A. Collins, A. K. Rodgers, M. F. R. Paraiso, M. D. Walters, and M. D. Barber, “Perioperative complications in obese women vs normal-weight women who undergo vaginal surgery,” *Am. J. Obstet. Gynecol.*, vol. 197, no. 1, 2007.
[28] C. Dumoulin, D. Bourbonnais, M. Morin, D. Gravel, and M. C. Lemieux, “Predictors of Success for Physiotherapy Treatment in Women With Persistent Postpartum Stress Urinary Incontinence,” *Arch. Phys. Med. Rehabil.*, vol. 91, no. 7, pp. 1059–1063, 2010.
[29] G. A. Digesu, D. Robinson, L. Cardozo, and V. Khullar, “Three-dimensional ultrasound of the urethral sphincter predicts continence surgery outcome,” *Neurourol. Urodyn.*, vol. 28, no. 1, pp. 90–94, Jan. 2009.
[30] S. J. Madill, S. Pontbriand-Drolet, A. Tang, and C. Dumoulin, “Changes in urethral sphincter size following rehabilitation in older women with stress urinary incontinence,” *Int. Urogynecol. J.*, vol. 26, no. 2, pp. 277–283, 2015.
[31] R. M. Caputo and J. T. Bension, “The Q-tip test and urethrovesical junction mobility,” *Obstet. Gynecol.*, vol. 82, no. 6, pp. 892–896, 1993.
[32] A. M. Weber, “Is urethral pressure profilometry a useful diagnostic test for stress urinary

incontinence?," *Obstet. Gynecol. Surv.*, vol. 56, no. 11, pp. 720–35, 2001.
[33] H. P. Dietz, "Ultrasound imaging of the pelvic floor. Part II: Three-dimensional or volume imaging," *Ultrasound Obstet. Gynecol.*, vol. 23, no. 6, pp. 615–625, 2004.
[34] P. Türker, G. Kilic, and T. Tarcan, "The presence of transurethral cystometry catheter and type of stress test affect the measurement of abdominal leak point pressure (ALPP) in women with stress urinary incontinence (SUI)," *Neurourol. Urodyn.*, vol. 34, no. 3, p. n/a-n/a, 2009.
[35] W. C. Huang, S. H. Yang, and J. M. Yang, "Anatomical and functional significance of urogenital hiatus in primary urodynamic stress incontinence," *Ultrasound Obstet. Gynecol.*, vol. 27, no. 1, pp. 71–77, 2006.
[36] M. Barbič, B. Kralj, and A. Cör, "Compliance of the bladder neck supporting structures: Importance of activity pattern of levator ani muscle and content of elastic fibers of endopelvic fascia," *Neurourol. Urodyn.*, vol. 22, no. 4, pp. 269–276, 2003.
[37] A. P. Reddy, J. O. L. DeLancey, L. M. Zwica, and J. A. Ashton-Miller, "On-screen vector-based ultrasound assessment of vesical neck movement," *Am. J. Obstet. Gynecol.*, vol. 185, no. 1, pp. 65–70, 2001.
[38] G. Lose, D. Griffiths, G. Hosker, S. Kulseng-Hanssen, D. Perucchini, W. Schfer, P. Thind, and E. Versi, "Standardisation of urethral pressure measurement: Report from the standardisation sub-committee of the International Continence Society," *Neurourol. Urodyn.*, vol. 21, no. 3, pp. 258–260, 2002.
[39] H. P. Dietz, "Ultrasound imaging of the pelvic floor. Part I: Two-dimensional aspects," *Ultrasound Obstet. Gynecol.*, vol. 23, no. 1, pp. 80–92, 2004.
[40] F. S. Q. D. S. Brandão, M. P. L. Parente, P. A. G. G. Rocha, M. T. D. Q. E. C. D. M. Saraiva, I. M. A. P. Ramos, and R. M. Natal Jorge, "Modeling the contraction of the pelvic floor muscles," *Comput. Methods Biomech. Biomed. Engin.*, vol. 5842, no. July, pp. 1–10, 2015.
[41] M. Morin, S. Bergeron, S. Khalifé, M. H. Mayrand, and Y. M. Binik, "Morphometry of the Pelvic Floor Muscles in Women With and Without Provoked Vestibulodynia Using 4D Ultrasound," *J. Sex. Med.*, vol. 11, no. 3, pp. 776–785, 2014.
[42] L. McLean, S. Thibault-Gagnon, K. Brooks, C. Goldfinger, C. Pukall, and S. Chamberlain, "Differences in Pelvic Morphology Between Women With and Without Provoked Vestibulodynia," *J. Sex. Med.*, vol. 13, no. 6, pp. 963–971, Jun. 2016.
[43] C. Naranjo-Ortiz, K. L. Shek, A. J. Martin, and H. P. Dietz, "What is normal bladder neck anatomy?," *Int. Urogynecol. J.*, 2015.
[44] D. Gordon, M. Pearce, P. Norton, and S. L. Stanton, "Comparison of ultrasound and lateral chain urethrocystography in the determination of bladder neck descent," *Am. J. Obstet. Gynecol.*, vol. 160, no. 1, pp. 182–185, 1989.
[45] Q. Peng, R. C. Jones, and C. E. Constantinou, "2D ultrasound image processing in identifying responses of urogenital structures to pelvic floor muscle activity," *Ann. Biomed. Eng.*, vol. 34, no. 3, pp. 477–493, 2006.
[46] R. C. Lovegrove Jones, Q. Peng, M. Stokes, V. F. Humphrey, C. Payne, and C. E. Constantinou, "Mechanisms of Pelvic Floor Muscle Function and the Effect on the Urethra during a Cough," *Eur. Urol.*, vol. 57, no. 6, pp. 1101–1110, 2010.
[47] J. O. L. DeLancey, "Structural support of the urethra as it relates to stress urinary incontinence: The hammock hypothesis," *Am. J. Obstet. Gynecol.*, vol. 170, no. 6, pp. 1713–1723, 1994.

[48] J. A. Ashton-Miller, D. Howard, and J. O. L. DeLancey, “Functional Anatomy of the Female Pelvic Floor,” *Ann. N. Y. Acad. Sci.*, vol. 1101, no. 1, pp. 266–296, Feb. 2007.
[49] Q. Peng, R. Jones, K. Shishido, S. Omata, and C. E. Constantinou, “Spatial distribution of vaginal closure pressures of continent and stress urinary incontinent women.,” *Physiol. Meas.*, vol. 28, no. 11, pp. 1429–1450, 2007.
[50] R. E. Stafford, G. Coughlin, N. J. Lutton, and P. W. Hodges, “Validity of Estimation of Pelvic Floor Muscle Activity from Transperineal Ultrasound Imaging in Men,” *PLoS One*, vol. 10, no. 12, p. e0144342, 2015.
[51] H. O. Critchley, J. S. Dixon, and J. A. Gosling, “Comparative Study of the Periurethral and Perianal Parts of the Human Levator ani Muscle,” *Urol. Int.*, vol. 35, no. 3, pp. 226–32, 1980.
[52] S. Thibault-Gagnon and M. Morin, “Active and Passive Components of Pelvic Floor Muscle Tone in Women with Provoked Vestibulodynia: A Perspective Based on a Review of the Literature,” *J. Sex. Med.*, vol. 12, no. 11, pp. 2178–2189, 2015.
[53] L. J. Tuttle, O. T. Nguyen, M. S. Cook, M. Alperin, S. B. Shah, S. R. Ward, and R. L. Lieber, “Architectural design of the pelvic floor is consistent with muscle functional subspecialization,” *Int. Urogynecol. J. Pelvic Floor Dysfunct.*, vol. 25, no. 2, pp. 205–212, 2014.
[54] E. Versi, L. D. Cardozo, J. W. Studd, M. Brincat, T. M. O’Dowd, and D. J. Cooper, “Internal urinary sphincter in maintenance of female continence.,” *Br. Med. J. (Clin. Res. Ed).*, vol. 292, no. 6514, pp. 166–7, 1986.
[55] K. Strohbehn, J. Elus, J. Strohbehn, and J. O. L. Delancey, “Magnetic resonance imaging of the levator ani with anatomic correlation,” *Obstet. Gynecol.*, vol. 87, no. 2, pp. 277–285, Feb. 1996.
[56] H. P. Dietz, C. Shek, and B. Clarke, “Biometry of the pubovisceral muscle and levator hiatus by three-dimensional pelvic floor ultrasound,” *Ultrasound Obstet. Gynecol.*, vol. 25, no. 6, pp. 580–585, 2005.
[57] S. Costantini, F. Esposito, C. Nadalini, D. Lijoi, S. Morano, P. Lantieri, and E. Mistrangelo, “Ultrasound imaging of the female perineum: The effect of vaginal delivery on pelvic floor dynamics,” *Ultrasound Obstet. Gynecol.*, vol. 27, no. 2, pp. 183–187, 2006.
[58] U. M. Peschers, D. B. Voduek, G. Fanger, G. N. Schaer, J. O. L. Delancey, and B. Schuessler, “Pelvic muscle activity in nulliparous volunteers,” *Neurourol. Urodyn.*, vol. 20, no. 3, pp. 269–275, 2001.
[59] G. N. Schaer, “Ultrasonography of the lower urinary tract,” *Curr. Opin. Obstet. Gynecol.*, vol. 9, no. 5, p. 313???316, Oct. 1997.
[60] U. M. Peschers, G. Fanger, G. N. Schaer, D. B. Vodusek, J. O. L. DeLancey, and B. Schuessler, “Bladder neck mobility in continent nulliparous women,” *Br. J. Obstet. Gynaecol.*, vol. 108, no. 3, pp. 320–324, 2001.
[61] H. P. Dietz, B. Clarke, and P. Herbison, “Bladder Neck Mobility and Urethral Closure Pressure as Predictors of Genuine Stress Incontinence,” *Int. Urogynecol. J.*, vol. 13, no. 5, pp. 289–293, Oct. 2002.
[62] J. Cassadó, A. Pessarrodona, R. Tulleuda, L. Cabero, M. Valls, S. Quintana, and M. Rodríguez-Carballeira, “Introital ultrasonography: A comparison of women with stress incontinence due to urethral hypermobility and continent women,” *BJU Int.*, vol. 98, no. 4, pp. 822–828, 2006.

[63] R. Pregazzi, A. Sartore, P. Bortoli, E. Grimaldi, L. Troiano, and S. Guaschino, “Perineal ultrasound evaluation of urethral angle and bladder neck mobility in women with stress urinary incontinence,” *BJOG An Int. J. Obstet. Gynaecol.*, vol. 109, no. 7, pp. 821–827, 2002.
[64] C. Auchincloss, S. Thibault-Gagnon, R. Graham, and L. McLean, “Validity of estimation of pelvic floor muscle activation through transperineal ultrasound imaging in women,” *Int. Soc. Electromyogr. Kinesiol.*, vol. Poster Abs, p. 45, 2016.
[65] C. S. Czyrnyj, M. R. Labrosse, and L. McLean, “Urogenital kinematics mesaured in the sagittal plane using a novel ultrasound image processing approach,” in *2016 IEEE EMBS International Student Conference (ISC)*, 2016, pp. 1–4.
[66] G. N. Schaer, O. Koechli, B. Schuessler, and U. Haller, “Perineal ultrasound for evaluating the bladder neck in urinary stress incontinence,” *Obstet. Gynecol.*, vol. 85, no. 2, pp. 220–224, Feb. 1995.
[67] A. K. Örnö and H. P. Dietz, “Levator co-activation is a significant confounder of pelvic organ descent on Valsalva maneuver,” *Ultrasound Obstet. Gynecol.*, vol. 30, no. 3, pp. 346–350, Sep. 2007.
[68] J. A. Kruger, S. W. Heap, B. a. Murphy, and H. P. Dietz, “How best to measure the levator hiatus: Evidence for the non-Euclidean nature of the ‘plane of minimal dimensions,’” *Ultrasound Obstet. Gynecol.*, vol. 36, no. 6, pp. 755–758, 2010.
[69] M. Majida, I. H. Braekken, W. Umek, K. Bo, Š. Benth, and M. E. Engh, “Interobserver repeatability of three- and four-dimensional transperineal ultrasound assessment of pelvic floor muscle anatomy and function,” *Ultrasound Obstet. Gynecol.*, vol. 33, no. 5, pp. 567–573, 2009.
[70] C. Persu, C. R. Chapple, V. Cauni, S. Gutue, and P. Geavlete, “Pelvic Organ Prolapse Quantification System (POP-Q) - a new era in pelvic prolapse staging.,” *J. Med. Life*, vol. 4, no. 1, pp. 75–81, 2011.
[71] R. C. Lovegrove Jones, Q. Peng, M. Stokes, V. F. Humphrey, and C. E. Constantinou, “The Inter-Tester Reliability of 2D Ultrasound and Image Processing Methods To Evaluate the Pelvic Floor Muscles (Pfm) and Urethra During a Cough in Continent and Stress Urinary Incontinent (Sui) Women,” *38th Annu. Meet. Int. Cont. Soc.*, vol. Abstract 2, pp. 20–24, 2008.
[72] K. Bø and M. Sherburn, “Evaluation of Female Pelvic-Floor Muscle Function and Strength,” *Phys. Ther.*, vol. 85, no. 3, 2005.
[73] J. E. Hall, *Guyton and Hall Textbook of Medical Physiology*, 13th ed. Philadelphia: Elsevier, Inc., 2016.
[74] C. E. Constantinou and D. E. Govan, “Spatial distribution and timing of transmitted and reflexly generated urethral pressures in healthy women.,” *J. Urol.*, vol. 127, no. 5, pp. 964–9, 1982.
[75] Y. Ansquer, P. Fernander, S. Aimot, M. Bennis, L. Salomon, and B. Carbonne, “MRI urethrovesical junction mobility is associated with global pelvic floor laxity in female stress incontinence.,” *Acta Obstet. Gynecol. Scand.*, vol. 86, no. 10, pp. 1243–50, 2007.
[76] S. J. Madill and L. McLean, “Intravaginal pressure generated during voluntary pelvic floor muscle contractions and during coughing: The effect of age and continence status,” *Neurourol. Urodyn.*, vol. 34, no. 3, p. n/a-n/a, 2009.
[77] N. Keshwani and L. McLean, “Development of a differential suction electrode for improved intravaginal recordings of pelvic floor muscle activity: Reliability and motion

artifact assessment," *Neurourol. Urodyn.*, vol. 31, no. 8, pp. 1272–1278, Nov. 2012.
[78] K. Bø and C. E. Constantinou, "Reflex contraction of pelvic floor muscles during cough cannot be measured with vaginal pressure devices," *Neurourol. Urodyn.*, vol. 30, no. 7, p. 1404, 2011.
[79] M. Morin, D. Bourbonnais, D. Gravel, C. Dumoulin, and M. C. Lemieux, "Pelvic floor muscle function in continent and stress urinary incontinent women using dynamometric measurements," *Neurourol. Urodyn.*, vol. 23, no. 7, pp. 668–674, 2004.
[80] H. P. Dietz, P. D. Wilson, and B. Clarke, "The use of perineal ultrasound to quantify levator activity and teach pelvic floor muscle exercises," *Int. Urogynecol. J. Pelvic Floor Dysfunct.*, vol. 12, no. 3, pp. 166–169, 2001.
[81] H. P. Dietz and P. D. Wilson, "The influence of bladder volume on the position and mobility of the urethrovesical junction," *Int Urogynecol J Pelvic Floor Dysfunct*, vol. 10, no. 1, pp. 3–6, 1999.
[82] S. J. Madill and L. McLean, "Relationship between abdominal and pelvic floor muscle activation and intravaginal pressure during pelvic floor muscle contractions in healthy continent women," *Neurourol. Urodyn.*, vol. 25, no. 7, pp. 722–730, 2006.
[83] N. Keshwani and L. McLean, "A differential suction electrode for recording electromyographic activity from the pelvic floor muscles: Crosstalk evaluation," *J. Electromyogr. Kinesiol.*, vol. 23, no. 2, pp. 311–318, 2013.
[84] K. Bø, B. Kvarstein, R. Hagen, and S. Larsen, "Pelvic floor muscles exercise for the treatment of female stress urinary incontinence: II. Validity of vaginal pressure strength and the necessity of supplementary methods for control of correct contraction," *Neurol Urodyn*, vol. 9, pp. 479–87, 1990.
[85] J. Miller, J. A. Ashton-Miller, and J. O. L. DeLancey, "A Pelvic Muscle Precontraction Can Reduce Cough-Related Urine Loss in Selected Women with Mild SUI," *J. Am. Geriatr. Soc.*, vol. 46, no. 7, pp. 870–874, 1998.
[86] B. Ihnatsenka and A. P. Boezaart, "Ultrasound: Basic understanding and learning the language," *Int. J. Shoulder Surg.*, vol. 4, no. 3, pp. 55–62, 2010.
[87] J. W. Clark, M. R. Neuman, W. H. Olson, R. A. Peura, F. P. Primiano, M. P. Siedband, J. G. Webster, and L. A. Wheeler, *Medical Insturmentation Application and Design*, 4th ed. Hoboken: John Wiley & Sons, Inc., 2010.
[88] S. M. Creighton, J. M. Pearce, and S. L. Stanton, "Perineal video-ultrasonography in the assessment of vaginal prolapse: early observations," *BJOG An Int. J. Obstet. Gynaecol.*, vol. 99, no. 4, pp. 310–313, Apr. 1992.
[89] A. J. Vickers, "Parametric versus non-parametric statistics in the analysis of randomized trials with non-normally distributed data," *BMC Med. Res. Methodol.*, vol. 5, no. 1, p. 35, 2005.
[90] H. M. Perkin, E. A. Bond, J. Thompson, E. C. Woods, and C. Smith, "Real Time Ultrasound: An Objective Measure of Skeletal Muscle," *Phys. Ther. Rev.*, vol. 8, no. 2, pp. 99–108, Jun. 2003.
[91] L. Tan, K. L. Shek, I. K. Atan, R. G. Rojas, and H. P. Dietz, "The repeatability of sonographic measures of functional pelvic floor anatomy," *Int. Urogynecol. J. Pelvic Floor Dysfunct.*, vol. 26, no. 11, pp. 1667–1672, 2015.
[92] M. Dalstra, R. Huiskes, A. Odgaard, and L. van Erning, "Mechanical and textural properties of pelvic trabecular bone," *J. Biomech.*, vol. 26, no. 4–5, pp. 523–535, 1993.
[93] P. Bonneau, A. Branzan Albu, and C. Dumoulin, "A motion-tracking algorithm to

quantify kinematic parameters of the urethra and pelvic floor on 2D transperineal us," *Int. Urogynecol. J. Pelvic Floor Dysfunct.*, vol. 22, no. c, pp. S412–S413, 2011.
[94] L. Wilson, J. S. Brown, G. P. Shind, K. O. Luca, and L. L. Subak, "Annual direct cost of urinary incontinence," *Obstet. Gynecol.*, vol. 98, no. 3, pp. 398–406, 2001.
[95] E. C. Chong, A. A. Khan, and J. T. Anger, "The financial burden of stress urinary incontinence among women in the United States," *Curr. Urol. Rep.*, vol. 12, no. 5, pp. 358–362, 2011.
[96] P. Abrams, K. Avery, N. Gardener, and J. Donovan, "The international consultation on incontinence modular questionnaire: www.iciq.net," *J. Urol.*, vol. 175, no. 3, pp. 1063–1066, 2006.
[97] U. Peschers, G. Schaer, C. Anthuber, J. O. L. Delancey, and B. Schuessler, "Changes in vesical neck mobility following vaginal delivery," *Obstet. Gynecol.*, vol. 88, no. 6, pp. 1001–1006, 1996.
[98] H. P. Dietz and K. L. Shek, "The quantification of levator muscle resting tone by digital assessment," *Int. Urogynecol. J. Pelvic Floor Dysfunct.*, vol. 19, no. 11, pp. 1489–1493, 2008.
[99] J. L. Locher, P. S. Goode, D. L. Roth, R. L. Worrell, and K. L. Burgio, "Reliability assessment of the bladder diary for urinary incontinence in older women.," *J. Gerontol. A. Biol. Sci. Med. Sci.*, vol. 56, no. 1, pp. M32–M35, 2001.
[100] J. Laycock and D. Jerwood, "Pelvic Floor Muscle Assessment: The PERFECT Scheme," *Physiotherapy*, vol. 87, no. 12, pp. 631–642, 2001.
[101] K. Bø, M. Sherburn, and T. Allen, "Transabdominal ultrasound measurement of pelvic floor muscle activity when activated directly or via a transversus abdominis muscle contraction," *Neurourol. Urodyn.*, vol. 22, no. 6, pp. 582–588, 2003.
[102] C. Dumoulin, "Pelvic floor muscle training versus no treatment , or inactive control treatments , for urinary incontinence in women (Review)," no. 1, 2010.
[103] H. P. Dietz and A. B. Steensma, "The prevalence of major abnormalities of the levator ani in urogynaecological patients," *BJOG An Int. J. Obstet. Gynaecol.*, vol. 113, no. 2, pp. 225–230, 2006.
[104] K.-C. Lien, B. Mooney, J. O. L. DeLancey, and J. A. Ashton-Miller, "Levator Ani Muscle Stretch Induced by Simulated Vaginal Birth," *Obstet. Gynecol.*, vol. 103, no. 1, pp. 31–40, Jan. 2004.
[105] J. O. L. DeLancey, R. Kearney, Q. Chou, S. Speights, and S. Binno, "The appearance of levator ani muscle abnormalities in magnetic resonance images after vaginal delivery," *Obstet. Gynecol.*, vol. 101, no. 1, pp. 46–53, 2003.
[106] A. Padoa and T. Rosenbaum, *The Overactive Pelvic Floor*. Cham: Springer International Publishing, 2016.
[107] M. D. Smith, M. W. Coppieters, and P. W. Hodges, "Postural activity of the pelvic floor muscles is delayed during rapid arm movements in women with stress urinary incontinence," *Int. Urogynecol. J. Pelvic Floor Dysfunct.*, vol. 18, no. 8, pp. 901–911, 2007.
[108] G. Truijen, J. J. Wyndaele, and J. Weyler, "Original Article Conservative Treatment of Stress Urinary Incontinence in Women : Who will Benefit ?," *Int. Urogynecol. J.*, vol. 12, no. 6, pp. 386–390, 2001.
[109] C. Czyrnyj, M. Labrosse, and L. Mclean, "A Novel Computational Approach for Calculating Sagittal Place Urogenital Kinematics from Dynamic 2D Ultrasound," *2016 C.*

Conf. Proc., 2016.
[110] C. Czyrnyj, M. Labrosse, and L. Mclean, "Refined Analysis of Sagittal Plane Transperineal Ultrasound to Obtain Urethral Mobility Profile Kinematics," *19th Bienn. Meet. Can. Soc. Biomech.*, 2016.
[111] L. Hoyte, L. Schierlitz, K. Zou, G. Flesh, and J. R. Fielding, "Two- and 3-dimensional MRI comparison of levator ani structure, volume, and integrity in women with stress incontinence and prolapse," *Am. J. Obstet. Gynecol.*, vol. 185, no. 1, pp. 11–19, 2001.
[112] D. M. Morgan, G. Kaur, Y. Hsu, D. E. Fenner, K. Guire, J. Miller, J. A. Ashton-Miller, and J. O. L. Delancey, "Does vaginal closure force differ in the supine and standing positions?," *Am. J. Obstet. Gynecol.*, vol. 192, no. 5 SPEC. ISS., pp. 1722–1728, 2005.
[113] K. Bø and H. B. Finckenhagen, "Is there any difference in measurement of pelvic floor muscle strength in supine and standing position?," *Acta Obstet. Gynecol. Scand.*, vol. 82, no. 12, pp. 1120–1124, 2003.
[114] J. Laycock, "Comparison of vaginal electromyography (EMG) in lying, sitting and standing," Denver, Colarado, USA, 1999.